School of Production Engineering & Management
TECHNICAL UNIVERSITY of CRETE

Industrial Energy Environmental Systems Laboratory (IEESL)

Design and Implementation of Integrated Control System – Sensors for "Smart" Greenhouses, based on Internet of Things (IoT) Technologies

Evangelos Ntousakis

Supervisor professor Dr. Spiros Papaefthimiou

Chania, July 2021

Approved by the following examining committee:

Spiros Papaefthimiou
Associate Professor
School of Production Engineering and Management
Technical University of Crete, Chania, Greece

Michalis Konsolakis
Associate Professor
School of Production Engineering and Management
Technical University of Crete, Chania, Greece

Dimitris Ipsakis
Assistant Professor
School of Production Engineering and Management
Technical University of Crete, Chania, Greece

Abstract

The present thesis proposes an integrated smart greenhouse control system. The system will contain sensors for continuous data collection, such as climatic variables (temperature, relative humidity, soil moisture), altitude, atmospheric pressure, and CO-CO_2 concentrations. The measurements will be used to evaluate the quality, sensitivity, and durability of the sensors, as well as the stability and quality of greenhouse production. Based on the environmental measurements, each microcontroller will activate the systems (heating, irrigation, and ventilation) for the configuration of the optimal climatic conditions. Furthermore, based on the Internet of Things, wireless connectivity of components will provide real-time remote access to the environment and greenhouse equipment. This type of automation will reduce the amount of energy required for monitoring, control during the plant growth process. In addition, less energy and fewer resources will be wasted, as the actuators will only be activated when indicated by the sensors. Finally, an original model of the system will be implemented in an experimental indoor greenhouse to cross-check its operation and results. The entire system will be designed in such a way that it can be adapted to a real greenhouse regardless of dimensions and upgrade according to the needs for future work and modifications.

Σχεδιασμός και Υλοποίηση Ολοκληρωμένου Συστήματος Ελέγχου – Αισθητήρων για «Έξυπνα» Θερμοκήπια, με βάση Τεχνολογίες Διαδικτύου των Πραγμάτων (IoT).

Η παρούσα εργασία προτείνει ένα ολοκληρωμένο σύστημα ελέγχου «έξυπνου» θερμοκηπίου. Το σύστημα θα περιέχει αισθητήρες για τη συνεχή συλλογή δεδομένων όπως: κλιματικές μεταβλητές (θερμοκρασία, σχετική υγρασία, υγρασία εδάφους), υψόμετρο, ατμοσφαιρική πίεση και συγκεντρώσεις CO-CO_2. Οι μετρήσεις θα χρησιμοποιούνται για τη αξιολόγηση της ποιότητας, ευαισθησίας και αντοχής των αισθητήρων, καθώς και της σταθερότητας και ποιότητας παραγωγής του θερμοκηπίου. Με βάση τις περιβαλλοντικές μετρήσεις, οι μικρό-ελεγκτές του συστήματος θα ενεργοποιούν τα αντίστοιχα συστήματα (θέρμανσης, άρδευσης και αερισμού) για τη διαμόρφωση των ιδανικών κλιματικών συνθηκών. Επιπλέον, με βάση το Διαδίκτυο των πραγμάτων, η ασύρματη συνδεσιμότητα των εξαρτημάτων θα παρέχει απομακρυσμένη πρόσβαση στο περιβάλλον και στον εξοπλισμό του θερμοκηπίου σε πραγματικό χρόνο. Αυτού του είδους ο αυτοματισμός θα μειώνει την ποσότητα της ενέργειας που απαιτείται για την παρακολούθηση, τον έλεγχο κατά τη διαδικασία ανάπτυξης των φυτών. Επιπλέον, λιγότερη ενέργεια και λιγότεροι πόροι θα σπαταλούνται, καθώς οι ενεργοποιητές θα τίθενται σε λειτουργία μόνο όταν υποδεικνύεται από τους αισθητήρες. Τέλος, ένα πρωτότυπο μοντέλο του συστήματος θα υλοποιηθεί σε πειραματικό θερμοκήπιο εσωτερικού χώρου, για να επιβεβαιωθούν η λειτουργία και τα αποτελέσματά του. Ολόκληρο το σύστημα θα σχεδιαστεί με τρόπο ώστε να μπορεί να εφαρμοστεί σε ένα πραγματικό θερμοκήπιο, ανεξάρτητα από τις διαστάσεις του καθώς και να αναβαθμιστεί ανάλογα με τις ανάγκες για μελλοντικές εργασίες και τροποποιήσεις.

Acknowledgments

I would like to sincerely thank my supervisor Dr. Spiros Papaefthimiou for his valuable guidance and constructive advice in my thesis and the opportunity he gave me to get involved in this interesting project within the field of automatic control systems in smart agriculture. I also want to thank Ph.D. candidate Konstantinos Loukakis for the guidance and practical cooperation throughout this project.

Contents

CHAPTER 1

Chapter 1: Smart greenhouse background theory and related work

1.1 Introduction

One of the direct consequences of the continuous population growth worldwide is the increasing need for resources. Due to the depletion and decreasing availability in resources, it is urgent to achieve the highest efficiency possible for sustainability. In order to increase a crop's response, all the environmental parameters, including temperature, humidity, moisture, and CO_2 concentration, have to reach their optimal level. The climate can be controlled within metallic or wooden structures, covered with transparent materials such as glass or plastic, called greenhouses. While the primary purpose of the greenhouse is to trap the short-wavelength solar radiation and to store the long-wavelength thermal radiation, it also protects the crops from the exterior weather conditions, excess heat and cold, blizzards, and storms [1], [2].

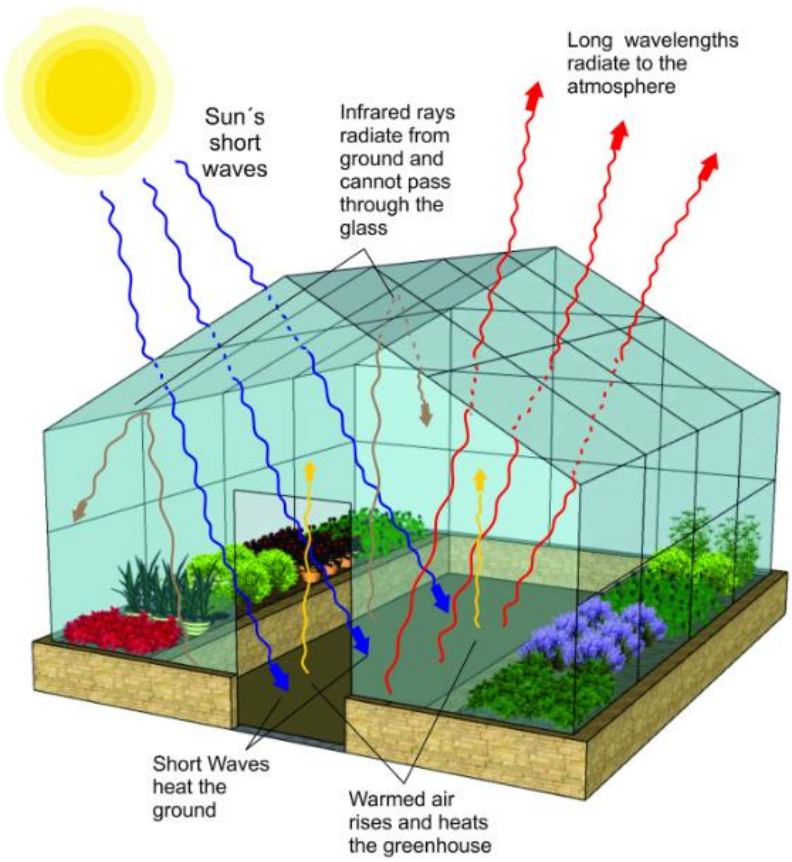

Figure 1.1: Operating principle of greenhouse [3].

Furthermore, the air movement inside the greenhouse is reduced, preventing the spread of plant diseases. Some other benefits of greenhouses include the ability to plant outside the farming season, throughout the whole year, with space optimization, to give an example, vertically. Last, the enclosed structure reduces evapotranspiration, subsequently energy losses, and filtrates harmful UV rays [1], [4].

Greenhouses include various systems for monitoring and controlling all the environmental forming factors. Continuous data acquisition and interpretation of interrelated parameters are laborious and complex processes. New atomization methods of "Precision farming" and "Smart agriculture" help farmers increase production while minimizing at the same time human labor and resources. Additionally, the Internet of Things (IoT) concept allows remote connectivity and communication across all devices over the internet in real-time [1], [4].

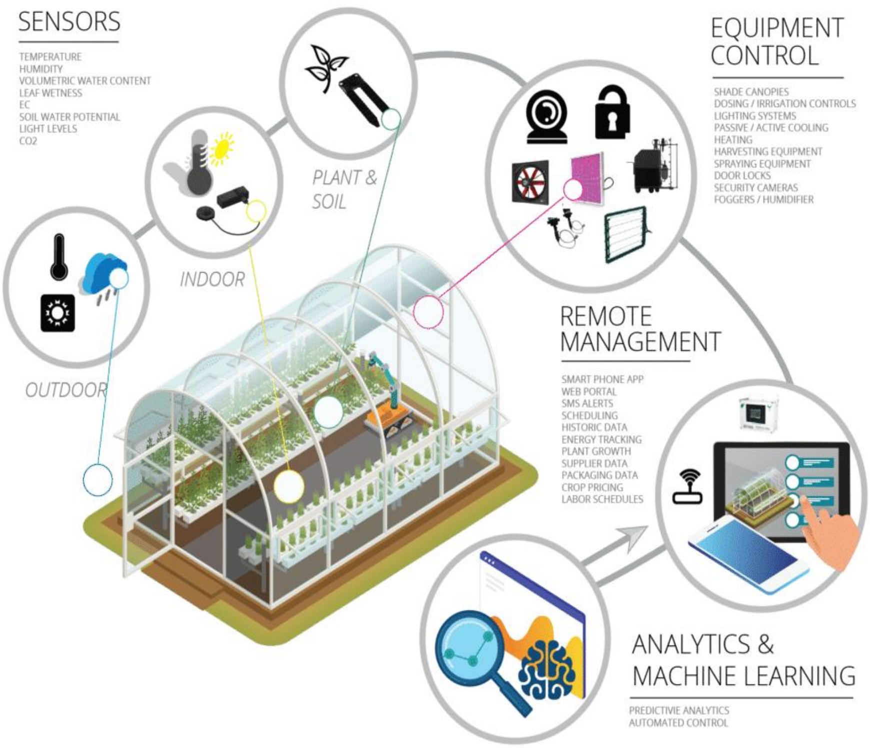

Figure 1.2: Smart greenhouse remote monitoring systems [5].

1.2 Greenhouse environmental variables

A number of factors contribute to greenhouse operations and efficiency, spanning from the good genetic properties of crops to the quality of fertilizers. Still what one needs to consider is the importance of continuous monitoring indoor and outdoor climate parameters: air and soil temperature, air humidity, soil moisture, solar radiation, light intensity, carbon dioxide (CO_2) concentration and soil PH, which directly contribute to the enhancement of plant growth as detailed below [6].

1.2.1 Solar radiation and light intensity

Solar energy is the main natural source of light and heat inside a greenhouse, where short-wavelength solar radiation is trapped and long-wavelength thermal radiation is stored. Short wavelength photosynthetically active radiation between 0.4-0.7μm is responsible for photosynthesis, and the rest of the spectrum is responsible for crop transpiration. At the same time, light is diffused when entering a greenhouse, creating a homogenous spectrum profile around the canopy, and enhancing the light processes. Besides the process of photosynthesis, throughout which carbon dioxide (CO_2) is converted to organic material with the help of light, the plant reactions to different types of light, called morphogenesis, and to different day lengths, called periodism, are also essential processes for plant growth. For this reason, it is necessary to measure the irradiance, the spectral quality, and the duration of light [6]–[8].

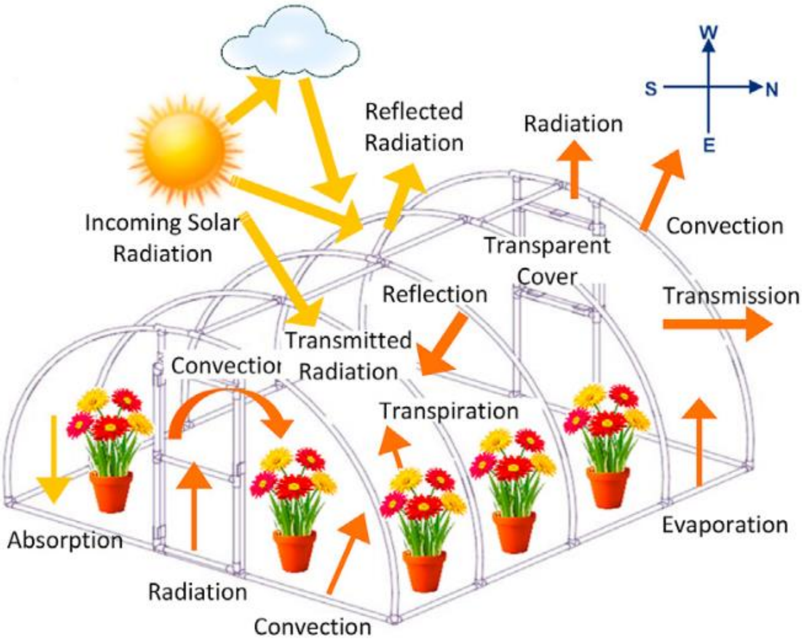

Figure 1.3: Energy transfer mechanisms [9].

1.2.2 Heat and temperature

The heat energy inside the greenhouse, and thereby the temperature, have a significant impact on chemical reactions and physical properties of crops both on plant and cellular level. The reason for that is that it regulates the transpiration rate and water status during photosynthesis. It should be noted that each species has unique requirements which vary during its development. What is more, temperature measurements are very important to closely and continuously monitor as they differ in height and length of the greenhouse, between day and night, throughout seasons, and are affected by light intensity, humidity and CO_2 concentration. Additionally, soil and plant temperatures provide vital information about the soil ecosystem and plant's health, respectively. Therefore, numerous temperature sensors to monitor the air, soil, and plant temperature are of equal and high importance [6], [8], [10].

1.2.3 Relative humidity

One of the most significant environmental factors is also humidity. Humidity influences all processes associated with transpiration, photosynthesis, pollination rate and ultimately the crop yield. Relative humidity and temperature are closely interlinked, as relative humidity indicates the ratio of dissolved water quantity in the air to the maximum amount without condensation at a specific temperature. Low percentages of relative humidity, which involve prolonged dry and extremely hot environments, can possibly lead plants to drought. On the contrary, high percentages and low temperatures make plants prone to fungus diseases and physiological disorders. Thus, it is necessary to monitor simultaneously both temperature and humidity [2], [6], [10]–[12].

1.2.4 Soil moisture

One more vital environmental parameter for plants is soil moisture in soil-based cultivation. A sufficient water level must be maintained in soil, where plants absorb all essential nutrients utilizing their roots. Monitoring soil moisture and supplying water according to each plant's needs not only protects the plants from being withered, when water is insufficient, and from various diseases, when there is an excess amount of water, but also limits the wasted water [8].

1.2.5 Carbon Dioxide - CO_2

Carbon dioxide (CO_2) is a fundamental element in photosynthesis, which plants absorb via stomata. Even though carbon dioxide and water are the only reactants in the chemical equation of photosynthesis (figure 1.4), temperature and humidity affect it by regulating the opening of stomata. The CO_2 concentration level can drop remarkably, even in a well-ventilated greenhouse, due to the dense crop growth. Unfortunately, CO_2 enrichment is not a widespread practice in mild climates. In an open environment, CO_2 concentration is about 400 ppm. However, in large-scale greenhouses, typically, levels as high as 1000-2000 ppm are ideal, capable of achieving over 20% cultivation increase [6], [8].

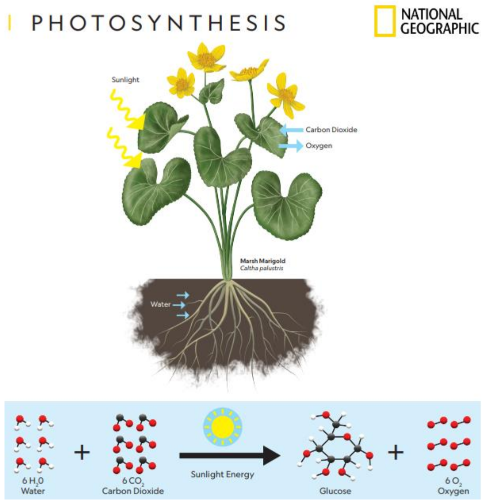

Figure 1.4: Chemical equation of photosynthesis [13].

1.2.6 Soil pH

One more chemical variable responsible for crop growth is soil pH, determining if the soil can receive nutrients. It ranges from 0 to 14, indicating the concentration of hydrogen ions. Usually, soil ranges from 4.0 to 8.5, but more favourable values are between 5.5 and 6.5. In alkaline soil (high pH values; above 7) nutrients are separated, depriving the plant of sustenance. On the other hand, in considerably acidic soil (low pH values; below 7) nutrients are more densely concentrated, becoming harmful for the plant. All in all, the pH level must meet each plant's requirements to grow and thrive. The soil pH characteristics can be modified by specially formulated fertilizers [12], [14].

Figure 1.5: Greenhouse environmental variables [15].

1.2.7 Outdoor weather conditions

Even though greenhouses are autonomous structures with their artificial environment, they are influenced by the outside weather conditions to a great level. Outdoor temperature and relative humidity affect the indoor parameters and the greenhouse's overall energy through air exchanges and heat transfer. Additionally, the wind speed, wind direction, and rainfall quantity may influence the rate of those exchanges [6].

1.3 Greenhouse variables regulating systems

Various systems are installed in a greenhouse to control the indoor environment parameters, adjust and maintain them at the optimal level of each crop's type and state. As mentioned above, all parameters inside and outside of the greenhouse are interrelated. Hence, a different combination of systems is needed every time (see table 1.1). Sensor data acquisition plays a significant role for the systems, as it provides feedback and controls their necessary activation and efficient operation.

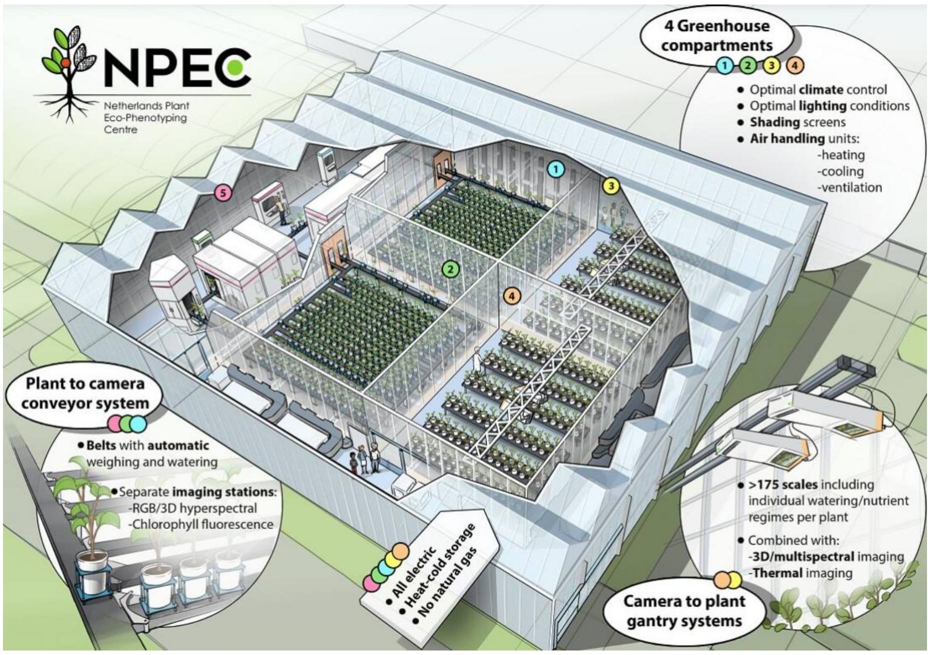

Figure 1.6: Automated greenhouse monitor and control model design [16].

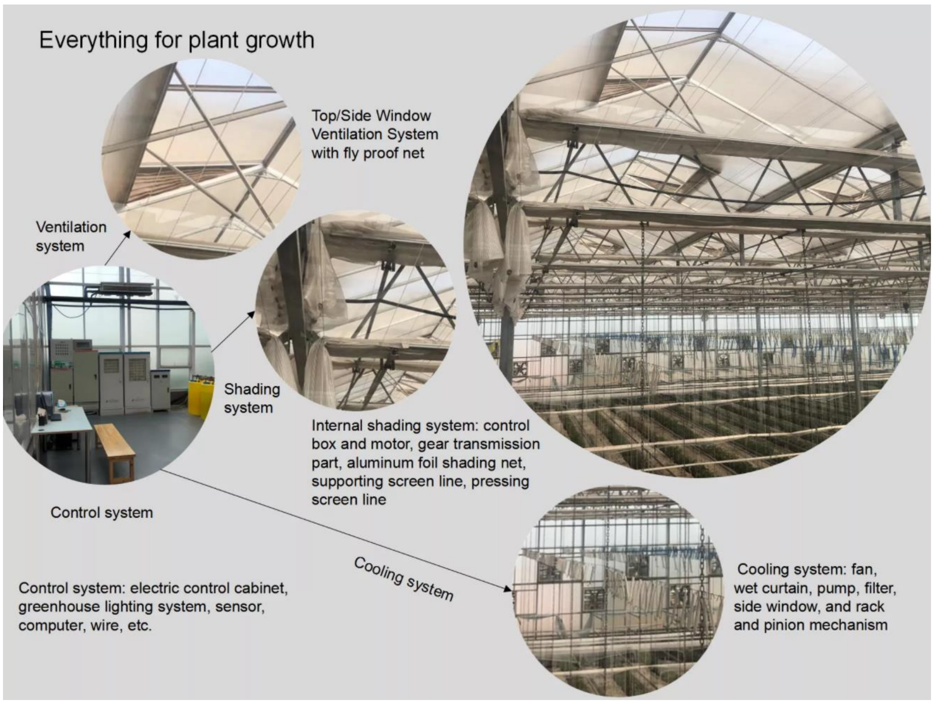

Figure 1.7: Implemented greenhouse control, ventilation, shading, and cooling systems.

Table 1.1: Impact of solar radiation, evaporative cooling and ventilation to the greenhouse variables (air temperature, relative humidity, VPD, irrigation needs, evapotranspiration) [17] [Μαυρογιαννόπουλος Ν. Γ., «Θερμοκήπια, Περιβάλλον-Υλικά-Κατασκευή- Εξοπλισμός», Δ'Έκδοση, Εκδόσεις Σταμούλη Α.Ε, Αθήνα, (2005)].

Systems and variables correlation	Air temperature	Relative humidity	VPD	Irrigation needs	Evapotranspiration
Solar radiation	+increase	-reduction	+increase	+increase	+increase
Evaporative cooling	-reduction	+ increase	-reduction	-reduction	-reduction
Ventilation	-reduction	-reduction	+ increase	+ increase	+ increase

1.3.1 Lighting and shading systems

Artificial lighting system

Most of the greenhouses use only solar as a light source. However, when natural light is absent or insufficient to cover the plant's needs, an auxiliary light is required to help plants continue their photo-processes relentlessly. Even when natural light is abundant and sufficient, artificial light at specific bands has proven its enhancements to plant growth, as shown in figure 1.9 [8], [18]. Most lighting systems include LED bulbs, fluorescent lights, tube lamps, metal halides lamps, or heat lamps [6].

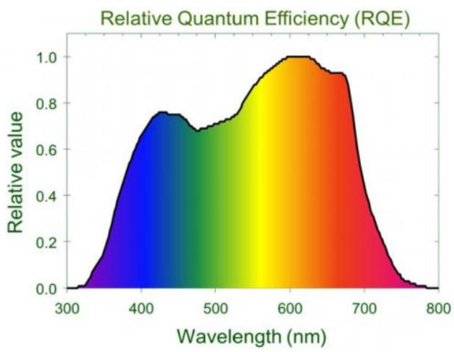

Figure 1.8: Relative quantum efficiency curve [19].

Figure 1.9: Greenhouse artificial lighting system utilizing the most efficient wavelengths for photosynthesis [20].

Shading system

In a different scenario, where solar radiation and light intensity exceed the optimal levels, resulting in excessively high temperatures and low relative humidity values (see table 1.1), shading systems are the only solution.

The most straightforward shading practices consist of internal or external shade screens, paints, and nets-fabrics with different opacity levels [6], [21].

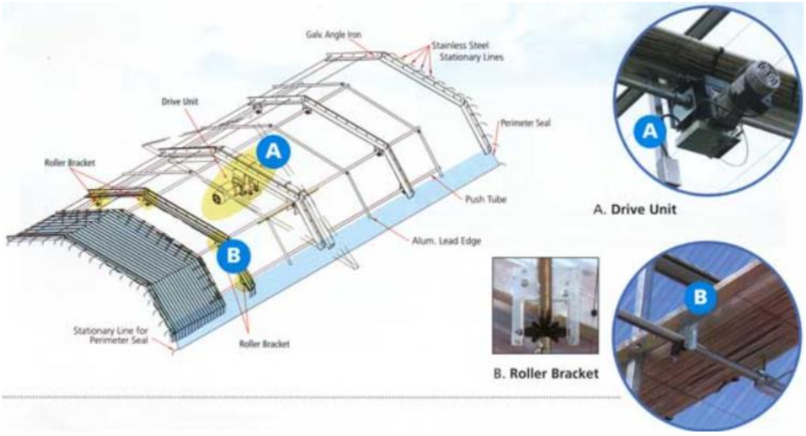

Figure 1.10: Internal shade screen mechanism [22].

A more advanced, innovative, and eco-friendly solution at a prototype level is proposed [23], [24] exploiting renewable energy sources and providing sustainability. This shading system contains semi-transparent photovoltaic (PV) modules, which are parallel oriented to the roof surface (figure 1.11.a) to provide shading and electricity production, or vertically (figure 1.11.b) to allow solar irradiance and sunlight intake.

Figure 1.11: Semi-transparent PV modules positioned parallel (a) or perpendicular (b) to the roof surface [23].

Additional information about more common practices for the industrial use of photovoltaics and shading systems can be found in [9].

1.3.2 Heating system

As mentioned before, a greenhouse's principal operation is to trap heat and maintain high temperature levels. However, solar thermal radiation may be limited due to outdoor weather conditions or greenhouse structures. Simultaneously, heat energy is lost through conduction with the ground and convection with the outside of the greenhouse, when air escapes through windows, doors, ventilation, or the covering materials that are not sufficiently insulated. Because heating systems have a great impact on greenhouse profitability, all lost heat must be replenished efficiently and accurately [12].

Unit heaters and convectors are used to heat air, which is uniformly distributed in the greenhouse through a ventilation system (figure 1.12).

Central heaters are more advanced systems that use various sources (electricity, fossil fuels, geothermal) to heat water in boilers and circulate it through wall pipes coils, overhead pipes, bed-pipe, and pipe rails. In this way, soil, plant, and air temperatures are controlled (figure 1.13) [6].

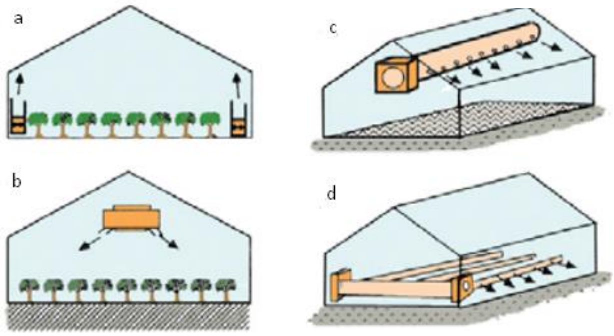

Figure 1.12: Greenhouse heating system using convectors (a), air-installed fan heaters (b), high-installed air channel (c), and low-mounted air channels (d) [25].

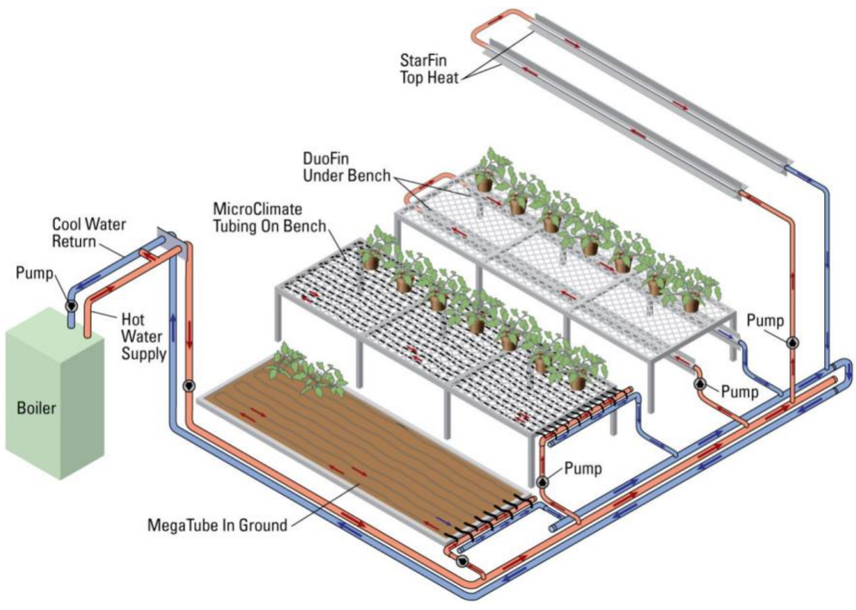

Figure 1.13: Greenhouse central heating system with in-bed pipes, rail pipes, and overhead pipes [26].

Infrared lights are also used in heating systems to compensate for the canopy's heat losses. Infrared light lamps warm only surfaces-plants and soil-, while they do not require auxiliary systems, such as boilers, transmissions, lines, or fans. This is a very simple but efficient system, as it responds instantly to outside temperature changes and does not dry out the air at a meager cost. [27].

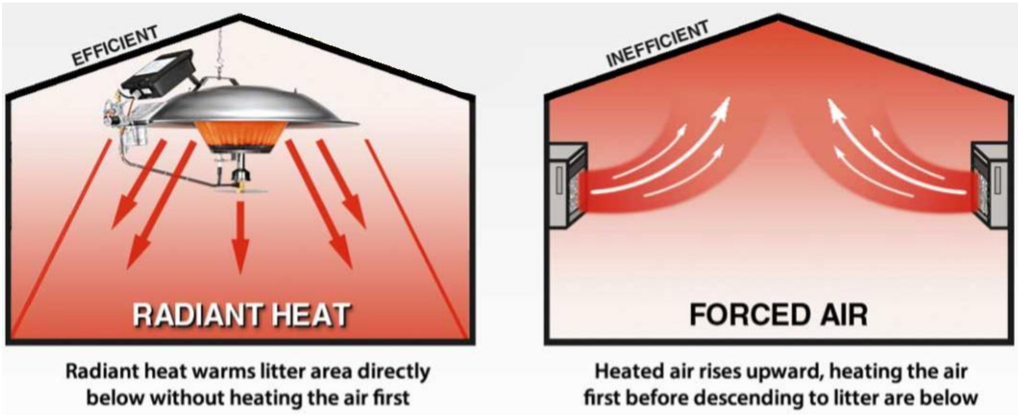

Figure 1.14: Illustration of radiant vs. forced air heat system efficiency [28].

1.3.3 Ventilation system

Air circulation is mainly controlled by a ventilation system, which affects the air temperature, relative humidity, CO_2 concentration and provides a uniform distribution of these characteristics across the greenhouse. Ventilation is divided into two categories: natural and dynamic.

Natural ventilation is based on two physical phenomena: temperature and pressure difference between the inside and outside of the greenhouse. The first one, also known as "thermal buoyancy", results in warm air rising due to its lower density. The second one, called the "wind effect", is causing the outside low-pressure wind to move from the windward to the greenhouse's leeward side. Side vents and windows are commonly used to create the appropriate openings and let the airflow.

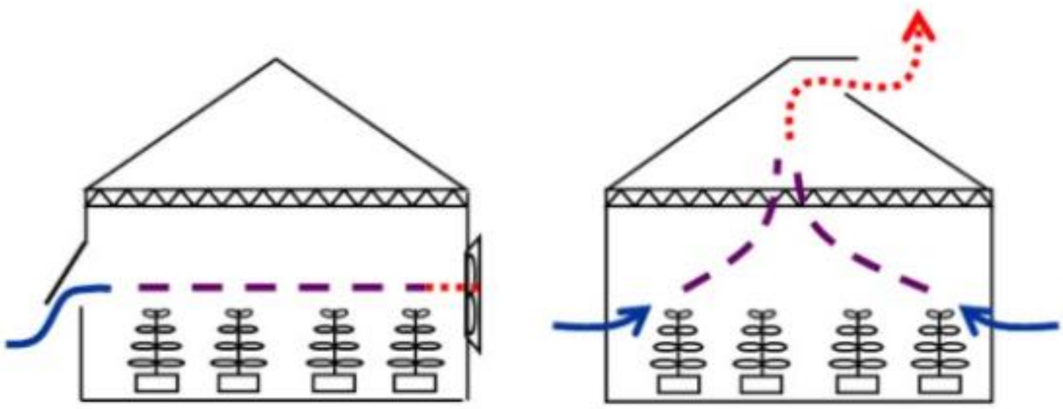

Figure 1.15: Active and Passive air circulation through side vents, fans, and roof windows [29].

Dynamic ventilation is inevitable for large greenhouses because the outside wind is unstable, cannot be controlled, and the inside air needs to be evenly distributed in length and height. Large arrays of fans are installed at the sides and inside the greenhouse to actively intake fresh air, circulate, distribute, and exhaust it. Active ventilation systems are more efficient than passive, but they consume electricity and require more expensive equipment. The use of dynamic ventilation systems is inevitable for industrial use, as it consists of an integrated part of cooling systems, which are detailed below [2], [6], [30].

Figure 1.16: Fans arrays of dynamic greenhouse ventilation system [31].

1.3.4 Cooling system

Apart from heating systems, cooling systems are also necessary to control the temperature and maintain within the optimal boundaries. Shading and ventilation systems consist a part of the cooling system, too; by limiting solar radiation and exchanging indoor hot air with cooler from the outside.

The most effective cooling method to control the temperature and humidity inside a greenhouse is evaporative cooling, which converses sensible heat into latent through sprinklers (misters or foggers) or evaporative pads and fans.

Sprinklers meet this goal by spraying tiny water droplets in the air, which increases the water surface contacting the air. Their low freefall velocity helps them to be distributed across the greenhouse. This method is also used to create a high relative humidity environment, along with cooling inside the greenhouse.

Figure 1.17: Sprinkler cooling system [32].

The **evaporative pad system** consists of a wet pad and a blower, which absorb heat from the air while water runs over the pad. Pads are made of wood, wool, swelling clay minerals, or impregnated cellulose paper and require as large a surface as possible.

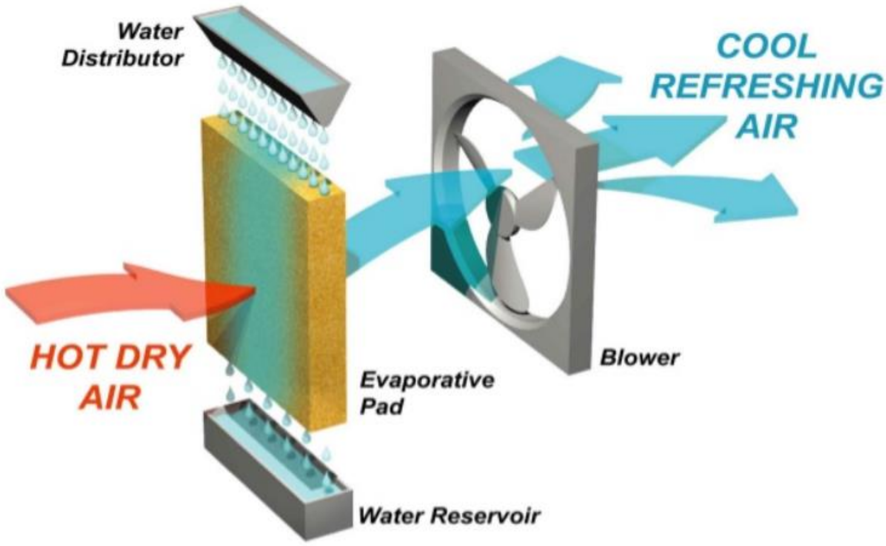

Figure 1.18: Evaporative cooling using a wet pad [33].

The main advantage of sprinklers over evaporative pad systems is the elimination of the need for forced ventilation and airtight enclosure, thanks to the uniformity of conditions throughout the greenhouse that they provide. Although, sprinklers require more expensive installation with higher operation and maintenance costs [2], [6], [30].

1.3.5 Air humidification and dehumidification systems

Air humidification is mainly controlled by shading and cooling systems, which reduce light, temperature and increase water surface contacting the air. In addition, relative humidity is generally maintained at high levels when plants are growing-transpiration- and due to water evaporation from the soil. The combination of these two natural phenomena, which represents the sum of water moving from the ground to the air, is called evapotranspiration.

Nevertheless, there are systems explicitly for air humidification at higher rates, which do not influence the rest parameters of the greenhouse. Steam boilers and heaters create and supply the greenhouse with saturated vapor. High-pressure humidifiers compress air, split water into droplets, and filtrate the dry air [6], [12].
When relative humidity exceeds the optimal range, various dehumidification practices are applied to lower and regulate it. Opening windows and roof ventilators is the simplest method to let the hot air with water vapor escape. Another simple and inexpensive solution is covering the greenhouse interior with anti-dripping films, which eliminate droplets and form thin layers of water running down the sides instead. More elaborate dehumidification methods are condensation on a cold surface, forced ventilation with a heat exchanger, and absorption of hygroscopic dehumidifier [2], [6].

1.3.6 Irrigation and fertigation systems

An irrigation system is responsible for water supply to the plants and soil moisture control. Depending on the greenhouse demands, an irrigation system consists of drip tubes, overhead sprinklers, sub-irrigation containers, or a combination of those methods.

The irrigation delivery system is also cooperating with the fertigation system to meet the crops' nutritional needs, regulate soil pH, and guarantee maximum growth [34].

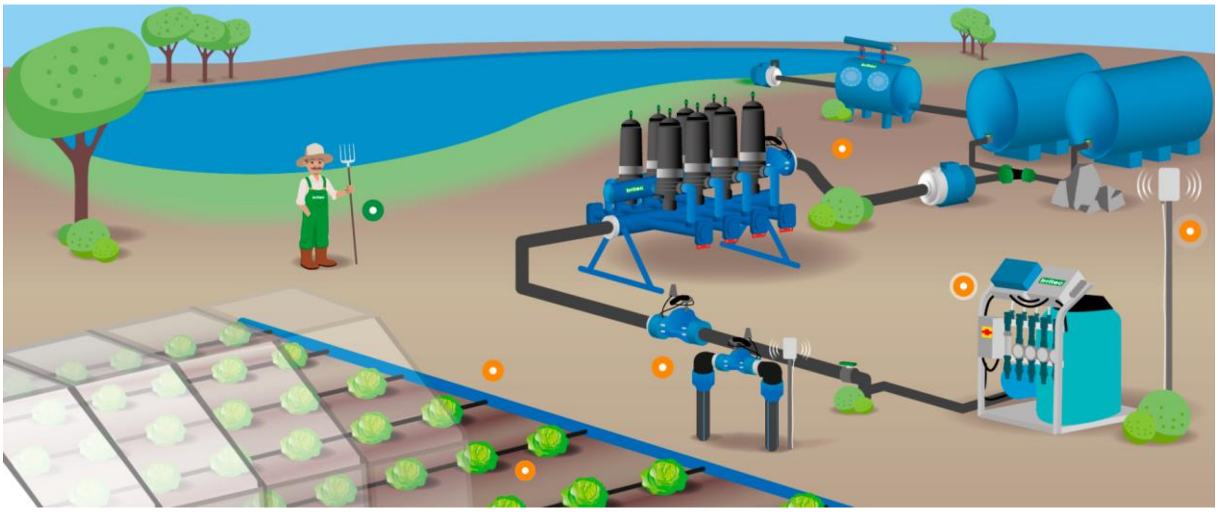

Figure 1.19: Irrigation and fertigation systems illustration [35].

1.3.7 Carbon dioxide - CO_2 enrichment system

Carbon dioxide is essential for the photosynthesis process and consequently plant survival and development. When air ventilation system cannot sufficiently replenish lost CO_2 and maintain it above 400 ppm, or at an industrial level where the recommended CO_2 concentration is between 1,000 ppm and 2,000 ppm, more progressives systems are implemented [12].

An advanced technic of carbon dioxide enrichment consists of liquid CO_2 pumping from containers into the greenhouse.

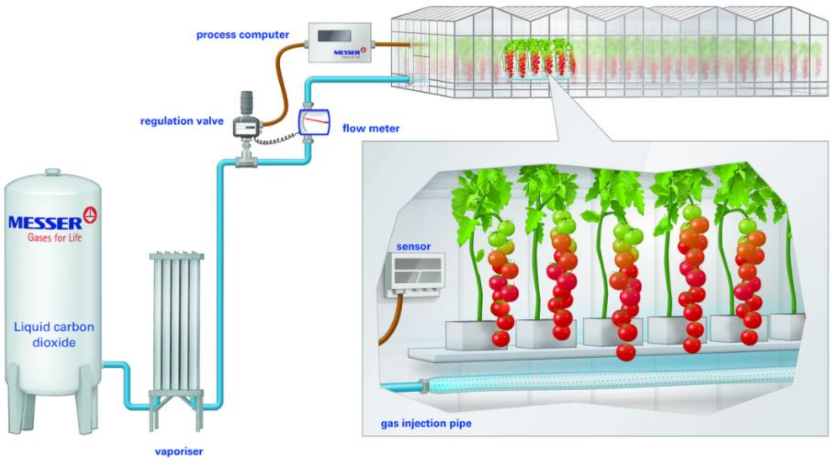

Figure 1.20: CO_2 enrichment system with liquid carbon dioxide [36].

Another method of CO_2 enrichment is achieved as a part of gas emissions through burners. Simultaneously, fossil fuel combustion or burning produces heat, which often is the primary reason for this installation. Thus, CO_2 can only be provided when heat is required [6].

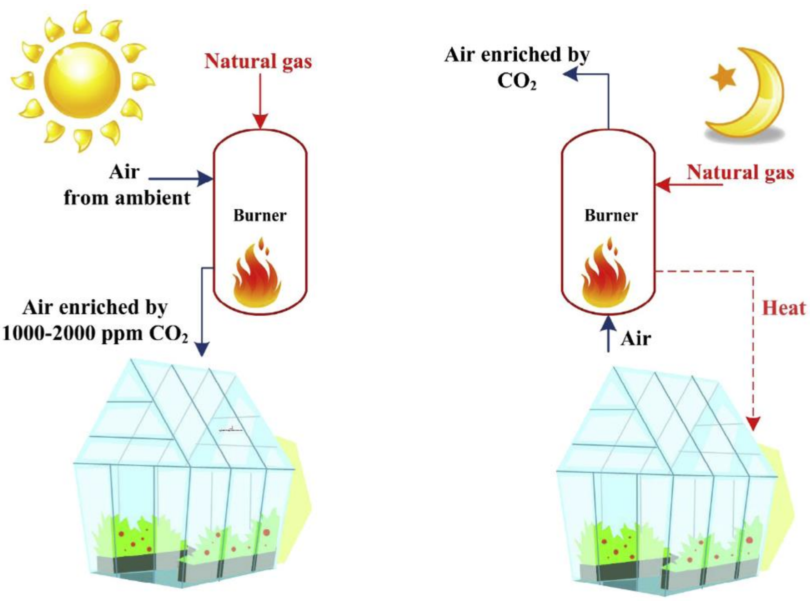

Figure 1.21: Schematic diagram of the conventional natural gas process providing CO_2 and heat in the greenhouse [37].

1.4 Related work

Greenhouses are simple structures. Conversely, but their operation is a complex and challenging process requiring monitoring several variables both inside and outside the greenhouse, visual inspection of the plant growth, as well as controlling various systems. Hand-operated greenhouses are time-consuming, vulnerable to human error and therefore less accurate, reliable, and practical. Fully automatized greenhouses are considered to be a more effective solution for precision farming.

Smart agriculture utilizing Internet of Things technology is an inevitable trend for precision farming. IoT technology allows connecting sensors, applications, and controlling them over a network. Consequently, an IoT-based smart greenhouse system allows monitoring and controlling over a network remotely, with high accuracy and real-time data. The incorporated sensors send triggers provided that parameters fluctuate above or below predefined values and help take proactive measures to protect plants from damage. As a result, higher crop yield and profit are achieved.

Various companies provide precision farming and smart agriculture solutions, including integrated systems of sensors, actuators, controllers, and remote management applications. Generally, the cost of these systems is considerably high and is aimed at exclusively to professionals for industrial use. Therefore, researchers have proceeded to the recreation of similar systems with low-cost materials and free applications, which are more accessible to the broader public.

A literature review of related work is fundamental in order to evaluate each layer, evaluate the advantages and disadvantages, identify and choose the most appropriate parts, which may enable us to optimize our proposed system.

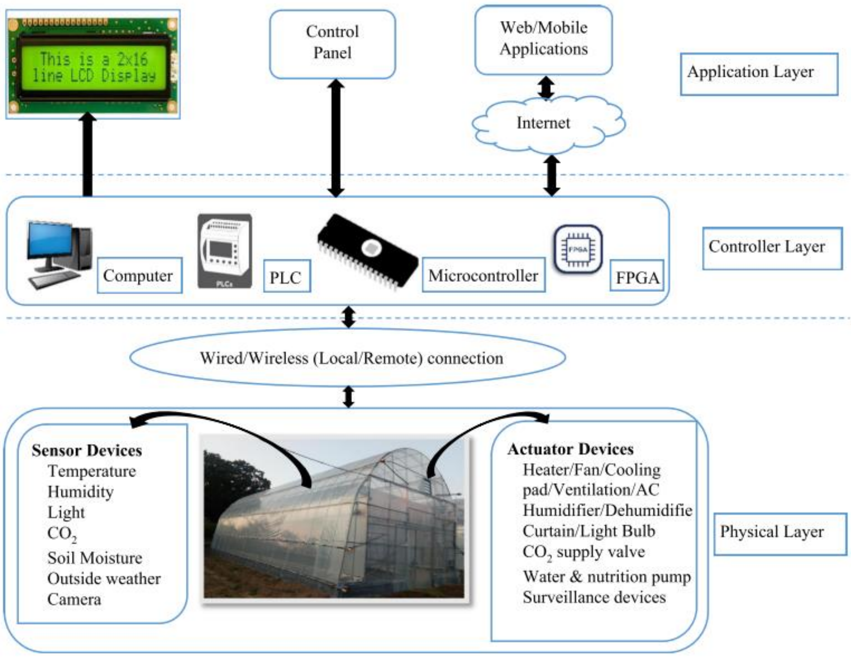

Figure 1.22: Greenhouse control system layers [8].

On the physical layer, a variety of sensors and actuators are implemented on each project. As can be seen in figure 1.23**,** the most common sensors of each category are compared and thus their providing pros and cons in terms of accuracy, sensitivity, range, energy consumption, size, and cost are identified.

Sensors	Sensing domain	Advantages	Disadvantages	References	Online reference
DHT22/A-M2302	Temperature and relative humidity	Low cost, good accuracy (2–5% for 0 to 100% RH and ± 0.5% for − 40 °C to 80°), digital output	Medium operating range, expensive than DHT11	Rodríguez et al. 2017; Zou et al. 2018;	Adafruit DHT22, Adrafruit AM2302
DHT11	"	Low cost, small in size, digital output	Small operating range (20–90% RH, 0–50 °C), low accuracy and precision	Türk et al. 2016; Siddiqui et al. 2018	Adafruit DHT11
MDA 300 Sensor board	"	Multifunction data acquisition board, up to 11 channels,	Specifically designed to work in specific mote	Pahuja et al. 2017	Memsic MDA 300
SHT11	"	High accuracy (± 4% for RH and ± 0.4% for temp.)	Active device, obsolete (replacing by SHT3x series)	Liu and Zhang 2017; Liu et al. 2016; Liao et al. 2017; Ismail et al. 2017	Sensirion humidity-sensors
AM2301	"	Digital output, high sensitivity (0.1% RH and 0.1 °C temp.), good accuracy, range (0–100% RH, − 40 to 80 °C)	Active device, high cost	Chen et al. 2017	Aosong AM2301
SHT71	"	Digital, low power, wide range (0–100% RH, − 40 to 125 °C), quick response time	Obsolete (replacing by SHT85)	Liang-Ying et al. 2015; Ferentinos et al. 2017	Sensirion SHT71
SHT 75	"	Similar to SHT71 but higher accuracy than SHT71	Obsolete (replacing by SHT85)	Ferentinos et al. 2017	Mouser SHT75
HD9009TR	"	Range (− 40 to 80 °C, 0–100% RH), high accuracy, module with transmitter	Output voltage range 0–1 V, medium cost, slow response time	Ferentinos et al. 2017	Deltaohm-9009t
MCH-383SD	Temperature, relative humidity, and CO_2	Real-time data recorder, low power, long battery life	Limited range (0–50 °C, 10–90% RH, 0–4000 ppm),	(Basak et al. 2019)	Lutron
LM35	Temperature	Linear, wide range (− 55 to 150 °C), self-heating very low	Active device	Erazo et al. 2015	ti/lm35
MCP9700A	"	Low cost, low power, linear, wide range of temperature and voltage	Analog, active device, low accuracy (± 2 °C for 0 to 70 °C)	Martinović and Simon 2014	Mouser 9700
SY HS220	Humidity	Low power, small size	Small operating range (30–90% RH), analog, low accuracy	S.Asolkar and S. Bhadade 2014	Tme HS220
DWYER 657	"	Wide range (0 to 100% RH), ± 2% accuracy for 10% to 90% RH range and ± 3% for beyond range, reliable	Medium in size, high cost	Erazo et al. 2015	Dwyer 657
808H5V5	"	Full range (0 to 100% RH), small size	Low accuracy (4%), high responding time	Martinović and Simon 2014	Tme 808
LDR/ Photoresistor	Light	Small, easy, cheap, passive devices	Less sensitive, non-linear, slow response time	S.Asolkar and S. Bhadade 2014; Erazo et al. 2015; Ismail et al. 2017	Components LDR
ISL29010	"	Digital, high sensitivity, low power, adjustable resolution	Variable sensitivity peak at 540 nm, sensitive to visible light only	Zou et al. 2018	bdtic/ISL29010
BH1750	"	Digital, wide range of light intensity with high resolution	Narrow range (almost human eye spectral response)	Liu and Zhang 2017	Mouser BH1750
S505	"	Low power, small size, wireless, wide range 0–100,000 Lux	Low accuracy up to 7%, operating temperature − 5 to 40 °C	Liang-Ying et al. 2015	Easte S505
S1087–01	"	Wide range of spectrum response 320–1100 nm (peak at 960 nm), linear, fast response time	High shunt resistance with temperature	Achouak et al. 2019	Hamamatsu S1087
TGS4161	CO_2 concentration	Low humidity dependency, small size, low power consumption, long life	Low accuracy ± 20% at 1000 ppm CO_2	Martinović and Simon 2014;	Datasheet4u TGS4161
MQ5	"	Wide detecting scope (200 to 10,000 ppm), stable and long life, fast response, and high sensitivity	Less sensitivity to alcohol and smoke	S.Asolkar and S. Bhadade 2014	mouser/Seeed_ 101020056-1217-478
H550	"	Wide range (0–10,000 ppm), NDIR sensing technique, precise (± 30 ppm ± 5%)	Low operating temperature (0–50 °C),	Liang-Ying et al. 2015	Funnykit H-550
AIRSENSE 310	"	Fast response time (< 1 min), accuracy ± 5% or ± 75 ppm whichever higher	Medium range 0 to 5000 ppm, annual drift ± 75 ppm, large size	Erazo et al. 2015	Enercorp 310
FC-22	Soil moisture	Easy to use, based on soil resistivity, good sensitivity	-	Rodríguez et al. 2017	Mouser FC-22
FC-28-B	"	Easy to use, both analog and digital output, threshold adjustment	-	Bajer and Krejcar 2015	Artofcircuits FC-28
FDS100	"	Small size, easy to use, portable, measuring range 0–100% and − 40 to 85 °C, digital, accuracy ± 3% and ± 0.2 °C, fast response	Medium cost, cable length 1.5 m	Zou et al. 2018	FDS-100 Soil sensor
DS18B20	Soil moisture and temperature	High accurate (± 0.5 °C for − 10 to 80 °C), software compatible, operating range − 55 to 100 °C, waterproof	-	Liang-Ying et al. 2015; Chen et al. 2017	Datasheets DS18B20
PT100	"	Accurate and robust, low cost, extendable cable length	-	Martinović and Simon 2014	Soil PT100
TES1333R	Solar radiation	Wide spectral range (400–1100 nm),	Annual drift < ± 2%, operating range 0–50 °C	Taki et al. 2018	Tes 133R
SQ-110	"	Self-powered, rugged, 0 to 800 mV output, spectral range 410 to 655 nm, small size, fast response	High cost	Martinović and Simon 2014	Apogeeinstruments SQ-110
SU-100	UV radiation	Very fast response (< 1 ms), spectral range 250–400 nm, operating environment − 40 to 70 °C and 0 to 100% RH	Analog, not suitable for long term outdoor use	Martinović and Simon 2014	Apogeeinstruments SU-100
MPX4115A	Air pressure	Range (15 to 115 kPa), easy to use, low error (< 1.5% over 0 to 85 °C), durable	Analog, error linearly increase beyond 0 to 85 °C	Martinović and Simon 2014	Nxp MPX4115
AVT Marlin F145-C2	Color image	Color picture, picture size 1280 × 960 pixels, transfer rate 100, 200, 400 Mbit/s, manual and auto gain control, built in image pre-processing	Operating temperature 5 to 45 °C	Yang et al. 2014	Adept AVT
AVT Marlin F145-B2	NIR image	Black and white picture, other similar to AVT Marlin F145-C2	Operating temperature 5 to 45 °C	Yang et al. 2014	Adept F145B
Zytemp TN9	Thermal infrared image	Wide range (− 33 to 220 °C), high accurate, low voltage operation (3/5 V), high resolution, suitable for widely changing environment	Operating temperature − 10 to 50 °C,	Ferentinos et al. 2017	Zytemp TN9

Figure 1.23: Comparison of greenhouse sensors [8].

Some examples of such sensors used on related projects [1], [38]–[41] are given in figure 1.24.

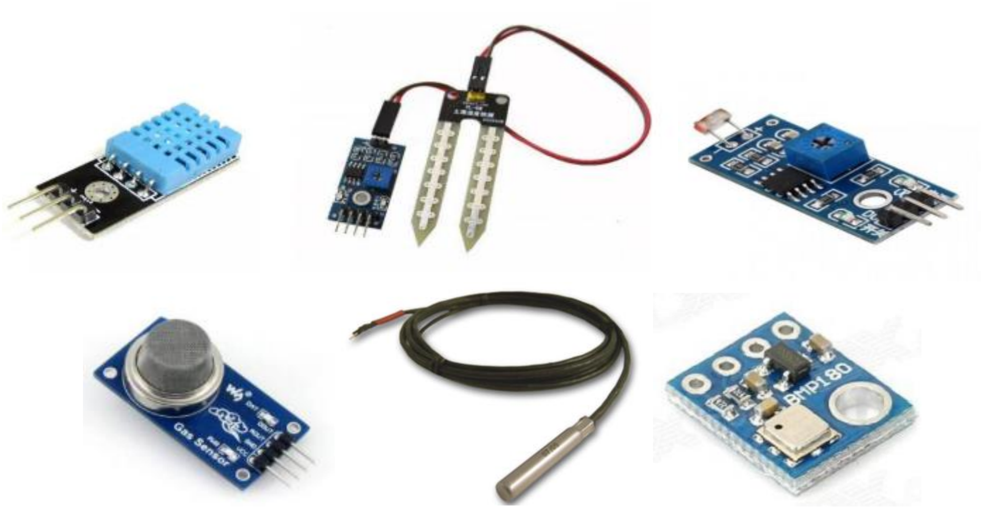

Figure 1.24: (a) DHT11 Air temperature and humidity sensor [1], (b) SN-M114 soil moisture sensor, (c) light-dependent resistor [38], (d) MQ-2 gas sensor [39], (e) DS18B20 soil temperature sensor [40], (f) BMP180 Barometric pressure sensor [41].

Supplementary types of sensors for monitoring rainfall [39], soil pH [38], water tank level [1], movement, fire sources [42], and a VGA camera for plant disease detection [43] are implemented on more advanced systems (see figure 1.25).

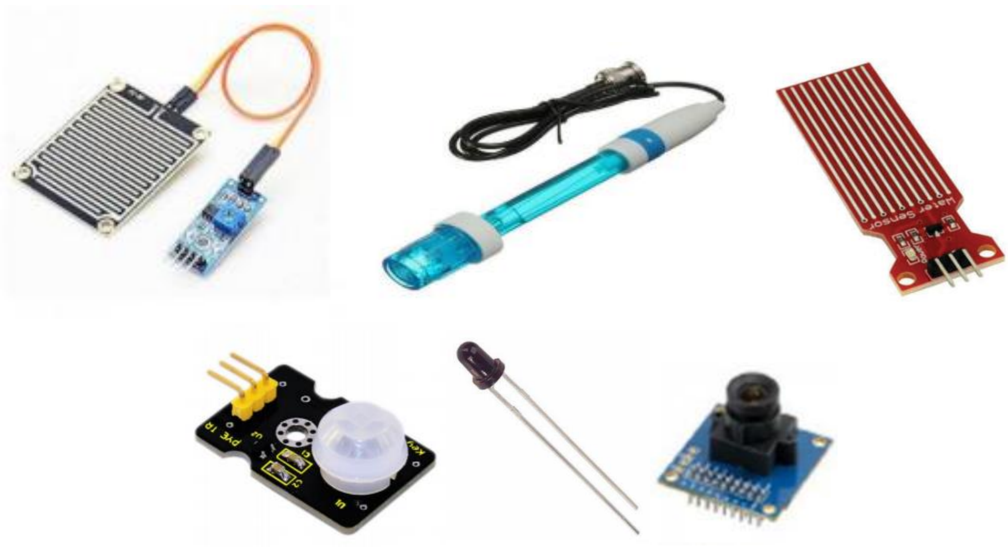

Figure 1.25: (a) Rainfall detection sensor [39], (b) soil pH sensor [38], (c) water level sensor [1], (d) PIR movement sensor, (e) HPTB3b-14D fire sensor [42], (f) VGA camera OV7670 module [43].

In contrast to sensors, installing the same actuators in small-scale greenhouse models is not an easy task. The most widespread devices implemented on related projects to simulate large-scale regulating systems are fans for ventilating and cooling [44]–[46], lamps for enhancing plant growth [44], [45], water pumps [40], [45] or electromechanically operated valves [47] for irrigation.

Figure 1.26: (a) LED strip, (b) fan, (c) water pump [44], (d) electromechanically operated valve [47].

An essential electronic part for almost each actuator is the electrically operated switch-relay. It controls circuits using independent low-power signals. Therefore, microcontrollers can operate any device regardless of its size and energy consumption.

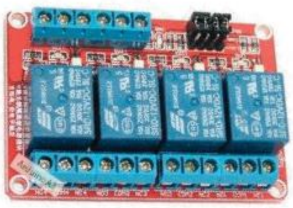

Figure 1.27: Four-channel relay [47].

Controller layer

Microcontrollers are the core of the system. They connect all the devices together and are responsible for reading data from the sensors, analyzing, sending them to the user and controlling the actuators. Various microcontrollers are incorporated depending on the system's requirements, devices' specifications, project's cost and communication technology needed.

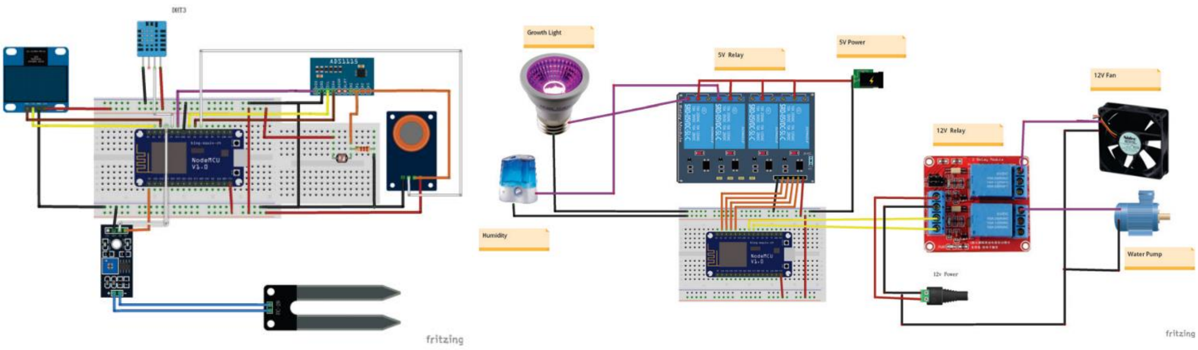

Figure 1.28: Fritzing schematics of sensors (a-left) and actuators (b-right) connecting to microcontroller ESP8266 [44]

Raspberry pi 4 is quite a powerful computer for its size with many GPIO pins, ports, and various connectivity capabilities: ethernet, Wi-Fi, and Bluetooth. Despite its advantages, the cost, the high-power consumption, and the advanced programming required render it unpopular among small-scale projects. However it is effective for executing multiple programs and working as a gateway [1], [48].

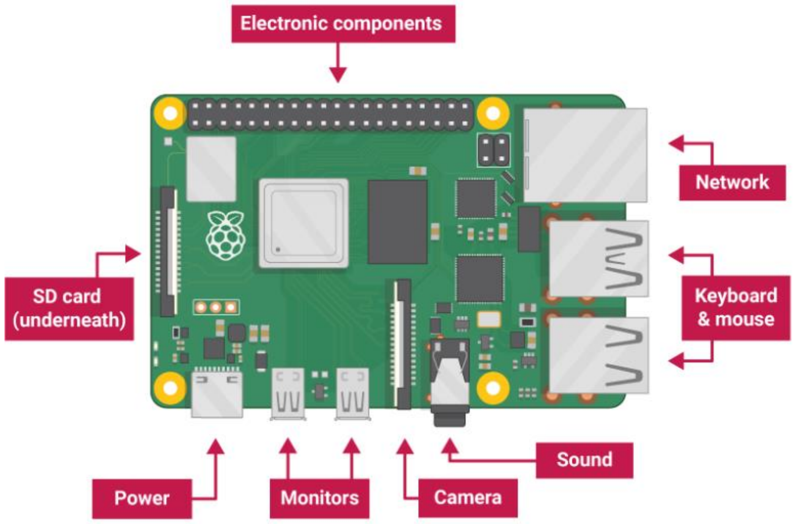

Figure 1.29: Raspberry pi 4 microcontroller [49]

A simpler board than Raspberry is the microcontroller Arduino. It is cheaper, less power consuming, features with a wide range of boards and extension shields to cover each project's needs, and uses the open-source program Arduino IDE. Therefore, the vast majority of projects include it [4], [11], [38]–[40], [43], [45], [50]–[52].

NodeMCU boards are similar to Arduino but more compact. They are smaller, even cheaper, and hence adequate for nodes in Wireless Sensors Networks [44], [47], [53]–[55].

Brand	Board	Processor	Clock Speed	GPIO/PWM	ADC/DAC	Internet	SD card slot	Dimensions	Price($)	Picture
Arduino	Uno wifi	8-bit ATMEGA4809	16 MHz	14/5	6/0	Wifi	-	68*54	45	
	Yun	8-bit ATmega32U4 + 16-bit Atheros AR9331	16 MHz + 400 MHz	20/7	12/0	Ethernet + Wifi	Yes	68*54	60	
NodeMCU	ESP8266	32-bit Xtensa Single-core	80 MHz	17/4	1/0	Wifi	-	49*25	8	
	ESP32	32-bit Xtensa Dual-Core	160 MHz	25/16	16/2	Wifi + BT V4	-	51*28	9	

Figure 1.30: Technical specification comparison of Arduino and NodeMCU microcontrollers [56].

Wireless communication

In a **hardwired sensor system**, all sensor devices and nodes are directly connected via cables to the central system. The connection through electric cables is feasible as long as the central monitoring system is either quite close to it or in the field. The sensor system in question is suitable in small-scale greenhouses when there are fewer parameters to monitor and control. Compared to the wireless systems, the acquisition and transmission of low-power signals generated by various sensors in hardwired systems are more secure and interference-free, without signal loss problems. However, the hardwired system faces several constraints with the increase in the greenhouse size, monitoring parameters, number of sensor nodes, and distance between the terminals. With the increase in distributed sensor networks, traditional star networks cannot handle a large number of sensor nodes. The mesh network, on the contrary, allows communication between each node through the gateway controller, thereby handling thousands of sensor nodes. Therefore, it is not an applicable system in commercial greenhouses. On the contrary, a hybrid system, combination of wired and wireless, satisfactorily makes us of the benefits of both systems [8].

Wireless Sensors Networks are an integral part of precision agriculture, as it provides self-configured and infrastructure-less communication. Wireless communication systems have become the reliable alternative in terms of system simplicity, flexibility, cost-effectiveness, and remote communication. The ease of installing and relocating sensor nodes is critical for a heterogeneous and extensive system. Each project meets different requirements, and each technology provides its own unique characteristics. Therefore, it is necessary to compare the benefits and drawbacks of each wireless communication technology, which detailed in figure 1.31 [8].

Specifications	ZigBee	Bluetooth	Wibree	Wi-Fi	LoRa	Sigfox	NB-IoT	Mobile network
Frequency band	2.4 GHz	2.4 GHz	2.4 GHz	2.4 GHz	Unlicensed ISM	Unlicensed ISM	Licensed LTE	Telecom license band
Range	0.03–1.6 km	10–100 m	Up to 3 m	30–45 m	3 km	10–40 km	1–10 km	No limit
Data rate	250 kbps	1 mbps	1 mbps	11–54 mbps	0.3–50 kbps	100 bps	200 kbps	0.3–100 mbps
Power consumption	Low	Medium	Low	High	Medium	Low	High	Medium
Cost	Low	Low	Low	High	Low	Low	Low	Medium
Modulation/protocol	DSSS	CSMA/CA	FHSS	DSSS/CCK	CSS	BPSK	QPSK	CDMA
Security	128 bit	64 bit	128 bit	128 bit	128 bit	Unique device ID	128 bit	128 bit

Where *DSSS*: direct-sequence spread spectrum, *CSMA/CA*: carrier-sense multiple access with collision avoidance, *FHSS*: frequency-hopping spread spectrum, *DSSS/CCK*: direct-sequence spread spectrum/complementary code keying, *CSS*: chirp spread spectrum, *BPSK*: binary phase-shift keying, *QPSK*: quadrature phase-shift keying, *CDMA*: code-division multiple access, *ISM band*: industrial, scientific and medical band, *BTS*: base transceiver station

Figure 1.31: Technical comparison of wireless communication technologies in WSNs [8].

ZigBee is the most widespread technology in WSNs due to its low cost, low power consumption, and medium-range connection. Nevertheless, it requires advanced programming skills, additional parts to establish a connection, and has low data rate transfer [8], [46], [57].

Wi-Fi antennas are usually integrated into most microcontrollers. Wi-Fi provides high connection speeds in WLANs. Therefore, the constitute a common practice means for connecting to the internet, as used in many projects [44], [47], [53]–[55].

On the contrary, **mobile network** is a special case because requires no network equipment and has no distance limitations. Its advancing technology, like 5G, offers great speeds and extensive coverage area by using a specific adaptor [41].

Application layer

Remote management technology is a convenient and essential feature for Internet of Things applications in modern agriculture, which provides long-distance control and continuous monitoring. Companies offer integrated monitoring systems that, besides microcontrollers, sensors, and gateway devices, frequently include remote management software.

Most experienced researchers have created their own applications in their projects based on their goals and needs [1], [46], [53], [54], [58]. However, IoT project-builder applications are available online such as ThingSpeak, Blynk, and Cayenne with numerous features and possibilities.

Both ThingSpeak and Blynk IoT platforms were included in the greenhouse managing project of [44]. **ThingSpeak** is an IoT analytics platform service that allows us to aggregate, visualize, and analyze live data streams in the cloud figure 1.32 (a). **Blynk** is a hardware-agnostic IoT platform with white-label mobile apps, private clouds, device management, data analytics, and machine learning. It can also display the environmental parameters (air humidity, soil moisture, temperature, CO_2 concentration) received from microcontrollers (see figure 1.32 (b)) and control greenhouse's equipment-relay modules (fans, light growing system, water pump) (see figure 1.32 (c)).

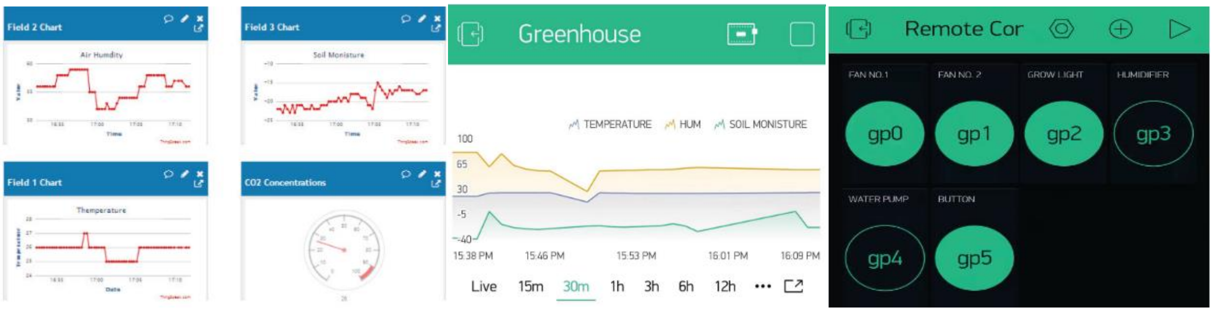

Figure 1.32: (a) Data visualization on ThingSpeak, (b) data visualization, and (c) equipment control using Blynk [44].

CHAPTER 2

Chapter 2: Smart greenhouse design

2.1 Introduction

The design and implementation of an integrated smart greenhouse control system on an experimental small-scale greenhouse is central to this thesis. Initially, the greenhouse equipment and their technical specifications are examined, including the Hobolink, Meazon, Agenso, proposed sensors and the proposed actuators. The electric circuits of the proposed sensors and actuators are explained in more detail. The provided schematics of the electric circuits were created using the Fritzing software. Furthermore, the algorithms executed by the greenhouse microcontrollers, which monitor and control the greenhouse, are presented. The microcontrollers run codes in Arduino language, similar to C++ language. Finally, the features of Cayenne IoT project builder used to remotely check the conditions of the greenhouse micro-climate and the status of the actuators are described.

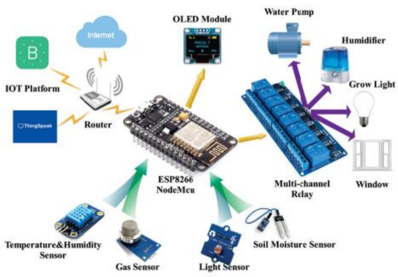

Figure 2.1: Greenhouse micro-climate control system [44].

2.2 Smart greenhouse equipment

There are four integrated systems installed in the experimental greenhouse model, i.e. Hobolink, Meazon, Agenso and a proposed greenhouse micro-climate monitoring system. All four systems are thoroughly detailed below.

Hobolink system includes a data logger, three relay modules, a wireless sensor manager, a solar radiation shield and sensors of solar radiation, PA radiation, UV, soil moisture, temperature-soil moisture-soil conductivity, multi-depth, CO_2-CO, rainfall, temperature, and relative humidity.

Meazon system consists of a gateway, three remotely controlled plugs, a temperature-relative humidity and an air quality-temperature-relative humidity sensor.

There are two Agenso stations with a base station, a weather station, which measures temperature, relative humidity, air pressure, wind speed, wind direction, wind gust, solar radiation, UV and rainfall, a soil temperature sensor and a soil moisture sensor.

The proposed greenhouse micro-climate monitoring system features two microcontrollers and sensors which monitor temperature, relative humidity, soil temperature and moisture, CO_2 and CO concentrations, TVOC level, atmospheric pressure and altitude.

2.2.1 Hobolink

HOBO® RX3002 Wi-Fi remote monitoring station data logger

RX3002 station is the primary component of the cost-effective and scalable HOBOnet Field Monitoring System for crop management, environmental research and greenhouse operations. It provides continuous logging for a broad range of energy and weather monitoring applications with up to ten smart sensors, optional analog sensors, water level sensors, relay modules, and wireless sensor motes. Data from RX3002 station is transferred at regular connection intervals to HOBOlink® web-based software through Wi-Fi, where we can check the latest conditions, view graphs, configure sensors and alarms, set up a dashboard, download data, or schedule data delivery via email or FTP. Inside its weatherproof enclosure, this durable station has a built-in LCD screen to check the current system configuration and status, start and stop logging, add and remove smart sensors, and connect to HOBOlink on demand. Up to three individual relays can be activated on the optional relay module, while the optional analog module has four analog inputs which support excitation power, scaling, and statistics measurements. An optional RXW Manager module is also available for the station to set up the HOBOnet Wireless Sensor Network, which can support up to 50 motes. All easy-to-install modules can be configured with HOBOlink.

Operating Range	-40° to 60°C (-40° to 140°F); no remote communications for battery voltage less than 3.9 V DC
Smart Sensor Connectors	10
Smart Sensor Network Cable Length	100 m (328 ft) maximum
Smart Sensor Data Channels	Maximum of 15 (some smart sensors use more than one data channel; see sensor manual for details)
Module Slots	2
Logging Rate	1 second (RX3001 and RX3002) or 1 minute (RX3003 and RX3004) to 18 hours
Time Accuracy	±8 seconds per month in 0° to 40°C (32°F to 104°F) range; ±30 seconds per month in -40° to 60°C (-40° to 140°F) range
Battery Type/Power Source	4 Volt, 10 AHr, rechargeable sealed lead-acid; external power required using one of these options: AC power adapter (AC-U30), solar panel (SOLAR-xW), or external power source 5 V DC to 17 V DC with external DC power cable (CABLE-RX-PWR)
Rechargeable Battery Service Life	Typical 3–5 years when operated in the temperature range -20° to 40°C (-4°F to 104°F); operation outside this range will reduce the battery service life
Memory	32 MB, 2 million measurements, continuous logging
Alarm Notification Latency	Logging interval plus 2–4 minutes, typical
Enclosure Access	Hinged door secured by two latches with eyelets for use with user-supplied padlocks
LCD	LCD is visible from 0° to 50°C (32° to 122°F); the LCD may react slowly or go blank in temperatures outside this range
Materials	Outer enclosure: Polycarbonate/PBT blend with stainless steel hinge pins and brass inserts; Inner enclosure: Polycarbonate; Gaskets: Silicone rubber; Cable channel: EPDM rubber; Cable opening cover: Aluminum with ABS plastic thumb screws; U-Bolts: Steel with zinc dichromate finish
Size	18.6 x 18.1 x 11.8 cm (7.3 x 7.1 x 4.7 in.); see diagrams on next page
Weight	2.2 kg (4.85 lb)
Mounting	3.8 cm (1.5 inch) mast or wall mount
Environmental Rating	Weatherproof enclosure, NEMA 4X (requires proper installation of cable channel system)
CE	The CE Marking identifies this product as complying with all relevant directives in the European Union (EU)
FC	See last page

Figure 2.2: RX3002 Wi-Fi remote monitoring station specifications [59].

RX3002 relay module / HOBO RXMOD-R1

HOBO RXMOD-R1 Relay Module allows for up to three individual relays to be activated or pulsed in response to alarms. Each relay contact closure can be configured as normally open or normally closed through HOBOlink.

Relays	Three independent relays
Alarm Output Relays	Each relay contact closure can be configured as normally open or normally closed. Relays can be activated or pulsed in response to alarms.
Voltage	30 V max
Current	1 Amp max

Figure 2.3: Relay module HOBO RXMOD-R1 specifications [59].

HOBO RX3002 RXW Manager / RXMOD-RXW-868

RXW Manager module transmits data wirelessly from sensor motes across the network to RX3002 station and then uploads them to HOBOlink® web-based software. HOBOlink can be used to monitor the network, view graphs, set up alarms, download data, and more.

Operating Temperature Range	-25° to 60°C (-13° to 140°F)
Radio Power	12.6 mW (+11 dBm) non-adjustable
Transmission Range	Reliable connection to 457.2 m (1,500 ft) line of sight at 1.8 m (6 ft) high Reliable connection to 609.6 m (2,000 ft) line of sight at 3 m (10 ft) high
Wireless Data Standard	IEEE 802.15.4
Radio Operating Frequencies	RXMOD-RXW-900: 904–924 MHz RXMOD-RXW-868: 866.5 MHz RXMOD-RXW-921: 921 MHz RXMOD-RXW-922: 916–924 MHz
Modulation Employed	OQPSK (Offset Quadrature Phase Shift Keying)
Data Rate	Up to 250 kbps, non-adjustable
Duty Cycle	<1%
Maximum Number of Motes	Up to 50 wireless sensors or 336 data channels per one HOBO RX station
Power Source	Powered by the RX3000 station
Dimensions	Mote: 16.2 x 8.59 x 4.14 cm (6.38 x 3.38 x 1.63 inches) Cable length: 2 m (6.56 ft)
Weight	Mote: 159 g (5.62 oz)
Materials	Mote: PCPBT, silicone rubber seal
Environmental Rating	Mote: IP67, NEMA 6

Figure 2.4: HOBOnet wireless sensor network manager RXMOD-RXW-868 specifications [59].

Pyranometers

<u>HOBOnet PAR sensor / RXW-LIA-868</u>

HOBOnet wireless sensors communicate data directly to HOBO RX3002 and then upload it to HOBOlink® web-based software. Each sensor is preconfigured and ready to deploy, and data is accessed through HOBOlink, Onset's innovative cloud-based software platform. It merely requires a button-push to join the HOBOnet wireless network. Lastly, each wireless sensor includes onboard memory to ensure no data loss and photovoltaic solar panel modules to recharge their batteries.

HOBOnet Wireless Photosynthetic Active Radiation (PAR) Sensor measures light intensity for frequencies relevant to photosynthesis.

Sensor

Measurement Range	0 to 2500 mol/m2/sec, wavelengths 400 to 700 nm
Accuracy	±5 mol/m2/sec or ± 5%, whichever is greater in sunlight; Additional temperature induced error ±0.75 mol/m2/sec/°C from 25°C (0.42 mol/m2/sec/°F from 77°F)
Angular Accuracy	Cosine corrected 0 to 80 degrees from vertical; Azimuth Error <2% error at 45 degrees from vertical, 360 degree rotation
Resolution	2.5 mol/m2/sec
Drift	<±2% per year

Wireless Mote

Operating Temperature Range	-25° to 60°C (-13° to 140°F) with rechargeable batteries -40 to 70°C (-40 to 158°F) with lithium batteries
Radio Power	12.6 mW (+11 dBm) non-adjustable
Transmission Range	Reliable connection to 457.2 m (1,500 ft) line of sight at 1.8 m (6 ft) high Reliable connection to 609.6 m (2,000 ft) line of sight at 3 m (10 ft) high
Wireless Data Standard	IEEE 802.15.4
Radio Operating Frequencies	RXW-LIA-900: 904–924 MHz RXW-LIA-868: 866.5 MHz RXW-LIA-922: 916–924 MHz RXW-LIA-921: 921 MHz
Modulation Employed	OQPSK (Offset Quadrature Phase Shift Keying)
Data Rate	Up to 250 kbps, non-adjustable
Duty Cycle	<1%
Maximum Number of Motes	Up to 50 wireless sensors or 336 data channels per one HOBO RX station
Logging Rate	1 minute to 18 hours
Number of Data Channels	2
Battery Type/ Power Source	Two AA 1.2V rechargeable NiMH batteries, powered by built-in solar panel or two AA 1.5 V lithium batteries for operating conditions of -40 to 70°C (-40 to 158°F)
Battery Life	With NiMH batteries: Typical 3–5 years when operated in the temperature range -20° to 40°C (-4°F to 104°F) and positioned toward the sun (see Deployment and Mounting), operation outside this range will reduce the battery service life With lithium batteries: 1 year, typical use
Memory	16 MB
Dimensions	Sensor: 4.1 cm height x 3.2 cm diameter (1.61 x 1.26 inches) Cable length: 2 m (6.56 ft) Mote: 16.2 x 8.59 x 4.14 cm (6.38 x 3.38 x 1.63 inches)
Weight	Sensor and cable: 109 g (3.85 oz) Mote: 223 g (7.87 oz)
Materials	Sensor: Anodized aluminum housing with acrylic diffuser and O-ring seal Mote: PCPBT, silicone rubber seal
Environmental Rating	Sensor: Weatherproof Mote: IP67, NEMA 6

Figure 2.5: PAR sensor RXW-LIA-868 and wireless mote specifications [59].

RXW Silicon Pyranometer Sensor (RXW-LIB-868)

HOBOnet Wireless Solar Radiation (Silicon Pyranometer) Sensor is calibrated to measure light intensity for frequencies relevant for solar radiation.

This sensor uses a silicon photodiode to measure solar power per unit area (watts per square meter). Silicon photodiodes are not ideal for use as solar radiation sensors, and the photodiode in this silicon pyranometer is no exception (see figure 2.6). An ideal pyranometer has an equal spectral response from 280 to 2800 nm. However, when appropriately calibrated and used correctly, the silicon pyranometer sensor should perform well in most situations.

The sensor is calibrated for use in sunlight (an Eppley Precision Spectral Pyranometer is used as a reference standard). Accordingly, if the sensor is used under natural sunlight, the measurement errors will be small. Note that significant errors may result from using the sensor under artificial light, within plant canopies, greenhouses, or any other conditions where the spectral content differs from sunlight.

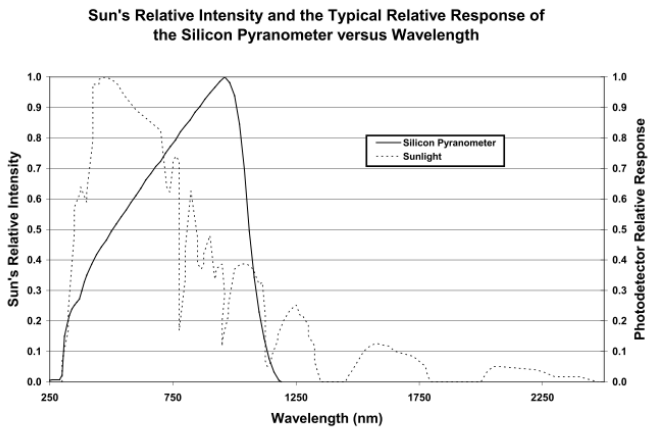

Figure 2.6: Silicon pyranometer sensor response curve [59].

Sensor	
Measurement Range	0 to 1280 W/m2
Spectral Range	300 to 1100 nm
Accuracy	Typically within ±10 W/m2 or ±5%, whichever is greater in sunlight; Additional temperature induced error ±0.38 W/m2/°C from 25°C (0.21 W/m2/°F from 77°F)
Angular Accuracy	Cosine corrected 0 to 80 degrees from vertical (see Plot B); Azimuth Error <±2% error at 45 degrees from vertical, 360 degree rotation
Resolution	1.25 W/m2
Drift	<±2% per year

Figure 2.7: Silicon pyranometer sensor RXW-LIB-868 specifications [59].

Solar Radiation (Silicon Pyranometer) Smart Sensor / HOBO® S-LIA-M003 Sensor

Silicon pyranometer HOBO S-LIA-M003 measures light intensity for frequencies relevant to photosynthesis (PAR). It has the same sensor as RXW-LIA-868 but does not include the wireless mote and connects wired to the RX3002 station.

Figure 2.8: Silicon pyranometer HOBO S-LIA-M003 [59].

Solar Radiation (Silicon Pyranometer) Smart Sensor / HOBO® S-LIB-M003 Sensor

Silicon pyranometer HOBO S-LIB-M003 measures light levels. It has the same sensor as RXW-LIB-868 but does not include the wireless mote and connects directly to the RX3002 station.

Figure 2.9: Silicon pyranometer HOBO S-LIB-M003 [59].

RK200-07 UV Radiation Sensor

RK200-07 UV Radiation Sensor is a precision instrument used to measure the atmosphere of the sun's ultraviolet radiation (UVA & UVB), supporting the product-related information acquisition instrument use can provide public concern: the UV index, UV erythema measurement, on the health effects of the UV and UV special biology and chemistry, highly meteorology, industry, construction, medical attention, are widely used in the exposure caused erythema dose, integrated environment ecological effect, the study of climate change and ultraviolet radiation monitoring and forecast.

Item	SPECIFICATIONS
Spectral range	280 ~ 400nm
Supply	5V,12-24VDC
Range	0-200W/m2, 0-200uW/cm2(only for 0-2V output), 0-15UV index
Output	0-2V,4-20mA(2 wires),0-5V,RS485
Accuracy	±5% rdg
Response time	≤1s
Cosine correction	≤±4%(Solar elevation angle=30°)
Non-linear	≤±3%
Temperature effect	±0.08%/°C
Stability	≤±2%/year
perating Temperature	-40°C-+85°C
Ingress Protection	IP65
Weight(unpacked)	150g
Shell material	Aluminum alloy
Storage Condition	10°C-60°C@20%-90%RH

Figure 2.10: RK200-07 UV radiation sensor specifications [60].

Soil moisture sensors

RXW-SMD-868 / RXW Soil moisture 10HS sensor

HOBOnet Wireless Soil Moisture Sensor integrates the field proven ECH_2O™ 10HS sensor and provides readings directly in volumetric water content. The 10cm probes measure soil moisture over a larger soil volume, helping to average out any soil variability. The sensor's high-frequency design minimizes sensitivity to salinity and textural effects and gives it a wide measurement range.

Figure 2.11: Soil moisture sensor 10HS / RXW-SMD-868 [59].

HOBO® RXW-SMC-868 Sensor / HOBOnet Soil Moisture EC-5 Sensor

HOBOnet Wireless Soil Moisture Sensor integrates the field proven ECH2O™ EC5 Sensor and provides readings directly in volumetric water content. The sensor's high-frequency design minimizes sensitivity to salinity and textural effects and gives it a wide measurement range.

Figure 2.12: Soil moisture sensor EC-5 / RXW-SMC-868 [59].

Note 1: (RXW-SMC and RXW-SMD) Given the nature of the sensors design operating frequency, the system has inherent susceptibilities to Radio Frequency signals. When subjected to certain RFI environments, such as those outlined in IEC 61000-4-3 and IEC 61000-4-6, the accuracy specification is reduced to 0.061 m /m. The system-level accuracy will be particularly affected when placed in an electric field of 3 V/m or greater in the 70 MHz range. RFI mitigation practices and physical deployment changes may reduce the system's susceptibility.

Note 2: (RXW-SMC and RXW-SMD) This is a system-level accuracy specification and is comprised of the probe’s accuracy of ±0.03 m /m typical (±0.02 m /m soil specific) plus the mote accuracy of ±0.003 m/m at 25°C. There are other temperature accuracy deviations of ±0.003 m/m/°C maximum for the probe across operating temperature environments, typical <0.001 m/m/°C. (The temperature dependence of the mote is negligible.)

	RXW-SMC-xxx	RXW-SMD-xxx
Measurement Range	In soil: 0 to 0.550 m /m (volumetric water content)	In soil: 0 to 0.570 m /m (volumetric water content)
Extended Range	-0.401 to 2.574 m /m ; see Note 1	-0.659 to 0.6026 m /m ; see Note 1
Accuracy	±0.031 m /m (±3.1%) typical 0 to 50°C (32° to 122°F) for mineral soils up to 8 dS/m and ±0.020 m /m (±2%) with soil specific calibration; see Notes 2 and 3	±0.033 m /m (±3.3%) typical 0 to 50°C (32° to 122°F) for mineral soils up to 10 dS/m and ±0.020 m /m (±2%) with soil specific calibration; see Notes 4 and 5
Resolution	0.0007 m /m (0.07%)	0.0008 m /m (0.08%)
Volume of Influence	0.3 liters (10.14 oz)	1 liter (33.81 oz)
Sensor Frequency	70 MHz	70 MHz
METER ECH2O Probe Part No.	EC-5	10HS
Sensor Operating Temperature Range	0° to 50°C (32° to 122°F). Although the sensor probe and cable can safely operate at below-freezing temperatures (to -40°C/F), the soil moisture data collected at these extreme temperatures is outside of the sensor's accurate measurement range.	0° to 50°C (32° to 122°F). Although the sensor probe and cable can safely operate at below-freezing temperatures (to -40°C/F), the soil moisture data collected at these extreme temperatures is outside of the sensor's accurate measurement range. Extended temperatures above 50°C (122°F) will decrease mote battery life.
Wireless Mote		
Operating Temperature Range	-25° to 60°C (-13° to 140°F) with rechargeable batteries -40° to 70°C (-40° to 158°F) with lithium batteries	
Radio Power	12.6 mW (+11 dBm) non-adjustable	
Transmission Range	Reliable connection to 457.2 m (1,500 ft) line of sight at 1.8 m (6 ft) high Reliable connection to 609.6 m (2,000 ft) line of sight at 3 m (10 ft) high	
Wireless Data Standard	IEEE 802.15.4	
Radio Operating Frequencies	RXW-SMC-900 and RXW-SMD-900: 904–924 MHz RXW-SMC-868 and RXW-SMD-868: 866.5 MHz RXW-SMC-921 and RXW-SMD-921: 921 MHz RXW-SMC-922 and RXW-SMD-922: 916–924 MHz	
Modulation Employed	OQPSK (Offset Quadrature Phase Shift Keying)	
Data Rate	Up to 250 kbps, non-adjustable	
Duty Cycle	<1%	
Maximum Number of Motes	Up to 50 wireless sensors or 336 data channels per one HOBO RX station	
Logging Rate	1 minute to 18 hours	
Number of Data Channels	2	
Battery Type/ Power Source	Two AA 1.2V rechargeable NiMH batteries, powered by built-in solar panel or two AA 1.5 V lithium batteries for operating conditions of -40° to 70°C (-40° to 158°F)	
Battery Life	With NiMH batteries: Typical 3–5 years when operated in the temperature range -20° to 40°C (-4°F to 104°F) and positioned toward the sun (see Deployment and Mounting), operation outside this range will reduce the battery service life With lithium batteries: 1 year, typical use	
Memory	16 MB	
Dimensions	RXW-SMC-xxx soil probe: 89 x 15 x 1.5 mm (3.5 x 0.62 x 0.06 in.) RXW-SMD-xxx soil probe: 160 x 32 x 2 mm (6.5 x 1.25 x 0.08 in.) Cable length: 5 m (16.4 ft) Mote: 16.2 x 8.59 x 4.14 cm (6.38 x 3.38 x 1.63 inches)	
Weight	RXW-SMC-xxx sensor and cable: 180 grams (6.3 oz) RXW-SMD-xxx sensor and cable: 190 grams (6.7 oz) Mote: 223 g (7.87 oz)	
Materials	Sensor: Weatherproof Mote: PCPBT, silicone rubber seal	

Figure 2.13: Soil moisture sensors HOBO RXW-SMD and RXW-SMC specifications [59].

Soil moisture, temperature, and electrical conductivity sensor / HOBO® RXW-T12-868 Sensor

HOBOnet T12 is a wireless sensor that works with the HOBOnet system to provide advanced soil moisture measurements (volumetric water content) with better accuracy and precision and measure soil temperature and electrical conductivity. Designed to withstand harsh environmental conditions, these durable sensors last up to 10 years. Sharpened stainless-steel probe tips make installation easy, even in hard soil, and a large volume of influence provides more accurate results. A trademark 70MHz frequency capacitance technology minimizes salinity and textural effects. Additionally, the verification clip offers a convenient way to confirm the operation and soil-moisture accuracy of HOBOnet T12 sensors. Attaching this clip to a sensor provides a known soil moisture level for verifying measurement accuracy without testing the sensor in actual soils, which requires typically weighing soil samples and drying them in an oven.

Soil Moisture: Volumetric Water Content (VWC)	
Measurement Range*	0.00 to 0.70 m /m in mineral soils
Accuracy	±0.030 m /m (±3%) typical from 0 to 50°C (32 to 122°F); ±0.020 m /m (±2%) with soil specific calibration
Resolution	0.001 m /m
Dielectric Measurement Frequency	70 MHz
Temperature**	
Measurement Range	-40 to 60°C (-40 to 140°F)
Accuracy	±0.5°C (0.9°F) from -40 to 0°C (-40 to 32°F) ±0.3°C (0.54°F) from 0 to 60°C (32 to 140°F)
Resolution	0.1°C (0.18°F)
Bulk Electrical Conductivity (EC)	
Measurement Range	0 to 20 dS/m (bulk)
Accuracy	±5% of reading + 0.01 dS/m from 0 to 10 dS/m ±8% of reading from 10 to 20 dS/m
Resolution	0.001 dS/m
Wireless Mote	
Operating Temperature Range	Sensor: -40 to 60°C (-40 to 140°F)
Radio Power	12.6 mW (+11 dBm) non-adjustable
Transmission Range	Reliable connection to 457.2 m (1,500 ft) line of sight at 1.8 m (6 ft) high Reliable connection to 609.6 m (2,000 ft) line of sight at 3 m (10 ft) high
Wireless Data Standard	IEEE 802.15.4
Radio Operating Frequencies	RXW-T12-900: 904–924 MHz RXW-T12-868: 866.5 MHz
Modulation Employed	OQPSK (Offset Quadrature Phase Shift Keying)
Data Rate	Up to 250 kbps, non-adjustable
Duty Cycle	<1%
Maximum Number of Motes	Up to 50 wireless sensors or 336 data channels per one HOBO RX station
Logging Rate	1 minute to 18 hours
Number of Data Channels	4
Dimensions	Sensor: 7.47 x 9.4 x 2.39 cm (2.94 x 3.7 x 0.94 inches) Sensor needle length: 5.4 cm (2.13 inches) Sensor needle diameter: 0.32 cm (0.13 inches) Cable length: 5 m (16.4 ft) Mote: 16.2 x 8.59 x 4.14 cm (6.38 x 3.38 x 1.63 inches)
Weight	RXW-T12-xxx sensor and cable: 245 grams (8.64 oz) Mote: 223 g (7.87 oz)
Materials	Sensor: ASA plastic body with polyurethane epoxy filling and stainless steel pins Cable: PVC, UV resistant and rodent repellent Mote: PCPBT, silicone rubber seal

Figure 2.14: HOBO® RXW-T12-868 sensor specifications [59].

HOBO® RXW-GP3-868 Sensor / HOBOnet multi-depth soil moisture and temperature sensor

HOBOnet multi-depth soil moisture sensor is a wireless sensor that works with the HOBOnet system to measure soil moisture and soil temperature at multiple depths with a single probe for fast and easy installation.

Featuring GroPoint's TDT5 technology with patented antenna design, this sensor measures soil moisture along the entire length of the probe segment, resulting in an enormous volume of influence per measurement section (2 L volume of influence per 15 cm segment). A high frequency of pulses (400,000 pulses per measurement) provides precise, consistent, and repeatable soil moisture data by eliminating outlying readings.

Soil Moisture: Volumetric Water Content (VWC)	
Measurement Range	0.000 to 1.000 m /m in most soils
Accuracy	±0.02 m /m (±2%) in most soils typical from 0° to 50°C (32° to 122°F)*
Resolution	0.001 m /m
Temperature	
Measurement Range	-20° to 70°C (-4° to 158°F)
Accuracy	±0.5°C (0.9°F)
Resolution	0.1°C (0.18°F)
Depths Measured (see below)	
RXW-GP3-xxx	45 cm (18 inches) total; three soil moisture zones, six temperature depths
Wireless Mote	
Operating Temperature Range	Sensor: -20° to 70°C (-4° to 158°F) Mote: -25° to 60°C (-13° to 140°F) with rechargeable batteries -40° to 70°C (-40° to 158°F) with lithium batteries
Radio Power	12.6 mW (+11 dBm) non-adjustable
Transmission Range	Reliable connection to 457.2 m (1,500 ft) line of sight at 1.8 m (6 ft) high Reliable connection to 609.6 m (2,000 ft) line of sight at 3 m (10 ft) high
Wireless Data Standard	IEEE 802.15.4
Radio Operating Frequencies	RXW-GPx-900: 904–924 MHz RXW-GPx-868: 866.5 MHz RXW-GPx-921: 921 MHz RXW-GPx-922: 916–924 MHz
Modulation Employed	OQPSK (Offset Quadrature Phase Shift Keying)
Data Rate	Up to 250 kbps, non-adjustable
Duty Cycle	<1%
Maximum Number of Motes	Up to 50 wireless sensors or 336 data channels per one HOBO RX station
Logging Rate	Maximum logging interval: 18 hours Recommended minimum logging interval: Using Solar Power with Rechargeable Batteries / **Using Non-Rechargeable Lithium Batteries** RXW-GP3-xxx: 5 minutes year round / 10 minutes
Number of Data Channels	RXW-GP3-xxx: 10
Battery Life	With NiMH batteries: Typical 3–5 years when operated in the temperature range -20° to 40°C (-4°F to 104°F) and positioned toward the sun (see Mounting and Positioning the Mote), operation outside this range will reduce the battery service life With non-rechargeable lithium batteries: RXW-GP3-xxx: 1 year with a 10-minute logging interval
Memory	16 MB
Dimensions	RXW-GP3-xxx sensor length: 53.2 cm (20.9 inches)
Weight	RXW-GP3-xxx sensor: 351 g (12.4 oz)
Materials	Sensor: Polycarbonate housing encasing epoxy sealed circuit board Cable: Polyurethane Mote: PCPBT, silicone rubber seal

Figure 2.15: Multi-depth soil moisture and temperature sensor RXW-GP3-868 specifications [59].

Dual Gas Transmitter / E2660-CO-CO_2

Dual Gas Transmitter E2660-CO-CO_2 belongs to the PluraSens® family of multifunctional measurement instruments. The device is intended for simultaneous detection of carbon dioxide-CO_2 and carbon monoxide-CO. The instrument utilizes electrochemical gas sensors with excellent repeatability, stability, and long lifetime. Two analog outputs (4-20 mA and 0-10 V) and RS485 digital interface with industry-standard Modbus RTU protocol can connect the transmitter to safety or building automation systems. The IP65 wall mount offers protected housing.

Calibration	carbon monoxide CO carbon dioxide CO_2
Sensors	CO: long-life electrochemical cell CO_2: optical (NDIR) sensor
Sampling method	diffusion
Detection ranges	0...1000 ppm CO 0...10 000 ppm CO_2 other ranges on request
Resolution	1 ppm CO 1 ppm CO_2
Response time T90	CO: ≤ 30 s; CO2: ca. 2-3 minutes
Signal update	every 1 second
Maintenance interval	CO: 6 months recommended CO_2: maintenance free
Sensor lifetime	CO: > 6 years (replaceable) CO_2 : > 10 years (non-replaceable)
Self-diagnostics	full functionality check at start-up
Warm-up time	≤ 1 min
Power supply	11...30 VDC, 24 VAC or 90...265 VAC
Power consumption	< 2 VA
Digital interface	RS485, Modbus RTU protocol
Analog outputs	2 × 4-20 mA / 0-10 V, user settable
Output scale widt	recommended: 20-100% of the range; > 10 × resolution in any case
Enclosure	light grey ABS plastic, wall mount, protection class IP65
Dimensions	H90 × W145× D55 mm
Sensor heads	M25
Remote sensor probe	protection IP65, shielded cable default cable length 3.0 m
Operating conditions	explosion safe areas; non-aggressive atmosphere without condensation; 0,9...1,1 atm; 0...+50 °C*, 0...85 %RH**

Figure 2.16: E2660 CO & CO_2 gas sensor specifications [59].

Davis 0.2 mm Rain Gauge Smart Sensor / HOBO® S-RGF-M002 Sensor

Davis® Rain Gauge Smart Sensors features the new AeroCone® design for better measurement accuracy in high-wind conditions. This gauge is made from UV-stabilized ABS plastic to provide a cost-effective sensor for rainfall measurement and is plug-and-play compatible with all HOBO weather stations. Its streamlined design reduces the amount of missed rain capture in windy conditions, resulting in more accurate rainfall data. In addition, improved debris screen locks in place to ensure it remains in place during high winds 16.5 cm collector opening meets World Meteorological Organization (WMO) guidelines.

Measurement Range	0 to 10.2 cm (0 to 4 in.) per hour, maximum 4,000 tips per logging interval
Accuracy	±4.0%, ±1 rainfall count between 0.2 and 50.0 mm (0.01 and 2.0 in.) per hour; ±5.0%, ±1 rainfall count between 50.0 and 100.0 mm (2.0 and 4.0 in.) per hour
Resolution	0.01 in. (S-RGC-M002) or 0.2 mm (S-RGF-M002)
Operating Temperature Range	0° to 50°C (32° to 122°F), survival -40° to 75°C (-40° to 167°F)
Environmental Rating	Weatherproof
Housing	UV-stabilized ABS plastic
Mechanism	Tipping spoon with magnetic reed switch pivots on metal shaft
Dimensions	16.5 cm opening diameter (6.5 in.) x 24 cm (9.5 in.) high; 214 cm^2 (33.2 $in.^2$) collection area
Weight	1.2 kg (2.7 lbs)
Bits per Sample	12
Number of Data Channels*	1
Measurement Averaging	No
Cable Length Available	2 m (6.6 ft)
Length of Smart Sensor Network Cable*	0.5 m (1.6 ft)
	The CE Marking identifies this product as complying with all relevant directives in the European Union (EU).

Figure 2.17: HOBO S-RGF-M002 rain gauge smart sensor specifications [59].

12-bit temperature & relative humidity (2m cable) smart sensor / HOBO® S-THB-M002

HOBO S-THB-M002 12-bit temperature and relative humidity smart sensor is designed to work with all Onset data loggers that accept smart sensors. All sensor parameters are stored inside the smart sensor, which automatically communicates configuration data information to the logger without any programming, calibration, or extensive user setup. This product meets CE specification EN61326 criterion C for ESD, criterion C for Radiated Immunity, criterion C for Fast Transient, criterion B for Conducted Immunity, criterion A for Power Frequency Magnetic Fields, and Radiated Emissions Group 1, Class B. To minimize measurement errors due to ambient RF, it is recommended to use the shortest possible probe cable length and keep the probe cable as far as possible from other cables.

Measurement Range
Temp: -40°C to 75°C (-40°F to 167°F)
RH: 0-100% RH at -40° to 75°C (-40° to 167°F); exposure to conditions below -20°C (-4°F) or above 95% RH may temporarily increase the maximum RH sensor error by an additional 1%

Accuracy
Temp: +/- 0.21°C from 0° to 50°C (0.38°F from 32° to 122°F)
RH: +/- 2.5% from 10% to 90% RH (typical), to a maximum of +/- 3.5% including hysteresis at 25°C (77°F); below 10% and above 90% ±5% typical

Resolution
Temp: 0.02°C at 25°C (0.04°F at 77°F)
RH: 0.1% RH

Bits Per Sample
Temp: 12
RH: 10

Drift
Temp: < 0.1°C (0.18°F) per year
RH: < 1% per year typical

Response Time (typical, to 90% of change)
Temp: 5 minutes in air moving 1 m/sec
RH: 5 minutes in air moving 1 m/sec with protective cap

Operating temperature range: -40°C to 75°C (-40°F to 167°F)
Environmental rating weatherproof: 0 to 100% RH intermittent condensing environments. For best results, the Temp/RH Smart Sensor should be mounted inside a protective enclosure, such as a solar radiation shield.
Housing PVC cable jacket with ASA styrene polymer RH sensor cap; modified hydrophobic polyethersulfone membrane
Sensor dimensions: 10 x 35 mm (0.39 x 1.39 in)
Weight: 110 g (3.88 oz)
Number of data channels: 2
Measurement averaging option: No
Cable lengths available: 2.5 m (8.2 ft)
Length of Smart Sensor network cable: 0.5 m (1.6 ft)

Figure 2.18: HOBO S-THB-M002 temperature & relative humidity smart sensor specifications [59].

Note: The sensor requires protection from rain or direct splashing; Radiation shield (RS3) strongly recommended for use in sunlight; sensors can be used in intermittent condensing environments up to 30°C and non-condensing above 30°C.

Solar radiation shield / HOBO RS3-B

RS3-B solar radiation shield improves the temperature and humidity measurements of HOBO external sensors in locations exposed to sunlight. This shield's small size and unobstructed airflow provide a faster response to changing conditions than larger radiation shields.

Time response: 2.5 times faster than the RS1 and M-RSA
Wind resistance: Tested in sustained winds up to 129 kph (80 mph), Tested in gusts up to 161 kph (100 mph)

Materials
Shield: ASA styrene (UV-stable)
Bracket: Glass-filled nylon (UV-stable)
Mounting hardware: Stainless steel and brass

Temperature: -40° to 75°C (-40° to 167°F)
Weight: 113 g (4 oz)
Height: 89 mm (3.5 inches); 159 mm (6.25 inches) with bracket
Diameter: 102 mm (4 inches); bracket protrudes an additional 51 mm (2 inches) from shield
Maximum Sensor Diameter: 1.22 cm (0.48 inches)
Mounting: Up to 51 mm (2 inches) mast diameter with hose clamp; unlimited with screws
Compatible sensors: S-THB-M00x, S-TMB-M0xx, RXW-THC-xxx, RXW-TMB-xxx, TMCx-HD, and external sensors from U23-00x or MX230x.

Note: This shield does not protect sensors from light reflected from below the shield at some angles. For deployments over reflective surfaces, consider using Onset's RS1 or M-RSA Solar Radiation Shields.

Figure 2.19: HOBO RS3-B solar radiation shield specifications [59].

2.2.2 Meazon

Meazon leads IoT energy management by using technology as leverage to unleash energy efficiency investments. Provides an energy IoT platform that can interface almost all available field level electrical loads (commercial, industrial, residential, electric vehicles, street lighting), gathers energy data using existing and emerging widely available networks such as NB-IoT, Wi-Fi & ZigBee, and channel them in a cost-efficient and secure manner to cloud connectivity & transport service. Meazon is fully committed to creating value for its customers and contributing to a greener planet, capitalizing on its technology, environmental policy, and quality policy. Offers public or private connectivity and transport data aggregation service with characteristics such as: distributed, real-time energy data collection & control of various sources (PV, EV, batteries) and loads (homes, buildings, HVAC, lighting, etc.). Additionally, Meazon features flexible energy submeters provisioning & management, cloud-based transparent connectivity, and a protocol bridge for Decision Support Systems and analytics platforms. Lastly, security across devices and users is provided, as well as insightful data analysis and visualization.

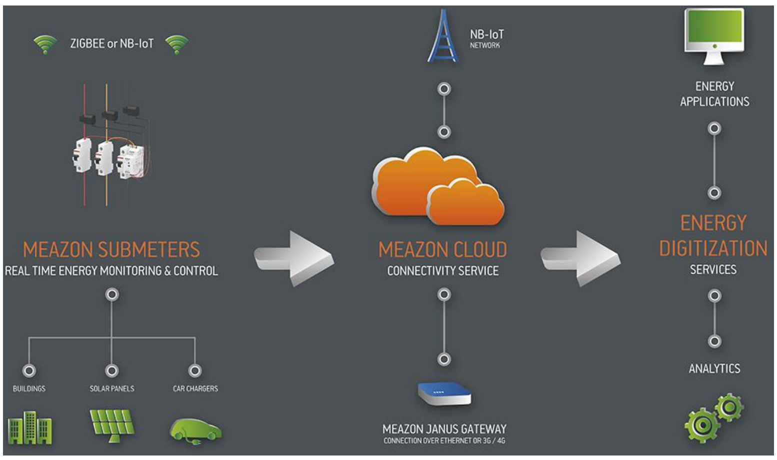

Figure 2.20: Meazon data connectivity and aggregation service flowchart [61].

Janus gateway

A Linux-based, small form factor appliance for provisioning, aggregating and backhauling data from Meazon metering and sensor devices to online analytics services (either Meazon Analytics or a preferred alternative solution) over Ethernet or 3G/4G. Thanks to the user-friendly provisioning web application UI, minimal configuration effort is required even for large-scale deployments. The Gateway can transmit control and data messages throughout the ZigBee network [62].

	Feature
Processor	1 GHz ARM Cortex-A8
Memory	512MB DDR3
USB 2.0 ports	2 x USB 2.0 type A host port, mini-USB 2.0 client port
Onboard storage	4 GB embedded MMC, microSD card
Network interfaces	10/100 RJ45, ZigBee, wM-Bus, WiFi (optional), Bluetooth (optional)
ZigBee	Home Automation 1.2
Protocol interfaces	MQTT, HTTP, WebSocket, FTP, openADR 2.0, SIA DC-09, NodeRed, ModBus
OSS applications	ZigPy, uBizy, NodeRed, SNMP
Power source	5.5mm/2.1mm Barrel connector, 5V@2A
Size	118 x 118 x 27 mm
Certifications	CE, FCC
Operating environment	Temperature: -20° C to 50° C Relative Humidity: 10% to 90% (RH), non-condensing

Figure 2.21: Meazon "Janus" Gateway device features [62].

Bizy type F plug

Meazon Bizy plug is used to control the power feed (on/off/scheduling) and measure energy & power consumed on electrical appliances. It connects an appliance wirelessly to the Home Area Network. It can measure I, V, Active and Reactive Power & Energy and Power Network Frequency. Finally, it can store on/off time schedules locally, as well as unread measurements making it robust to Internet and power outages [63].

Voltage	85 - 265 VAC 45-65 Hz
Maximum Load	16A
Internal relay	16A on/off state
Power consumption	Less than 0.5 W
Accuracy	Higher than 99%
Communications	IEEE 802.15.4 / ZigBee
ZigBee Standard	Home Automation 1.2
Frequency	2.4 GHz
Coverage Dimensions	Up to 50m indoor / mesh topology 43 x 87 x 87 (WxHxD) in mm
Operating Environment	Indoor rated : -20° C to 50° C

Figure 2.22: Bizy Type F Plug technical characteristics [63].

Humidity and temperature sensor / HMSZB-110

HMSZB-110 wireless humidity sensor helps maintain the ideal comfort level by supervising the temperature and relative humidity levels and protecting the interior, electronics, instruments, and other humidity-sensitive items. Additionally, the sensor is an essential part of any insurtech solution, as it will alert the user if indoor humidity fluctuates to undesirable levels. Readings from the sensor are sent wirelessly through the Janus gateway to the web-based platform. In order to reduce condensation levels, the humidity sensor can be set to activate, for instance, a ventilation system or a thermostat. The sensor features a long battery life (non-rechargeable) and accurate long-range temperature and humidity reporting. The sensor includes adhesive tape and screws, allowing the sensor to be easily mounted on the wall or the ground or near vulnerable and valuable items [64].

Dimensions (W x H)	70 x 70 x 21 mm
Colour	White
Power supply	Battery: 2 x AA, exchangeable Battery life: 5 years, reporting every 5 minutes Battery level and low battery warning can be reported
Radio	Sensitivity: -92 dBm Output power: +3 dBm
Environment	IP class: IP20 Operation temperature 0 to +50°C Relative humidity 5% - 85%, non condensing
Functions	
Temperature sensor	Range: 0 to +50°C Resolution: 0.1°C (accuracy Typ ±0.5°C and Max ±2°C) Sample time: config.: 2 s -65,000 s Reporting: configurable
Humidity sensor	Range: 0 to 100% rH Resolution: 1% rH (accuracy ± 3.5% rH, 20 - +80% rH)
Communication	
Wireless protocol	Zigbee Home Automation Zigbee end-device
Certifications	Conforming to CE, FCC, IC, ISED, RED and RoHS directives Zigbee Home Automation 1.2 certified

Figure 2.23: HMSZB-110 humidity and temperature sensor technical specifications [64].

Air quality, humidity, and temperature sensor / AQSZB-110

The wireless Air Quality Sensor is easy to integrate into IoT solutions. It features long-range and accurate reporting of (total) volatile organic compounds (TVOC) level, temperature, and humidity to ensure the best air quality possible [65].

Dimensions (W x H)	70 x 70 x 21 mm
Colour	White
Power supply	Battery: 2 x AA, exchangeable Battery life: 2 years, reporting every 5 minutes Resolution: 0.1 Volt
Radio	Sensitivity: -97 dBm Output power: up to +7 dBm
Environment	Operation temperature 0 to +50°C IP class: IP20
Functions	
VOC sensor	Range: 0 to 60000 ppb Resolution: 1 - 32 ppb Reporting: configurable
Temperature sensor	Range: 0 to +50°C Resolution: 0.1°C (accuracy typical ± 0.2°C) Sample time: 30 s Reporting: configurable
Humidity sensor	Range: 0 to 100% RH Resolution: 1% RH (accuracy typical 2%, 20-80% RH)
Communication	
Wireless protocol	Zigbee Home Automation Zigbee end-device
Certifications	Conforming to CE, RED and RoHS directives

Figure 2.24: AQSZB-110 air quality sensor technical specifications [65].

LEVEL		HYGIENIC RATING	RECOMMENDATION	TVOC [µg/m³]	TVOC [ppb]
5	Unhealthy	Situation not acceptable	Intense ventilation necessary	10'000 - 25'000	2200 - 5500
4	Poor	Major objections	Intensified ventilation / airing necessary	3'000 - 10'000	660 - 2200
3	Moderate	Some objections	Intensified ventilation recommended	1'000 - 3'000	220 - 660
2	Good	No relevant objections	Ventilation/airing recommended	300 -1'000	65 - 220
1	Excellent	No objections	Target value	< 300	0 - 65

Figure 2.25: TVOC chart of air quality sensor [65].

2.2.3 Agenso

Agenso (Agricultural and environmental solutions) expertise spans in IoT solutions and Precision Agriculture (PA) services. Agenso specializes in the promotion of research and services in the areas of sustainable agricultural production, environmental sustainability and advanced technologies for agriculture and environment. Both offer integrated solutions featuring Internet of Things devices for agricultural and environmental purposes, data collection from field sensors and advanced spatial mapping techniques for data visualisation. Their integrated system includes a base station which transfers data to the Agenso cloud, a weather station with numerous sensors, two soil moisture sensors and a soil temperature sensor. All Agenso services and devices' specifications are detailed below.

Agenso features of services include:

- permanent connection via mobile network
- access to data through a web-based application
- weather forecast
- user calendar
- anti-theft system
- historical data storage
- personalized alerts
- data export
- 2 year of warranty

Base station

Figure 2.26: Agenso base station.

- 4G/3G/GPRS & GNSS connectivity
- Rechargeable battery with photovoltaic solar panel
- Measurements display monitor
- Integrated GPS
- Ingress Protection Code IP 67

Weather station

Figure 2.27: Agenso weather station.

Temperature sensor

- Range: -30°C – 60 °C
- Accuracy: ±1.0°C
- Resolution: 0.1°C

Relative humidity sensor

- Range: 1 - 99% RH
- Accuracy: ±5% RH

Air pressure sensor

- Range: 0 – 1100 hPa
- Accuracy: ±3 hPa
- Resolution: 0.1 hPa

Wind speed, direction and gust sensor

- Range: 0 - 50m/s
- Accuracy: ±1m/s (speed< 5m/s), ±10% (speed > 5m/s)

Solar intensity sensor

- Range: 0 – 300000Lux
- Accuracy: ±15%

UV radiation sensor

- Range: 0 – 11 UV

Rain gauge

- Range: 0 - 9999mm

Soil moisture sensor (HOBOnet soil moisture EC-5 sensor)

Figure 2.28: Agenso soil moisture sensor.

- Range: 0 - 100%
- Accuracy: ±0.03 m^3/m^3

Soil temperature sensor (GMCM D18B20 sensor)

- Range: -55°C - 125°C
- Accuracy: ±0.5°C

Figure 2.29: Agenso soil temperature sensor.

2.2.4 Proposed GMCM system

This thesis investigates the possibility of building a less expensive but reliable monitoring system. The parts included in the proposed Greenhouse Micro-Climate Monitoring system, the schematics and the operating principal are analysed in the following sections.

Microcontroller & data loggers

<u>NodeMCU Lolin v.3 ESP8266</u>

NodeMCU is based on the Esperessif ESP8266-12E Wi-Fi System-On-Chip, loaded with open-source, Lua-based firmware. It has more robust specs, including a 32-bit RISC processor clocked at 80MHz, along with a generous RAM complement and support for up to 16mb of external flash storage. The device is handy for IoT applications, thanks to its tiny footprint and built-in Wi-Fi support. NodeMCU board will read data from the sensors, control the actuators and communicate with Cayenne platform.

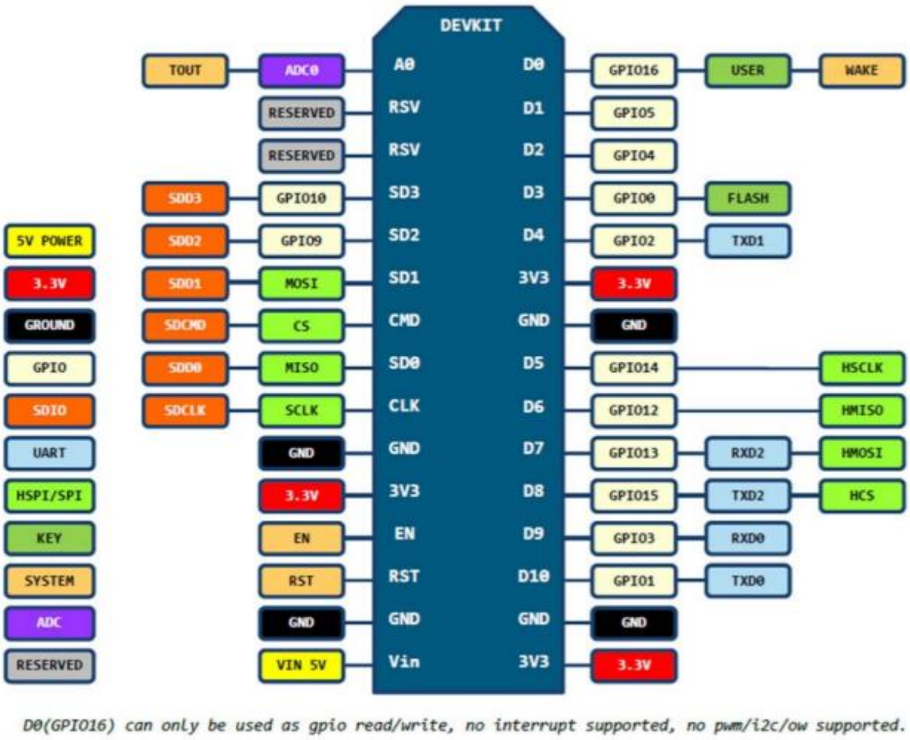

- Voltage:3.3V.
- Wi-Fi Direct (P2P), soft-AP.
- Current consumption: 10uA~170mA.
- Flash memory attachable: 16MB max (512K normal).
- Integrated TCP/IP protocol stack.
- Processor: Tensilica L106 32-bit.
- Processor speed: 80~160MHz.
- RAM: 32K + 80K.
- GPIOs: 17 (multiplexed with other functions).
- Analog to Digital: 1 input with 1024 step resolution.
- +19.5dBm output power in 802.11b mode
- 802.11 support: b/g/n.
- Maximum concurrent TCP connections: 5.

Figure 2.30: NodeMCU microcontroller pinout diagram and specifications [66].

ESP32

The Esp32 Developer Kit v1 is one of the development board created to evaluate the ESP-WROOM-32 module. It is based on the ESP32 microcontroller that boasts Wi-Fi, Bluetooth, Ethernet and Low Power support all in a single chip.

ESP32 is already integrated antenna and RF balun, power amplifier, low-noise amplifiers, filters, and power management module. The entire solution takes up the least amount of printed circuit board area. This board is used with 2.4 GHz dual-mode Wi-Fi and Bluetooth chips by TSMC 40nm low power technology, power and RF properties best, which is safe, reliable, and scalable to a variety of applications.

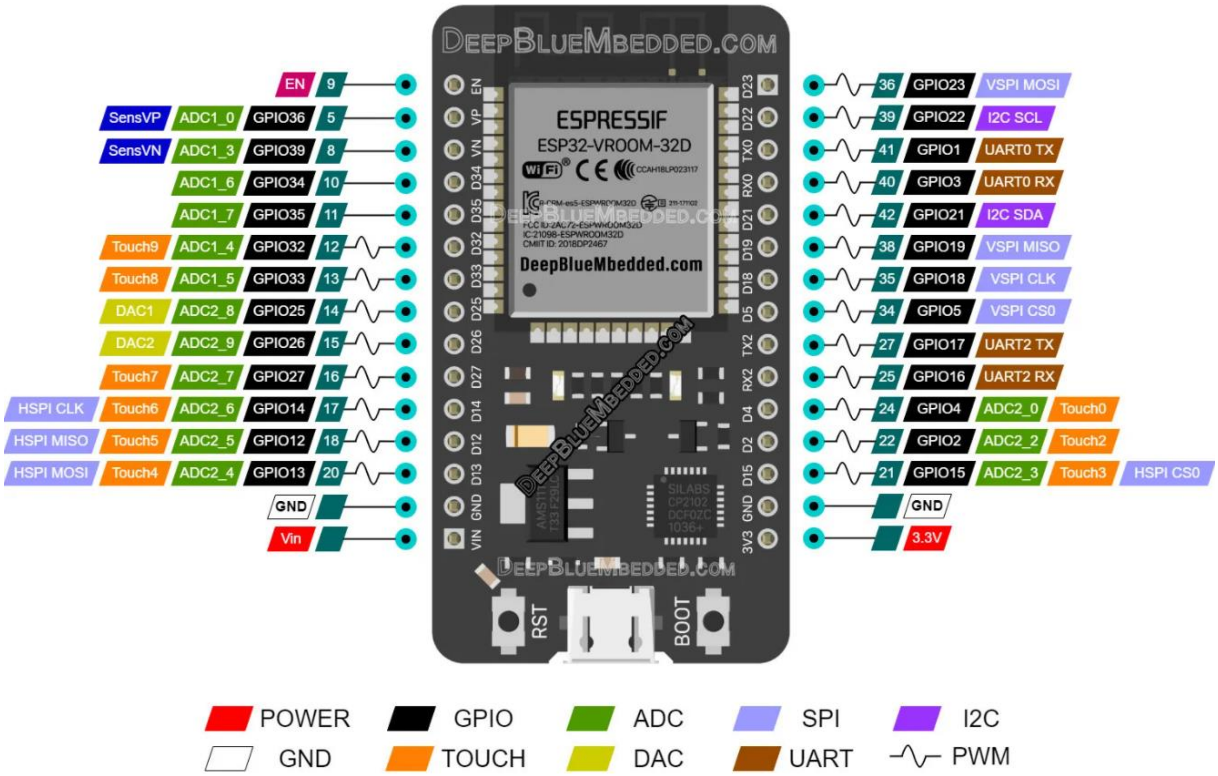

- Microcontroller: Tensilica 32-bit Single-/Dual-core CPU Xtensa LX6
- Operating Voltage: 3.3V
- Input Voltage: 7-12V
- Digital I/O Pins (DIO): 25
- Analog Input Pins (ADC): 6
- Analog Outputs Pins (DAC): 2
- UARTs: 3
- SPIs: 2
- I2Cs: 3
- Flash Memory: 4 MB
- SRAM: 520 KB
- Clock Speed: 240 Mhz
- Wi-Fi: IEEE 802.11 b/g/n/e/i:
  - Integrated TR switch, balun, LNA, power amplifier and matching network
  - WEP or WPA/WPA2 authentication, or open networks
- Dimensions: 51.5x29x5mm

Figure 2.31: ESP32 microcontroller pinout diagram and specifications [67], [68].

Sensors

<u>Air temperature and relative humidity sensor / DHT22 (AM2302)</u>

DHT22 is a basic, low-cost digital air temperature and humidity sensor. It utilizes exclusive digital-signal-collecting-technique and humidity sensing technology, assuring its reliability and stability. Its sensing elements are connected with an 8-bit single-chip computer, which uses a capacitive humidity sensor and a thermistor to measure the surrounding air. The only downside of this sensor is the possibility to get new data every 2 seconds. Each sensor of this model is temperature compensated and calibrated in an accurate calibration chamber. The calibration coefficient is saved in OTP memory. Small size and low consumption allow DHT22 to be suited in all kinds of harsh application occasions. Additionally, the single row packaged with four pins makes the connection very convenient. One capacitor valued at 100nF can be added between VDD and GND for wave filtering.

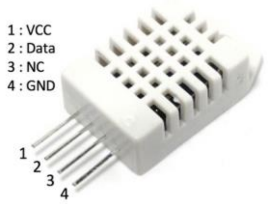

Model	DHT22
Power supply	3.3-6V DC
Output signal	digital signal via single-bus
Sensing element	Polymer capacitor
Operating range	humidity 0-100%RH; temperature -40~80Celsius
Accuracy	humidity +-2%RH(Max +-5%RH); temperature <+-0.5Celsius
Resolution or sensitivity	humidity 0.1%RH; temperature 0.1Celsius
Repeatability	humidity +-1%RH; temperature +-0.2Celsius
Humidity hysteresis	+-0.3%RH
Long-term Stability	+-0.5%RH/year
Sensing period	Average: 2s
Interchangeability	fully interchangeable
Dimensions	small size 14*18*5.5mm; big size 22*28*5mm

Figure 2.32: Technical specification of DHT22 sensor [69].

<u>Temperature sensor / DS 18B20 waterproof sensor cable</u>

DS18B20 digital thermometer provides temperature measurements from -55°C to +125°C in 750ms (max). The resolution of the DS18B20 is configurable (9, 10, 11, or 12 bits), with 12-bit readings of the factory default state. This equates to a temperature resolution of 0.5°C, 0.25°C, 0.125°C, or 0.0625°C. The DS18B20 communicates over a 1-Wire bus that by definition requires only one data line (and ground) for communication with a central microprocessor. In addition, the DS18B20 can derive power directly from the data line (parasite power), eliminating the need for an external power supply. Each DS18B20 has a its own 64-bit serial code, allowing multiple DS18B20s to function on the same 1-Wire bus. Thus, it is simple to use a microprocessor to control many DS18B20s distributed over an extensive area. Lastly, the stainless-steel probe head of the sensor makes it suitable for any wet or harsh environment.

Power supply range:	3.0V to 5.5V
Operating temperature range:	-55°C to +125°C
Storage temperature range:	-55°CC to +125°C
Accuracy over the range of -10°C to +85°C:	±0.5°C

Figure 2.33: DS18B20 sensor specifications [70].

Capacitive soil moisture sensor

SEN0193 soil moisture sensor measures soil moisture levels by capacitive sensing rather than resistive sensing like other sensors do. It is made of corrosion resistant material which gives it an excellent service life. It provides real-time soil moisture data by inserting it into the soil. This module includes an on-board voltage regulator which gives it an operating voltage range of 3.3-5.5V. It is compatible with all low-voltage MCUs, both 3.3V and 5V. For compatibility with a Raspberry Pi it will need an ADC converter. This soil moisture sensor is compatible with 3-pin "Gravity" interface, which can be directly connected to the Gravity I/O expansion shield.

- Operating Voltage: 3.3 ~ 5.5 VDC
- Output Voltage: 0 ~ 3.0VDC
- Operating Current: 5mA
- Interface: PH2.0-3P
- Dimensions: 3.86 x 0.905 inches (L x W)
- Weight: 15g

Figure 2.34: Technical specification of DHT22 sensor [71].

Photoelectric water sensor / FS-IR02

This is a photoelectric liquid level sensor which operates by using traditional optical principles. The advantages of this sensor include a high sensitivity and no need for mechanical parts - meaning less calibration. The corrosion resistant probe is easily mounted and can handle high temperatures and high pressures. The sensor is equipped with an interface adapter for compatibility with the DFRobot "Gravity" interface.

Liquid Level Sensor-FS-IR02 Pin Mappings

Num.	Name	Description
1 (Red)	GND	Probe_GND
2 (Yellow)	GND	Probe_GND
3 (Blue)	VCC	Probe_VCC
4 (White)	OUT	Signal Output

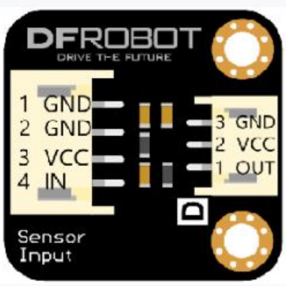

Liquid Level Sensor-FS-IR02 Pin Mapping

Num.	Name	Description
Left_1	GND	Probe_GND
Left_2	GND	Probe_GND
Left_3	VCC	Probe_VCC
Left_4	IN	Signal Input
Right_1	OUT	Signal Output
Right_2	VCC	VCC
Right_3	GND	GND

- Model: FS-IR02
- Type: Photoelectric Liquid Level Sensor
- Operating Voltage: 5V DC
- Output Current: 12mA
- Operating Temperature: - 25 ~ 105 ℃
- Low Level Output: < 0.1 V
- High Level Output: > 4.6 V
- Liquid Level Detection Accuracy: ±0.5 mm
- Material: Polycarbonate
- Measuring Range: No limit
- Life: 50,000 hours

Figure 2.35: Pinout diagram and technical specifications of FS-IR02 photoelectric water sensor [72].

Temperature, relative humidity, CO_2, TVOC, altitude, air pressure sensor / CCS811 & BME280

Based on the combination of CCS811 and BME280 chip, this module features high accuracy, IIC interface and fast-paced measurements. The BME280 can provide temperature and humidity compensation for CCS811 to improve the whole accuracy to a certain extent. It can be used to detect temperature, humidity, barometric pressure, altitude, TVOC and eCO_2 levels.

CCS811 air quality sensor uses AMS's unique micro-hot plate technology. Compared with conventional gas sensors, it has lower power consumption, shorter preheating time, and smaller size. The internally integrated ADC and MCU allow it to collect and process data and return via I2C.

BME280 is an environmental sensor that combines temperature sensor, humidity sensor and barometer in one board. It has high precision, multiple functions and small size. The sensor offers ±0.5°C temperature error and ±2% relative humidity error. It provides very stable performance within the detection temperature range. Besides, the offset temperature coefficient is ±1.5 Pa/K, equivalent to ±12.6 cm at 1°C temperature change.

- Operating Voltage: 3.3V~5.5 V
- Working Current: <20mA

CCS811 Parameter:

- Preheat Time: <15s
- I2C Address: 0x5A(in default)/0X5B
- Operating Temperature Range: -40℃~85℃
- Operating Humidity Range: 10%RH~95%RH
- eCO2 Measuring Range: 400ppm~8000ppm
- TVOC Measuring Range: 0ppb~1100ppb

BME280 Parameter:

- I2CAddress：0x76(in default)/0X77
- Operating Temperature: -40℃~85℃
- Temperature Measuring Range: -40℃~+85℃, resolution of 0.1℃, deviation of ±0.5℃
- Humidity Measuring Range: 0~100%RH, resolution of 0.1%RH, deviation of ±2%RH
- Pressure Measuring Range: 300~1100hPa

Figure 2.36: Technical specifications of module with CCS811 and BME280 sensors [73].

Carbon monoxide (CO) sensor / MQ-7

The MQ7 is a Carbon Monoxide (CO) sensor, suitable for sensing CO concentrations in the air. It can detect CO gas concentrations anywhere from 20 to 2000ppm. The sensitivity can be adjusted by the potentiometer.

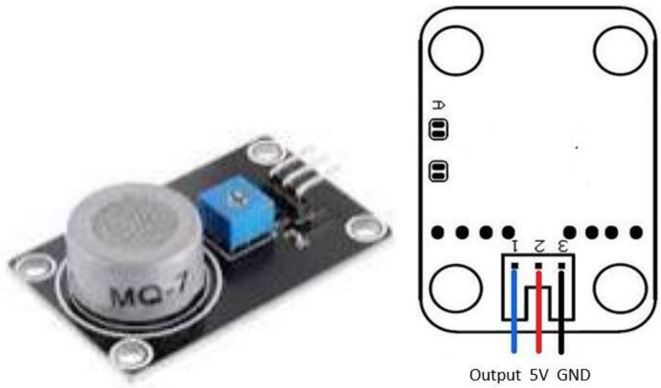

- Power supply needs: 5V
- Interface type: Analog
- Pin Definition: 1-Output 2-VCC 3-GND
- High sensitivity to carbon monoxide
- Fast response
- Stable and long life
- Size: 40x20mm

Figure 2.37: Pinout diagram and technical specifications of MQ-7 carbon monoxide sensor [74].

Magnetic door switch / MC 37B

MC-37 door sensor is a magnetic switch wired to the door or window to alarm when opened. No external power supply is required; simply connects to GND and digital GPIO ports directly to operate.

- Connecting Mode: N.C.
- Rated current: 100mA
- Rated voltage: 200VDC
- Operating distance: more than 15mm, less than 25mm
- Rated power: 3W
- Dimension: 28x15x0.9cm
- Cable Length: 30.5cm ± 12mm
- Switch output: normally closed (switch and magnet are together when the switch is closed)

Figure 2.38: Magnetic door switch MC 37B specifications [75].

2.2.5 Actuators

The greenhouse model includes a simulation of heating, forced ventilation, natural ventilation and irrigation systems. The heating system is simulated by using an infrared lamp and the forced ventilation system by using fans. The natural ventilation system is simulated by a window opening system, while the irrigation system by using a water pump. What is more, an air relative humidity and soil moisture control system is simulated by combining the infrared lamp, the water pump, the fans and the window opening system.

Creality 3D 42-40 stepper motor

Creality 3D 42-40 is a hybrid stepping motor with a 1.8° step angle (200 steps/revolution). Each phase draws 1.5 A at 4 V, allowing for a 4 kg*cm holding torque.

- Step Angle: 1.8
- Holding Torque: 4kg.cm
- Rated Voltage: 4.8Volt
- Rated Current: 1.5A/Phase
- Form Factor: NEMA 17

- Steps: 200
- Nominal Voltage: 4.83V
- Current Rating: 1.5A
- Rated speed: 1-1000rpm

- Rated torque: 0.4NM
- Ambient Temperatuar: -20 - 50℃
- Length: 40mm
- Shaft length: 24mm (D Shaft)

Figure 2.39: Creality 3D 42-40 stepper motor technical specifications [76].

A4988 stepper motor driver module

The A4988 is a micro-stepping driver for controlling bipolar stepper motors, which has a built-in translator for easy operation. Therefore, the stepper motor can be controlled with just two pins, one for controlling the rotation direction and the other for controlling the steps. The driver provides five different step resolutions: full-step, haft-step, quarter-step, eight-step, and sixteenth-step. Also, it has a potentiometer for adjusting the current output, over-temperature thermal shutdown, and crossover-current protection. Its logic voltage ranges from 3 to 5.5 V, and the maximum current per phase is 2A when sufficient cooling is provided or 1A continuous current per phase without a heat sink or cooling.

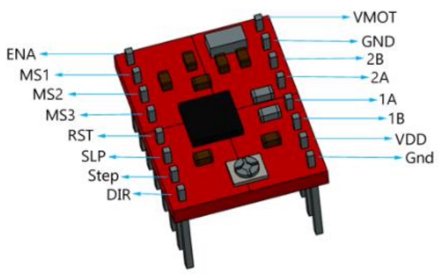

- Max. Operating Voltage: 35V
- Min. Operating Voltage: 8V
- Max. Current Per Phase: 2A
- Microstep resolution: Full step, ½ step, ¼ step, 1/8 and 1/16 step
- Reverse voltage protection: No
- Dimensions: 15.5 × 20.5 mm (0.6″ × 0.8″)
- Short-to-ground and shorted-load protection
- Low RDS(ON) outputs
- Thermal shutdown circuitry

Figure 2.40: A4988 stepper motor driver module pinout and technical specifications [77].

Pin Name	Description
VDD & GND	Connected to 5V and GND of Controller
VMOT & GND	Used to power the motor
1A, 1B, 2A, 2B	Connected to the 4 coils of motor
DIRECTION	Motor Direction Control pin
STEP	Steps Control Pin
MS1, MS2, MS3	Microstep Selection Pins
SLEEP	Pins For Controlling Power States

MS1	MS2	MS3	Resolution
LOW	LOW	LOW	Full Step
HIGH	LOW	LOW	Halft Step
LOW	HIGH	LOW	Quarter Step
HIGH	HIGH	LOW	Eighth step
HIGH	HIGH	HIGH	Sixteenth Step

Figure 2.41: A4988 driver module pinout description and function [77] [78].

The three pins (MS1, MS2, and MS3) are used for selecting one of the five-step resolutions according to the above figure (2.41). These pins have internal pull-down resistors, this means, in case they get disconnected, the board will operate in full-step mode.

Arctic P12 PWM PST CO fan

P12 PWM PST CO fan features premium quality Japanese dual ball bearing, which allows Continuous Operation 24/7 without the slightest compromise in performance. Thanks to the 4-pin connector, the RPM can be regulated in a broad spectrum via PWM. In this way, noise is kept at a minimum while maximum cooling performance is guaranteed when needed. Additionally, the Power Sharing Technology allows the fans to be powered and controlled synchronously with the same cable.

Fan	120 mm, 200–1800 RPM (Controlled by PWM)
Airflow	56.3 CFM/95.65 m³/h (@1800 RPM)
Static Pressure	2.2 mm H_2O (@1800 RPM)
Bearing	Dual Ball Bearing
Noise Level	0.3 Sone (@1800 RPM)
Voltage/Current	0.08 A/12 V DC
Connector	4-pin Connector + 4-pin Socket
Dimensions	120 (L) x 120 (W) x 25 (H) mm
Weight	145 g

Figure 2.42: Arctic P12 PWM PST CO fan pinout and technical specifications [79].

Avide infrared bulb E27 250W red

Infrared lamps are commonly used in radiant heating for industrial processes and building heating. Infrared heating provides electromagnetic radiation with wavelengths between 780 nm and 1 mm invisible to the eye. When infrared waves touch a surface, heat energy is released regardless of the surrounding air temperature.

Wattage:	250W
Voltage:	220-240V
Dimmability:	Yes
Lifetime:	5 000h
Energy class:	E
IP standard:	IP20

Figure 2.43: Avide infrared bulb E27 250W red specifications [80].

XiLong XL-780 submersible pump

XiLong XL-780 is a submersible water pump used for the model greenhouse's irrigation system. It is submerged in a water tank, from where it draws water and through the tubes pours it into the flowerpot. Into the soil of the flowerpot, all the soil sensors are installed.

Pump operation type	lifting
Input voltage	220-240V
Aquarium type	marine, freshwate
Pump performance	650 l / h
Feeding height	90 cm
Pump power	8 watts
Pump flow regulator	mechanical
Weight	310 g

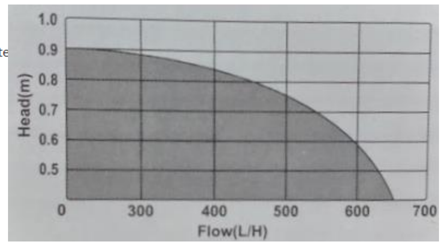

Figure 2.44: Submersible water pump XiLong XL-780 specifications and head-flow diagram.

Relay module 5V

Relay is an electromechanical device that uses an electric current to open or close the contacts of a switch. The single-channel relay module is much more than just a plain relay; it comprises components that make switching and connection easier and act as indicators to show if the module is powered and if the relay is active or not.

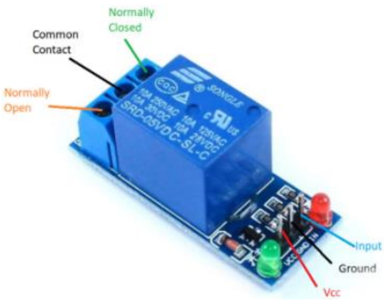

Pin Name	Description
Relay Trigger	Input to activate the relay
Ground	0V reference
VCC	Supply input for powering the relay coil
Normally Open	Normally open terminal of the relay
Common	Common terminal of the relay
Normally Closed	Normally closed contact of the relay

- Supply voltage – 3.75V to 6V
- Quiescent current: 2mA
- Current when the relay is active: ~70mA
- Relay maximum contact voltage – 250VAC or 30VDC
- Relay maximum current – 10A

Figure 2.45: Relay module pinout diagram, description and specifications [81].

2.3 Proposed smart greenhouse design

2.3.1 Electric circuits schematics

The electric circuits of the smart greenhouse project were designed in the Fritzing software. Fritzing is a free, open-source program that allows “breadboard” view, giving the sense of physical stacking of components. Additionally, it offers an electronic chart creation tool, in which the components and modules used in one of these views are automatically routed. Last, Fritzing features printed electronic circuit board creation tool.

Greenhouse Micro-Climate Monitoring system 1

The proposed Greenhouse Micro-Climate Monitoring system 1 includes NodeMCU Esp8266 microprocessor, DHT22 air temperature and relative humidity sensor, DS18B20 waterproof temperature sensor, a capacitive soil moisture sensor and a photoelectric water sensor. All sensors are powered with the 3.3 V pin of the microprocessor and grounded at the GND pin. DHT22, DS18B20 and water level sensors transfer data to digital GPIOs 5 (D2), 4 (D1) and 14 (D5) respectively, while the capacitive soil moisture sensor to the analog GPIO A0. It is recommended to add a 4.7kΩ resistor in the DS18B20 circuit for signal filtration. Finally, the microcontroller is powered with its 5V USB port.

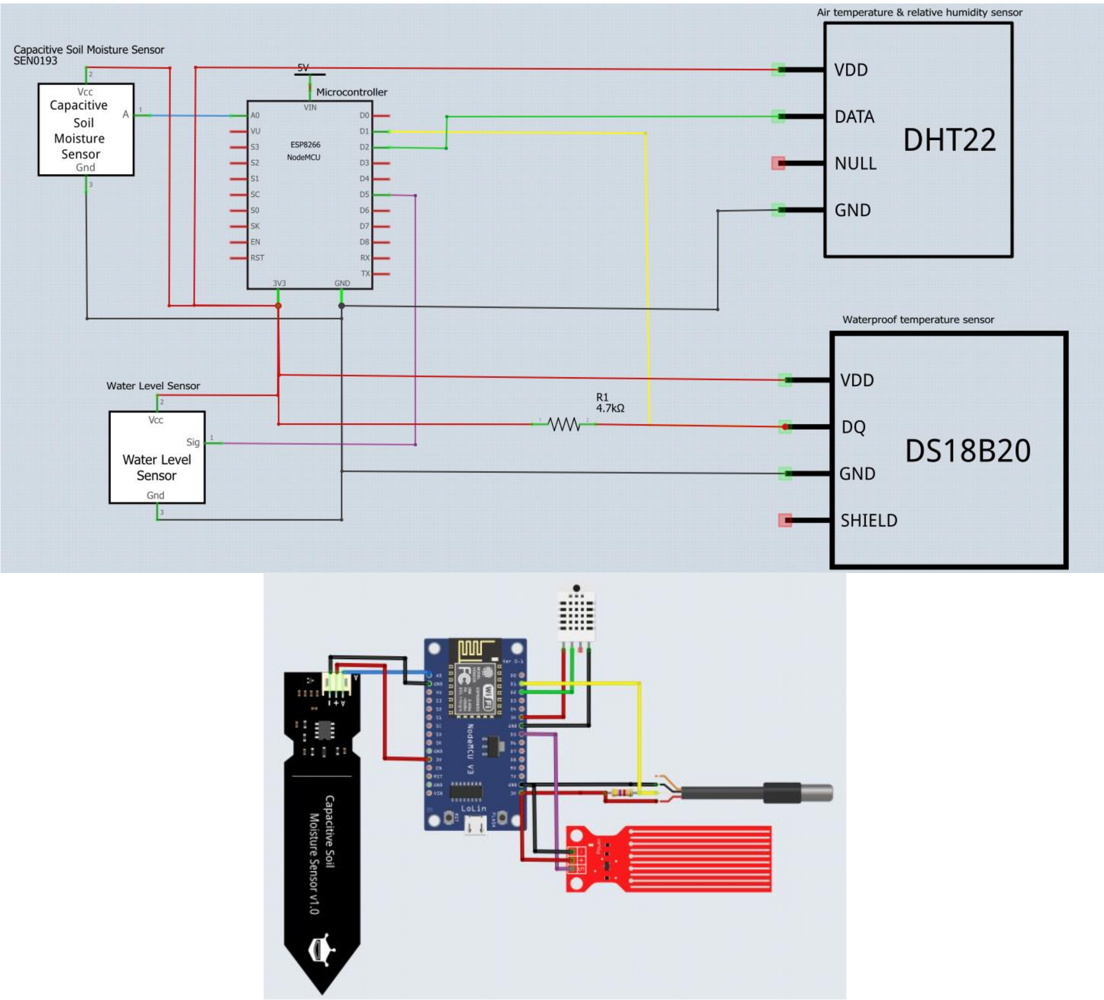

Figure 2.46: Fritzing and animated schematics of GMCM system 1.

Greenhouse Micro-Climate Monitoring system 2

The second node of Greenhouse Micro-Climate Monitoring system (2) includes ESP32 microprocessor, MQ-7 CO sensor, BME280 and CCS811 sensors. All sensors are powered with the 3.3 V pin of the microprocessor and grounded at the GND pin. MQ-7 sensor is connected to the digital GPIO 15. The module, which includes BME280 and CC811 sensors, sends data through SCL and SDA ports with I2C serial communication protocol. Therefore, ESP32 microcontroller is used, instead of a NodeMCU.

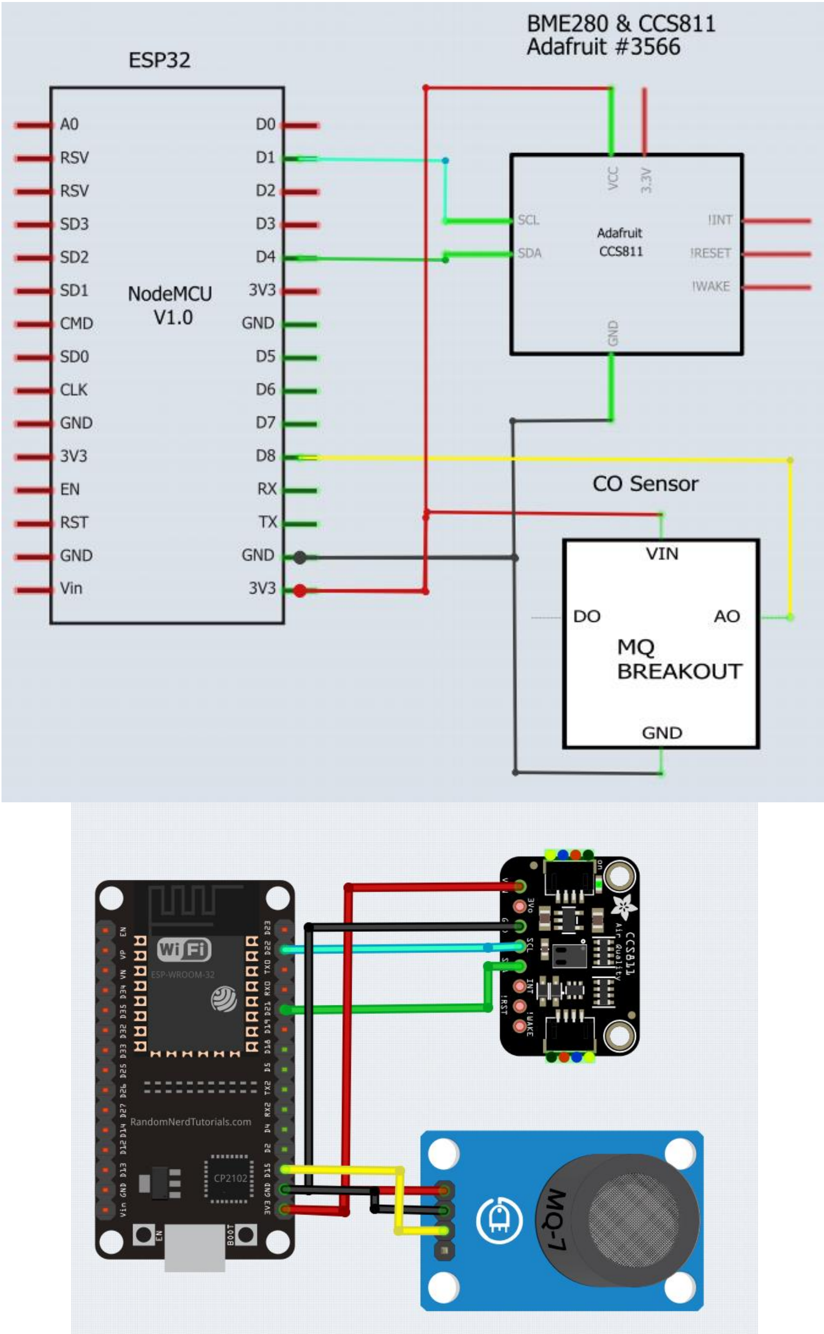

Figure 2.47: Fritzing and animated schematics of GMCM system 2.

Window opening mechanism

The window opening mechanism consists of NodeMCU microcontroller, Creality 3D 42-40 stepper motor, A4988 stepper motor driver, and two door magnet sensors. An external 12V DC power source is needed to power the stepper motor and a 100µF capacitor to protect it from voltage spikes. The driver module is powered by the microcontroller and controlled by "dir" and "step" pins connected to GPIO 4 and GPIO 5. A relay is installed to control the current flow through the stepper motor driver. MS1, MS2 and MS3 pins are connected to the power source of the microcontroller in order to provide sixteenth-step resolution. The stepper motor pins need to be connected as indicated in figure 2.48. Last, the magnetic door switches send signals to the connected GPIOs (GPIO 3 and GPIO 6), when the circuits are closed.

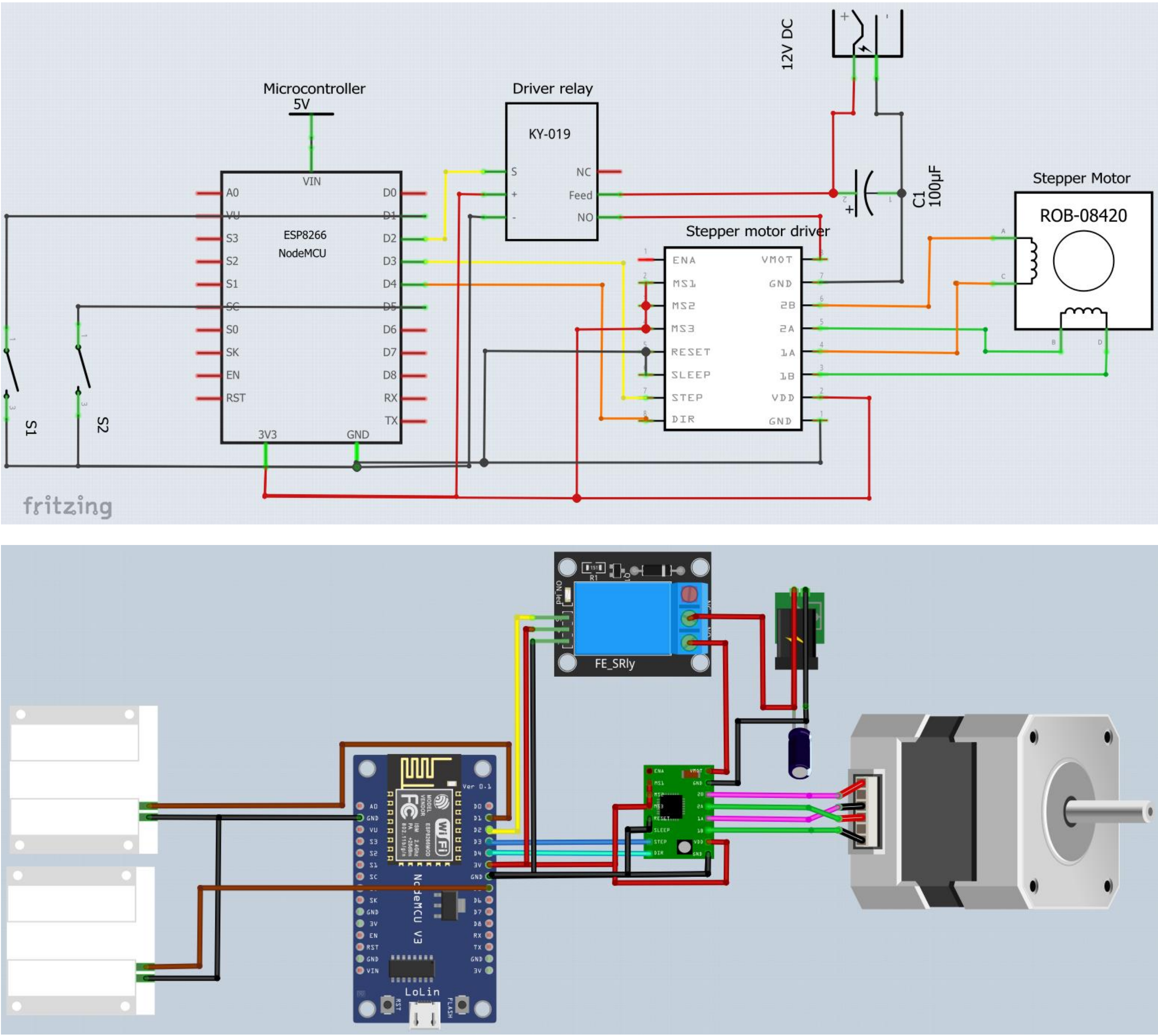

Figure 2.48: Fritzing and animated schematics of window opening mechanism.

Ventilation system

The ventilation system comprises six Arctic P12 PWM PST CO fans, a NodeMCU ESP8266 microcontroller and a relay. The two front fans and the four rear fans are connected in parallel. Therefore, a single PWM signal is needed for each set of fans. The set of front fans occupies microcontroller's GPIO 14, while the rear set occupies GPIO 12. The minimum speed of the fans is 200rpm, thus a relay is connected to the GPIO 13, which can shut them down completely. The fans require 12V DC. Therefore, an external power source is installed, as shown in figure 2.49. The external power source and the microcontroller need to be grounded so that the fans can be controlled by the PWM signals.

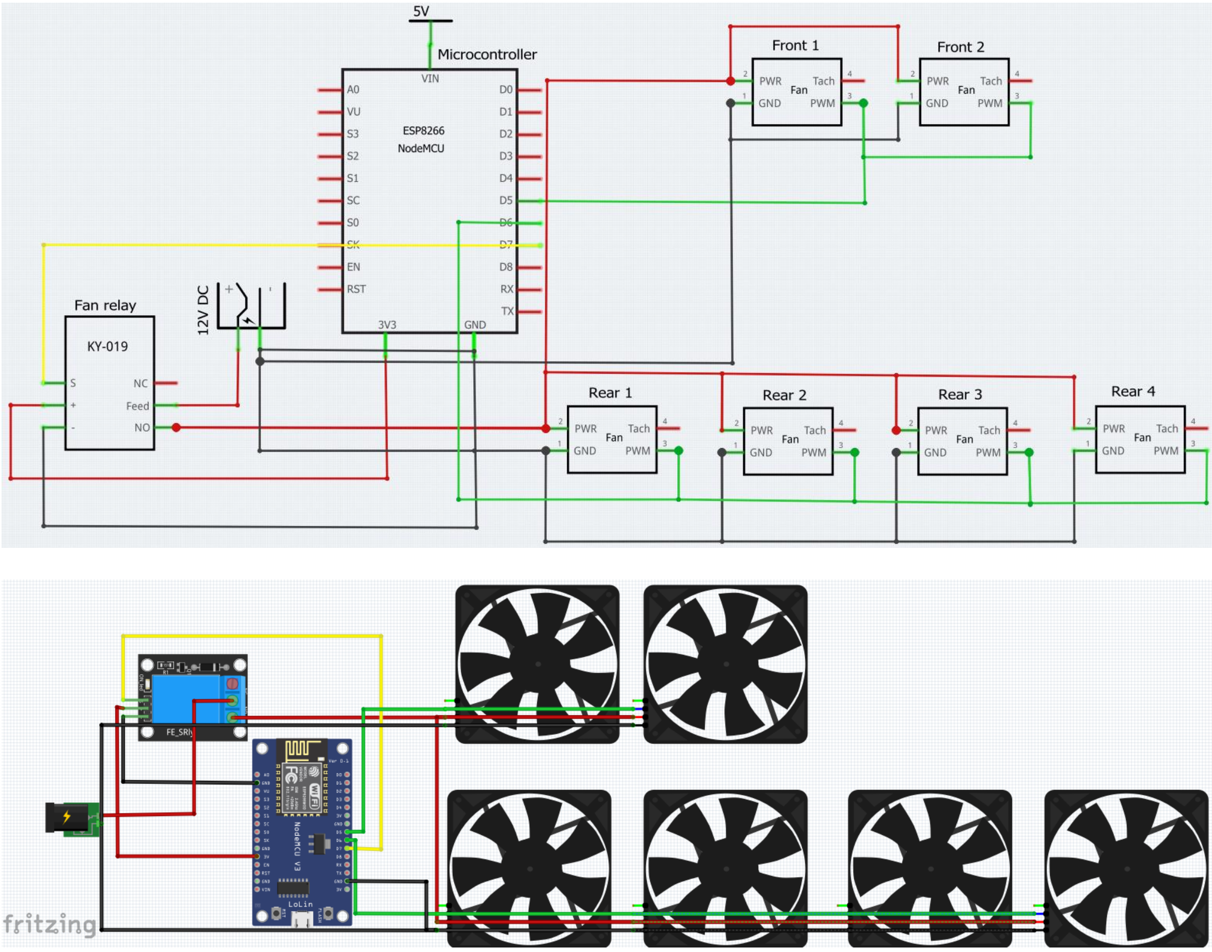

Figure 2.49: Fritzing and animated schematics of ventilation system.

Irrigation & Heating system

NodeMCU ESP8266 microcontroller manages the irrigation and heating system, in addition to the aforementioned systems. The water pump and the IR lamp need a 220-250V AC power source to operate. Two relays are installed in the circuit to control the state of the actuators. The relay modules are controlled and powered by the NodeMCU microcontroller. The relays are set in the Normally Open position, that is, the circuit is "open" when the relays are in the OFF state, whereas conversely, the circuit is "closed" when the relays are in the ON state.

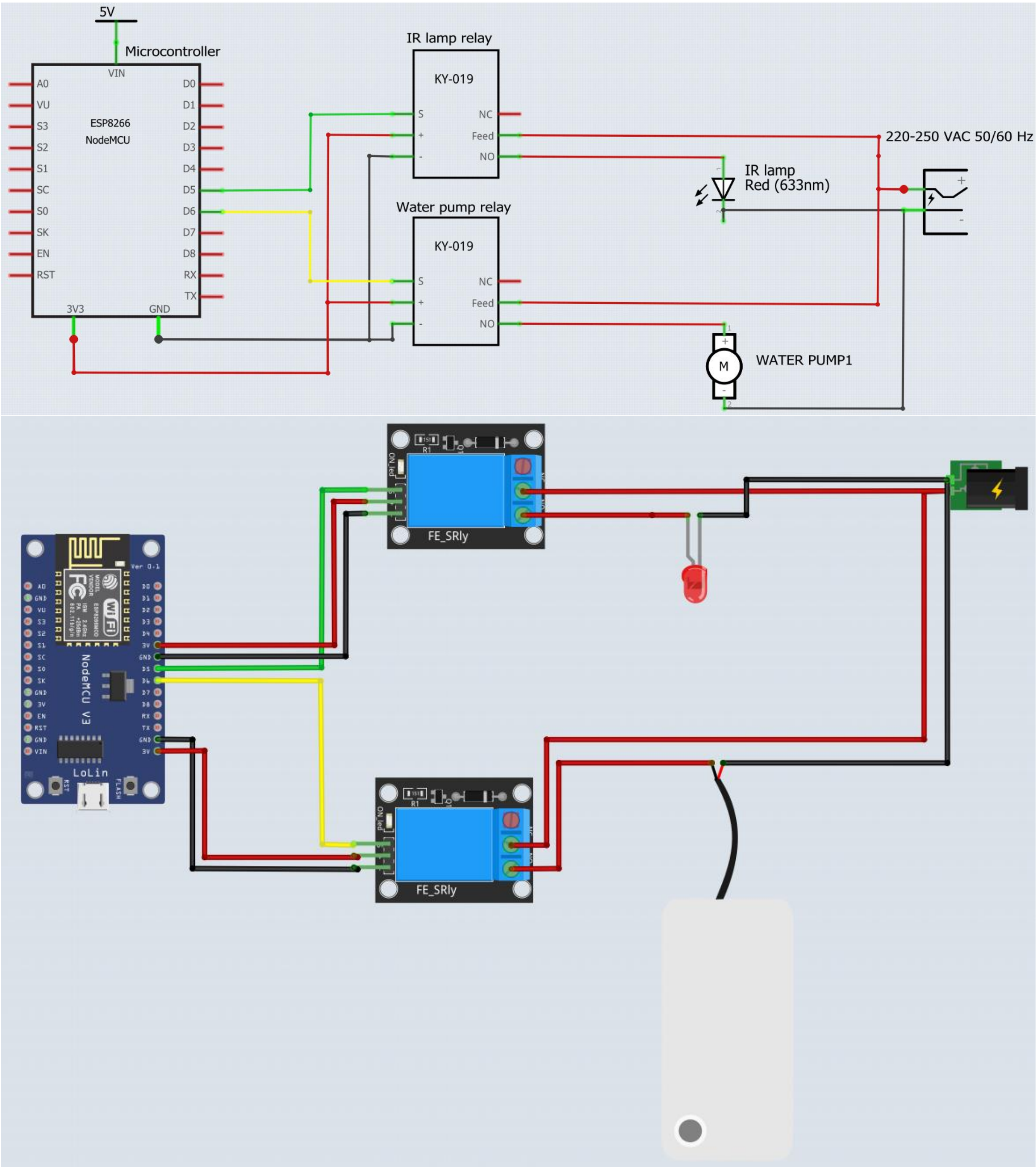

Figure 2.50: Fritzing and animated schematics of irrigation and heating systems.

2.3.2 Programming smart greenhouse

The microcontrollers NodeMCU ESP8266 v.3 and ESP32 boards were programmed with Arduino IDE software. These microcontrollers use the programming language of Arduinos, which is similar to C++. It is necessary to include the “ESP8266” board manager for the software to identify the boards and install the appropriate drivers to the computer used.

All boards communicate with Cayenne Application Programming Interface (API). As a result, “CayenneMQTTESP8266.h” library and “ssid”, “password”, “username”, “mqtt_password”, “client_id” credentials are required. Each device in the circuit sends and receives data through the virtual channels defined.

In the function “void setup” the code runs once and is generally used to setup the hardware, set initial values, start sensors, configure the actuators state, connect to Cayenne etc.

The codes in the functions “void loop” and “Cayenne.loop” are executed consecutively, as long as the board is powered. In this way, the microcontroller collects data from sensors, controls the actuators, and continuously communicates with the Cayenne API.

```
#include <CayenneMQTTESP8266.h>
#define CAYENNE_DEBUG
#define CAYENNE_PRINT Serial
char ssid[] = "Wi-Fi";
char password[] = "Wi-Fi password";
char username[] = "************************************";
char mqtt_password[] = "*******************************";
char client_id[] = "***********************************";
```

Figure 2.51: Cayenne setup code.

Greenhouse Micro-Climate Monitoring system 1

The GMCM system 1, as mentioned in the electronic circuit schematic, contains the DHT22, DS18B20, soil moisture and water level sensors. The code has to include their libraries “DHT.h”, “DallsTemperature.h” and “OneWire.h” to work correctly. The DHT22 sensor occupies two channels because it sends two data types to Cayenne: temperature and relative humidity. A loop is used to send data every 2 seconds due to the slow data reception of the sensor. The third virtual channel of Cayenne is dedicated to the DS 18B20 sensor, the fourth to the soil moisture sensor and the fifth to the water level sensor. The soil moisture sensor is calibrated by defining the measurements of 0% (air value) and at 100% (water value) water presence.

```
#include <DHT.h>
#include <DallasTemperature.h>
#include <OneWire.h>
#define DHTPIN 4
#define DHTTYPE DHT22
DHT dht(DHTPIN, DHTTYPE);
#define SENSOR_PIN 5
#define VIRTUAL_CHANNEL_DS18B20 3
OneWire oneWire(SENSOR_PIN);
DallasTemperature sensors(&oneWire);
#define VIRTUAL_CHANNEL_sm 4
#define VIRTUAL_CHANNEL_wl 5
int Liquid_level=0;
int wl=14;
const int AirValue = 780;
const int WaterValue = 400;
int soilMoistureValue = 0;
int perc=0;
const int sm=(A0);
int timeSinceLastRead = 0;

void setup() {
  Cayenne.begin(username, mqtt_password, client_id, ssid, password);
  pinMode(wl,INPUT);
  pinMode(sm,INPUT);
  dht.begin();
  sensors.begin();
}
void loop()
{ Cayenne.loop();
  if(timeSinceLastRead > 2000){
  float h = dht.readHumidity();
  float t = dht.readTemperature();
    if (isnan(h) || isnan(t) ){
      timeSinceLastRead = 0;
      return;}
  Cayenne.virtualWrite(1, t, TYPE_TEMPERATURE, UNIT_CELSIUS);
  Cayenne.virtualWrite(2, h, TYPE_RELATIVE_HUMIDITY, UNIT_PERCENT);
  timeSinceLastRead = 0;      }
  delay(1000);
  timeSinceLastRead += 100;
}
CAYENNE_OUT(VIRTUAL_CHANNEL_DS18B20)
{ sensors.requestTemperatures();
  Cayenne.celsiusWrite(VIRTUAL_CHANNEL_DS18B20, sensors.getTempCByIndex(0));
}
CAYENNE_OUT(VIRTUAL_CHANNEL_wl){
  Liquid_level=digitalRead(wl);
  Cayenne.virtualWrite(VIRTUAL_CHANNEL_wl, digitalRead(wl), "digital_sensor", "state");
  delay(5000);
}
CAYENNE_OUT(VIRTUAL_CHANNEL_sm){
  soilMoistureValue = analogRead(sm);
  perc=(100-100*(soilMoistureValue-WaterValue)/(AirValue-WaterValue));
  Cayenne.virtualWrite(VIRTUAL_CHANNEL_sm, perc, "analog_sensor", "%");
  delay(5000);
}
```

Figure 2.52: Greenhouse Micro-Climate Monitoring system 1.

Greenhouse Micro-Climate Monitoring system 2

Greenhouse micro-climate monitoring system 2 runs on ESP32 microcontroller, hence library “CayenneMQTTESP32.h” must be included. Furthermore, “DFRobot_CCS811”, “DFRobot_BME280” and “Wire” libraries are necessary for the sensors operation.

```
#include "DFRobot_CCS811.h"
#include "DFRobot_BME280.h"
#include "Wire.h"
#define VIRTUAL_CHANNEL_CO2 4
#define VIRTUAL_CHANNEL_TVOC 5
#define VIRTUAL_CHANNEL_AP 6
#define VIRTUAL_CHANNEL_ALT 7
#define VIRTUAL_CHANNEL_CO 9
#define SEA_LEVEL_PRESSURE    1015.0f
const int co=15;
int CO2=0;
int TVOC=0;
int coc=0;
typedef DFRobot_BME280_IIC    BME;
BME    bme(&Wire, 0x76);
DFRobot_CCS811 CCS811;

void setup(void)
{ Cayenne.begin(username, mqtt_password, client_id, ssid, password);
    pinMode(co,INPUT);
    while(CCS811.begin()!=0){
    delay(1000);}
    bme.reset();
    delay(200);
    while(bme.begin()!=0){
    delay(1000);}
    while(CCS811.checkDataReady() != true){delay(1000);}
}
void loop() {Cayenne.loop();}

CAYENNE_OUT(VIRTUAL_CHANNEL_CO2){
  CO2=CCS811.getCO2PPM();
  Cayenne.virtualWrite(VIRTUAL_CHANNEL_CO2, CO2, "analog_sensor", "ppm");
  delay(5000);}
CAYENNE_OUT(VIRTUAL_CHANNEL_TVOC){
  TVOC=CCS811.getTVOCPPB();
  Cayenne.virtualWrite(VIRTUAL_CHANNEL_TVOC, TVOC, "analog_sensor", "ppb");
  delay(5000);}
CAYENNE_OUT(VIRTUAL_CHANNEL_AP){
  uint32_t    press = bme.getPressure();
  Cayenne.virtualWrite(VIRTUAL_CHANNEL_AP, press, "analog_sensor", "Pa");
  delay(5000);}
CAYENNE_OUT(VIRTUAL_CHANNEL_ALT){
  uint32_t    press = bme.getPressure();
  float    alti = bme.calAltitude(SEA_LEVEL_PRESSURE, press);
  Cayenne.virtualWrite(VIRTUAL_CHANNEL_ALT, alti, "analog_sensor", "m");
  delay(5000);}
CAYENNE_OUT(VIRTUAL_CHANNEL_CO){
  coc = analogRead(co);
  Cayenne.virtualWrite(VIRTUAL_CHANNEL_CO, coc, "analog_sensor", "ppm");
  delay(5000);}
```

Figure 2.53: Greenhouse Micro-Climate Monitoring system 2.

Window opening mechanism

In the window opening mechanism code, five virtual channels are to be used. Two channels activate the stepper motor for opening or closing the window, one channel controls the state of the relay and two channels send data from the magnetic window sensors. In “void setup()”

function, pins of “step”, “dir”, and “relay” are set as output, “window1” and “window2” pins of magnetic switches are set as input and the relay is turned off with the “digitalWrite” function.

```
#define VIRTUAL_CHANNEL1 1
#define VIRTUAL_CHANNEL2 2
#define VIRTUAL_CHANNEL3 3
#define VIRTUAL_CHANNEL4 4
#define VIRTUAL_CHANNEL5 5
const int window1 = 5; //D1
const int window2 = 14; //D5
const int relay = 4; //D2
const int stepPin = 0; //D3
const int dirPin = 2; //D4

void setup()
{ Cayenne.begin(username, mqtt_password, client_id, ssid, password);
  pinMode(stepPin,OUTPUT);
  pinMode(dirPin,OUTPUT);
  pinMode(relay,OUTPUT);
  digitalWrite(relay, HIGH); //set relay off during setup
  pinMode(window1, INPUT_PULLUP);
  pinMode(window2, INPUT_PULLUP);
}
void loop() {  Cayenne.loop();}

CAYENNE_IN(VIRTUAL_CHANNEL1)
{ int enabled1 = getValue.asInt();
  if (enabled1 == 1) {
    digitalWrite(relay, LOW); //RELAY ON - INVERTED LOGIC
    delay(1000);
    digitalWrite(dirPin,LOW); // Enables the motor to move CCW
    // Makes 3200 pulses for making one full cycle rotation - window needs 2+ cycles
    for(int x = 0; x < 6700; x++) {
    digitalWrite(stepPin,HIGH);
    delayMicroseconds(100);
    digitalWrite(stepPin,LOW);
    delayMicroseconds(100);
}}}
CAYENNE_IN(VIRTUAL_CHANNEL2)
{  int enabled2 = getValue.asInt();
   if (enabled2 == 1) {
    digitalWrite(dirPin,HIGH); //Changes the rotations direction to CW
    for(int x = 0; x < 6700; x++) {
    digitalWrite(stepPin,HIGH);
    delayMicroseconds(100);
    digitalWrite(stepPin,LOW);
    delayMicroseconds(100);
    }delay(1000);
   digitalWrite(relay, HIGH); //RELAY OFF / POWER SAVE MODE - INVERTED LOGIC
}}
CAYENNE_IN(VIRTUAL_CHANNEL3)
{ if (getValue.asInt() == 0) {digitalWrite(relay, HIGH);}
  else {digitalWrite(relay, LOW);
}}
CAYENNE_OUT(VIRTUAL_CHANNEL4)
{  Cayenne.virtualWrite(VIRTUAL_CHANNEL4, digitalRead(window1), "digital_sensor", "d");}
CAYENNE_OUT(VIRTUAL_CHANNEL5)
{  Cayenne.virtualWrite(VIRTUAL_CHANNEL5, digitalRead(window2), "digital_sensor", "d");}
```

Figure 2.54: Window opening mechanism code.

Ventilation system

The ventilation system communicates with Cayenne by means of two channels; one to control the two front fans and a second one for the four rear fans. The fans are connected to PWM pins to regulate their speed with analog values in the range of 0-1023. The relay intercepts the current flow through the driver to prevent excess heat generation, when it is not in use.

Note: When there are no sensors to continuously communicate with the Cayenne, it is advised to use a virtual channel (0), which maintains the device online by sending continuous data.

```
#define VIRTUAL_CHANNEL_1 1
#define ACTUATOR_PIN_1 14
#define VIRTUAL_CHANNEL_2 2
#define ACTUATOR_PIN_2 12
#define VIRTUAL_CHANNEL_3 3
#define relay 13

void setup() {Cayenne.begin(username, mqtt_password, client_id, ssid, password);
              pinMode(ACTUATOR_PIN_1,OUTPUT);
              pinMode(ACTUATOR_PIN_2,OUTPUT);
              pinMode(relay,OUTPUT);
              digitalWrite(relay, HIGH);}
void loop() {Cayenne.loop();}

CAYENNE_IN(VIRTUAL_CHANNEL_1)
{ int value = getValue.asInt(); // 0 to 1023
  CAYENNE_LOG("Channel %d, pin %d, value %d", VIRTUAL_CHANNEL_1, ACTUATOR_PIN_1, value);
  // Write the value received to the PWM pin. analogWrite accepts a value from 0 to 1023
  analogWrite(ACTUATOR_PIN_1, value);
}
CAYENNE_IN(VIRTUAL_CHANNEL_2)
{ int value = getValue.asInt();
  CAYENNE_LOG("Channel %d, pin %d, value %d", VIRTUAL_CHANNEL_2, ACTUATOR_PIN_2, value);
  analogWrite(ACTUATOR_PIN_2, value);
}
CAYENNE_IN(VIRTUAL_CHANNEL_3)
{ if (getValue.asInt() == 0) {digitalWrite(relay, HIGH);}
  else {digitalWrite(relay, LOW); }
}
CAYENNE_OUT(0)
{ CAYENNE_LOG("Send data for Virtual Channel 0");
  Cayenne.virtualWrite(0, millis() / 1000);
}
```

Figure 2.55: Ventilation system code.

Irrigation and Heating system

The irrigation and heating systems contain complex devices, such as a water pump and an infrared light lamp, although they are controlled by the microprocessor and two relays. The relays are in Normally Open position and set OFF when the code runs. The relays are changing state by turning ON and OFF the buttons of the Cayenne trough the channels 1 and 2.

```
#define VIRTUAL_CHANNEL1 1
#define pump 12 //D6 Normally Open RELAY
#define VIRTUAL_CHANNEL2 2
#define irlamp 14 //D5 NO RELAY

void setup() { Cayenne.begin(username, mqtt_password, client_id, ssid, password);
  pinMode(pump, OUTPUT);
  pinMode(irlamp, OUTPUT);
  digitalWrite(pump, HIGH);
  digitalWrite(irlamp, HIGH);
}
void loop() {Cayenne.loop();}

CAYENNE_IN(VIRTUAL_CHANNEL1)
{ if (getValue.asInt() != 0) {
    digitalWrite(pump, LOW);} //WP ON
  else {digitalWrite(pump, HIGH);}// WP OFF
}
CAYENNE_IN(VIRTUAL_CHANNEL2)
{ if (getValue.asInt() != 0) {
    digitalWrite(irlamp, LOW);} //IR lamp ON
  else {digitalWrite(irlamp, HIGH); }// IR lamp OFF
}
```

Figure 2.56: Irrigation and heating systems code.

2.3.3 Cayenne IoT project builder

Cayenne is the world's first drag and drop IoT project builder that empowers developers, designers, and engineers to quickly prototype and share their connected device projects. Cayenne was designed to help users create Internet of Things prototypes and then bring them to production.

The Cayenne MQTT API is used to connect any device with the Cayenne Cloud. After connecting a device, it can send data to the Cayenne dashboard and display it using widgets.

Commands can also be received from Cayenne, allowing remote control and automation of your devices. Cayenne makes it easy to manage connected devices from anywhere. The online dashboard gives the possibility to monitor device status, make changes to devices, and control them.

Besides real-time data visualization, Cayenne also stores historical data that enables meaningful patterns of behavior recognition and thus improvements on IoT projects.

Cayenne allows to create scheduled events for Raspberry Pis, Arduinos, sensors, and actuators connected. Cayenne also allows creating triggered actions on and between devices based upon their state. Additionally, Cayenne enables to receive notifications when a has reached a certain state!

Lastly by using Cayenne's asset tracking features, the past and present location of the connected devices to Cayenne is indicated.

Figure 2.57: Cayenne API dashboard [82].

A particular feature of Cayenne is its setup. Setting up Cayenne is not demanding, considering that it sketches the code for compatible computers, microcontrollers, sensors, actuators, extensions etc. After uploading the code with the credentials on the board, this connects automatically to the platform while Cayenne detects any sensors and adds their channels.

Few widgets have to be manually added to the dashboard by setting up the name, the device connected, the channel, and the icon. All these features render Cayenne an ideal option for unexperienced and experienced users alike.

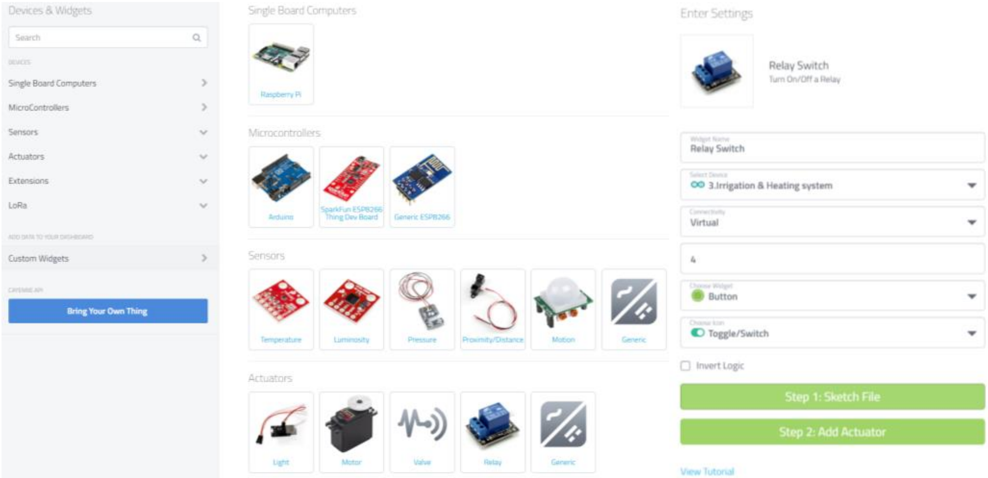

Figure 2.58: Setting up devices and widgets in Cayenne [82].

The dashboard of the proposed smart greenhouse system in Cayenne consists of:

- Nine graph widgets showing the sensors measurements
- Two button widgets activating the window opening mechanism in two directions
- Two motion widgets indicating the position of the window
- Two button widgets activating the heating and irrigation system
- Two widgets regulating the speed of the front and rear fans in the range of 0-1000‰
- A switch widget controlling the power supply of the fans
- A widget representing the water level sensor status

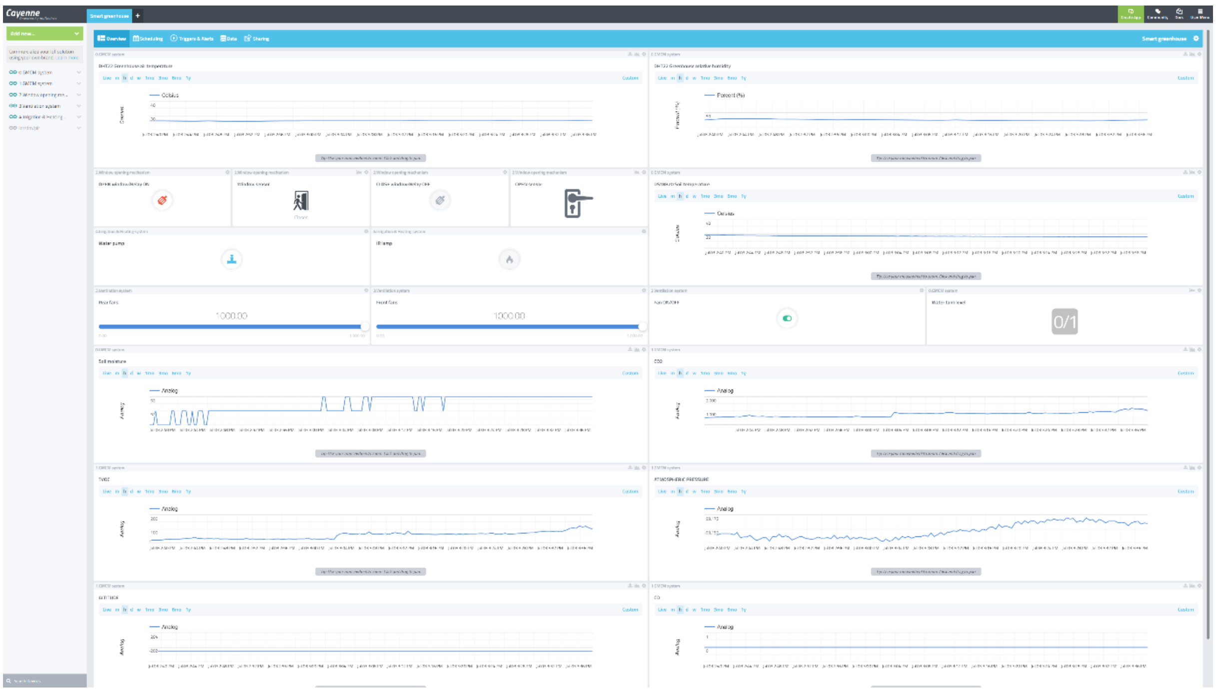

Figure 2.59: Proposed smart greenhouse project Cayenne dashboard.

CHAPTER 3

Chapter 3: Smart greenhouse implementation on experimental model

3.1 Introduction

The construction of an experimental model and the implementation of the smart greenhouse design consist the second part of the thesis. The experimental greenhouse model was placed in the Industrial Energy Environmental System Laboratory at Technical University of Crete, where all the aforementioned monitoring systems of Hobolink, Meazon, Agenso and the proposed were used to form the smart greenhouse. First, the construction of the experimental model and the installation of the equipment are analyzed. Second, the various user interfaces that give remote access to the greenhouse are presented. Finally, the measurement data collected from the sensors as well as the results from the actuators operation are examined.

3.2 Smart greenhouse implementation

The software used to design the experimental greenhouse model is FreeCAD. FreeCAD is a free and open-source general-purpose parametric 3D computer-aided design (CAD) modeler and a building information modeling (BIM) software with finite element method (FEM) support. FreeCAD also features a workbench for 2D technical drawing. FreeCAD saves files in “FCStd” format and can export “stl” files of the parts to allow 3D printing.

The 3D printed parts are made of PLA material. Their interior consists of nerves that form square cells. This significantly reduces their weight and printing time, without compromising their durability. Fillets were made in every 90-degree angle to avoid concentration of forces.

3.2.1 Experimental greenhouse model

In this section, the prototype model developed for the installation of the equipment is described. The metal structure of the greenhouse is 1m long, 1m wide and 1m high. The steel beams of the metal structure are 25mm thick. The exterior surface of the greenhouse is covered with 3mm plexiglass. There are four 120mm diameter holes at the side wall and two 120mm diameter holes at the gable, where fans for dynamic ventilation have been installed. Two 3D printed bases for the stepper motor and the sensors are mounted on the model, which are detailed in sections 3.2.1 and 3.2.2. The 2D technical drawings, the 3D model and the actual experimental smart greenhouse are shown in the following figures.

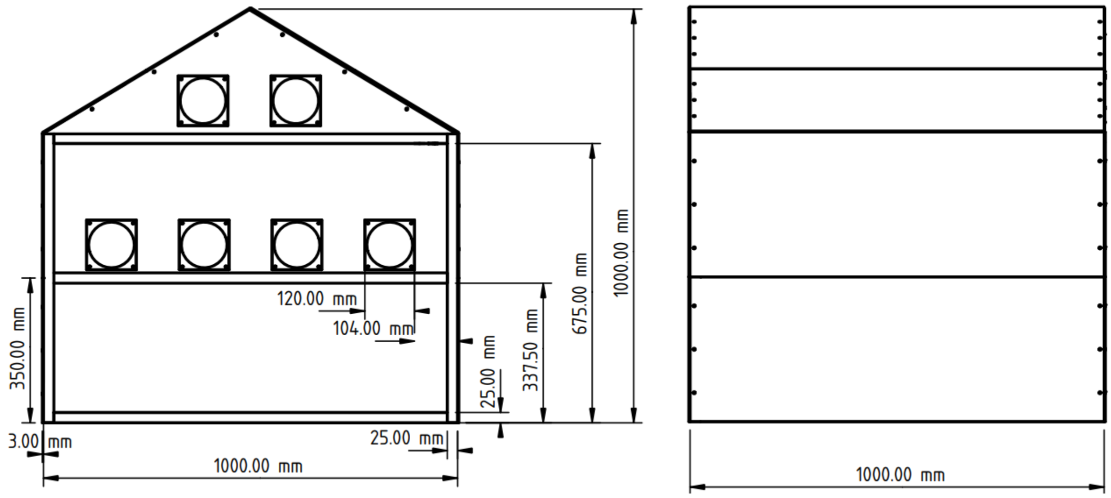

Figure 3.1: Front and left views of experimental greenhouse technical drawing in FreeCAD software.

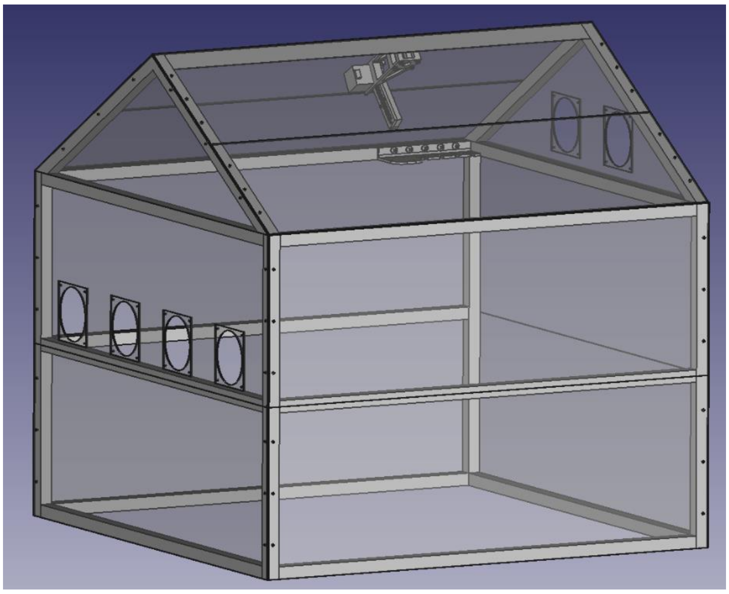

Figure 3.2: Experimental greenhouse 3D computer-aided design in FreeCAD.

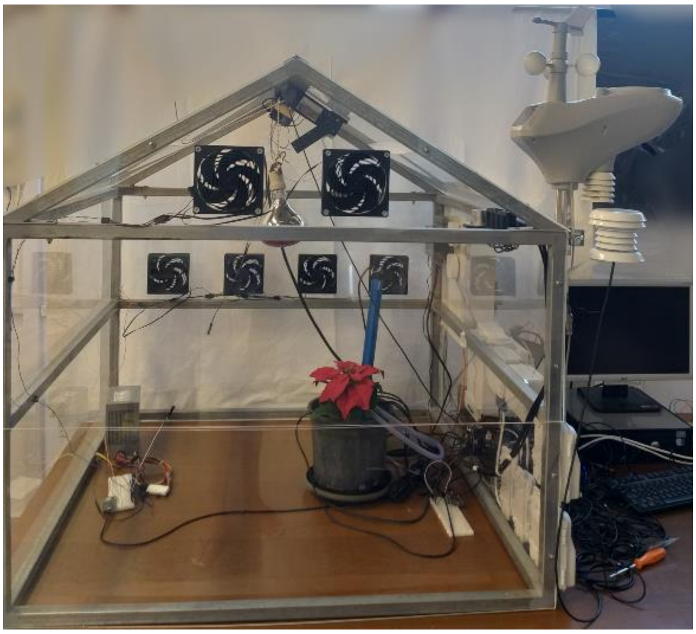

Figure 3.3: Experimental smart greenhouse model in TUC IEESL.

3.2.2 Sensors installation

Multiple sensors of different systems are installed inside and outside the greenhouse to measure and monitor the micro-climate and the exterior conditions. More precisely the installed sensors measure:

Room sensors

AGENSO

- Air temperature
- Relative humidity
- Air pressure
- Light intensity

HOBOLINK

- Air temperature
- Relative humidity
- Dew point

Greenhouse sensors

HOBOLINK

- PA radiation (2)
- Solar radiation (2)
- UV radiation
- CO-CO_2 concentration
- Rainfall
- Water content (4)
- Soil temperature (3)
- Soil conductivity

AGENSO

- Soil moisture (2)
- Soil temperature

MEAZON

- Air temperature (2)
- Relative humidity (2)
- Air quality
- TVOC level

PROPOSED GMCMs

- Air temperature
- Relative humidity
- Soil temperature
- Soil moisture
- Altitude
- Air pressure
- CO_2 concentration
- CO concentration
- TVOC level
- Water tank level

Sensors base

The five Hobolink sensors for solar radiation, PA radiation and UV radiation require a fixed face-up position, so that light enters. Therefore, a base was designed with 3D CAD software and 3D printed. The 2D technical drawings, the 3D CAD assembly and the mounted 3D printed part are shown in the following figures.

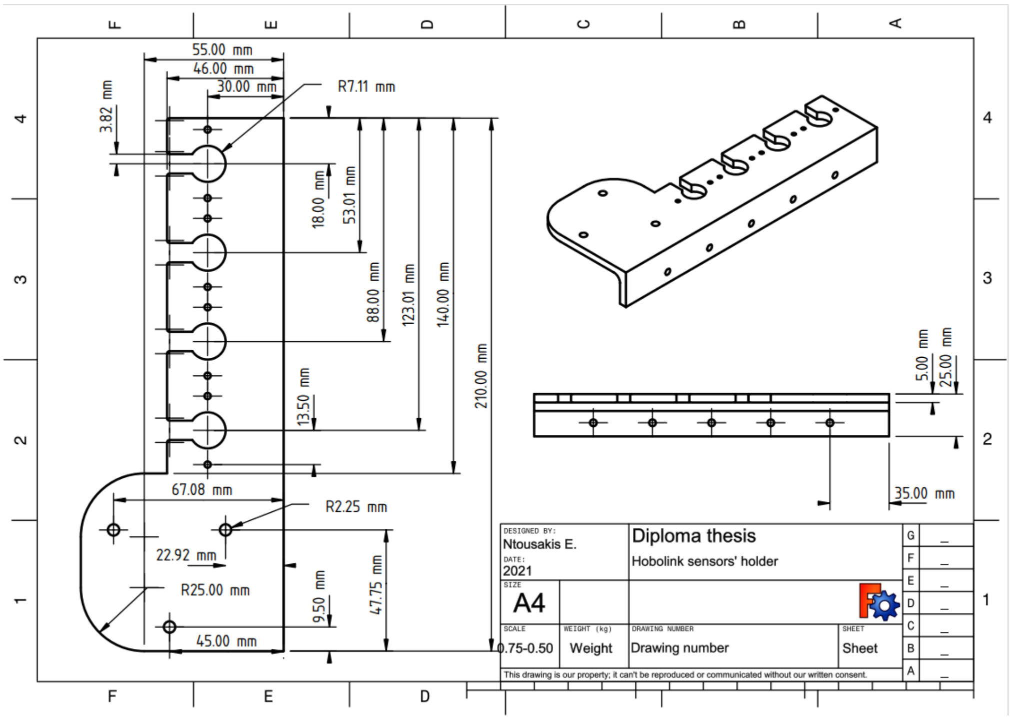

Figure 3.4: Top, left, and isometric views of sensors base.

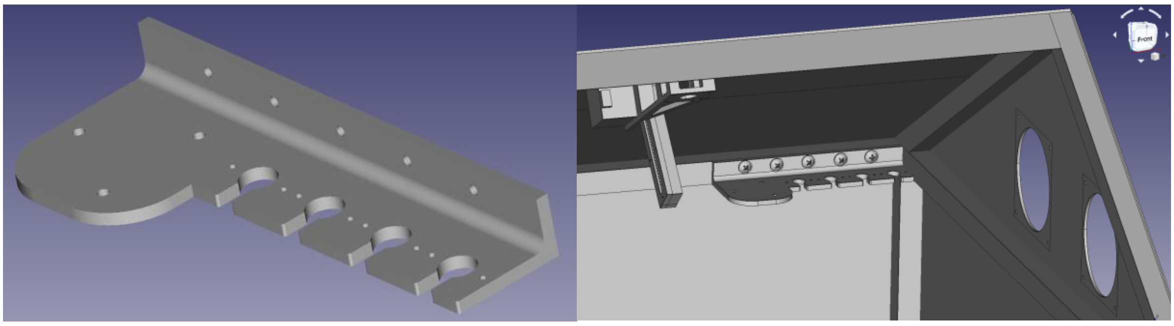

Figure 3.5: 3D computer-aided design of sensors holder.

Figure 3.6: 3D printed sensors holder.

3.3.3 Actuators installation

Window opening mechanism

The window opening mechanism is responsible for the natural ventilation of the experimental greenhouse. The whole assembly consists of a microcontroller, a stepper motor, a stepper motor driver, a relay, two magnetic switches and the 3D printed parts: stepper motor holder, gear, window slider and the two parts of rack. The rack is divided into two parts, so that the gear can be installed between them and not be transposed horizontally. Only the thin cylinder of the gear can pass through the second part of the rack. The stepper motor and the driver are powered by a PSU, while the microcontroller by a 5V USB port.

A stepper motor provides the required force to lift the plexiglass attached to the greenhouse roof with a hinge. The window is 1000mm long, 291.55mm high, 3mm wide and consecutively its volume is V=874.650mm^3. The average density of the plexiglass is ρ=1.180kg/m^3. The mass of the window, according to the equation m=V × ρ, equals to m=1.032087kg. The total mass of the window, the window slider and the racks does not overpass 1.5kg.

The stepper motor used has a maximum torque of 4kg*cm. The gear applying torque from the motor to the rack has a radius smaller than 1cm. As the motor easily lifts the window, the stepper motor driver is undervolted to prevent excess heat generated, that can harm the system.

The 2D technical drawings, the 3D models and the actual system are provided below.

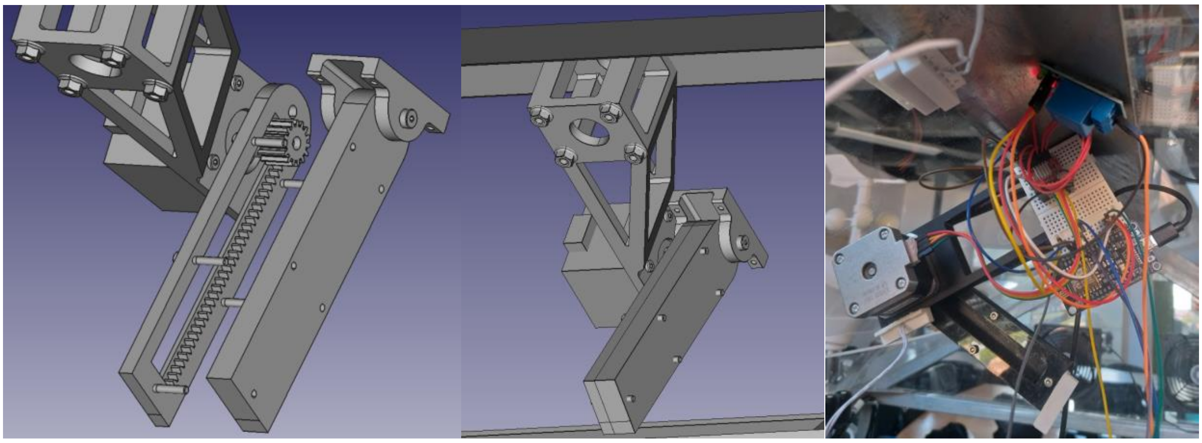

Figure 3.7: Window opening mechanism 3D CAD exploded view, assembly and implementation.

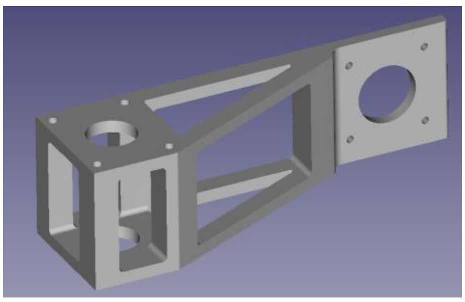

Figure 3.8: Stepper motor holder 3D CAD part.

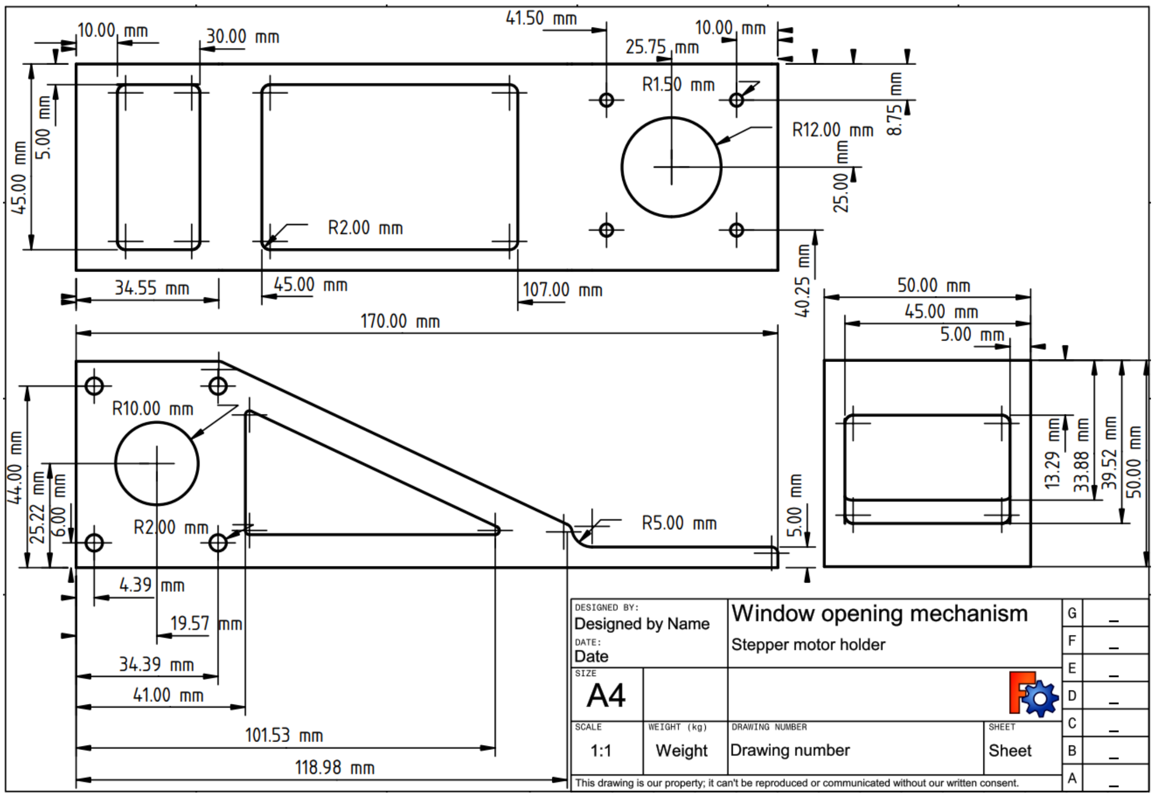

Figure 3.9: Front, top, and left views of stepper motor holder.

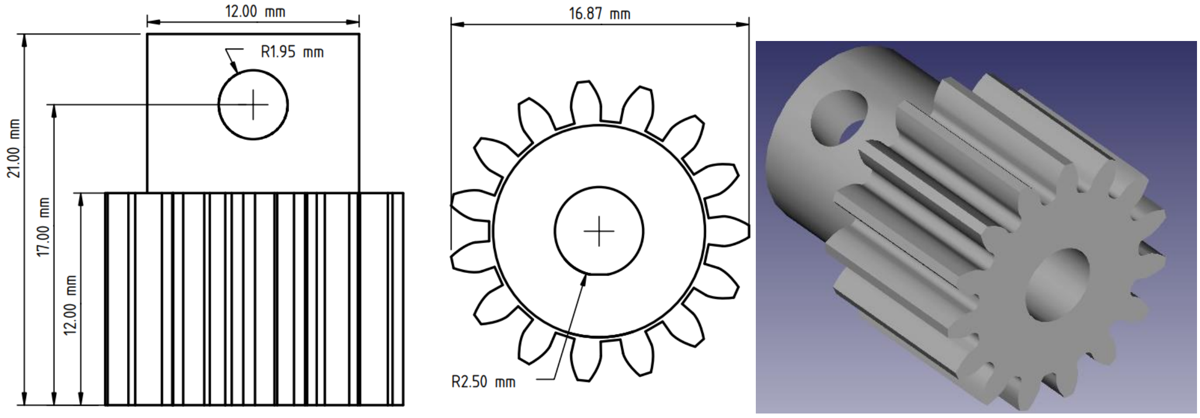

Figure 3.10: Front and top views of stepper motor gear.

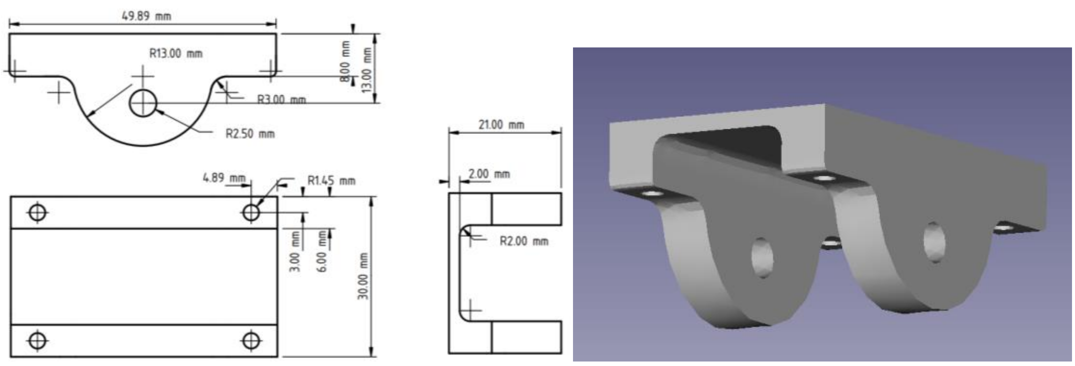

Figure 3.11: Front, top and left views of window slider.

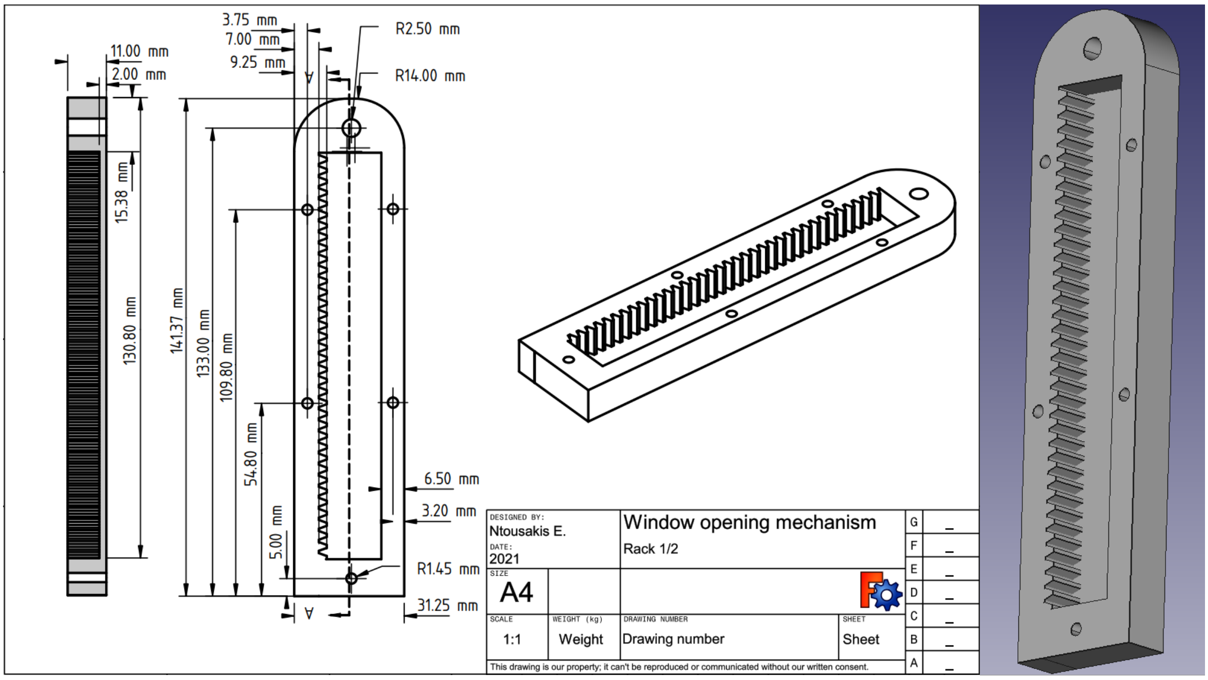

Figure 3.12: Front, right section, and isometric views of rack part 1.

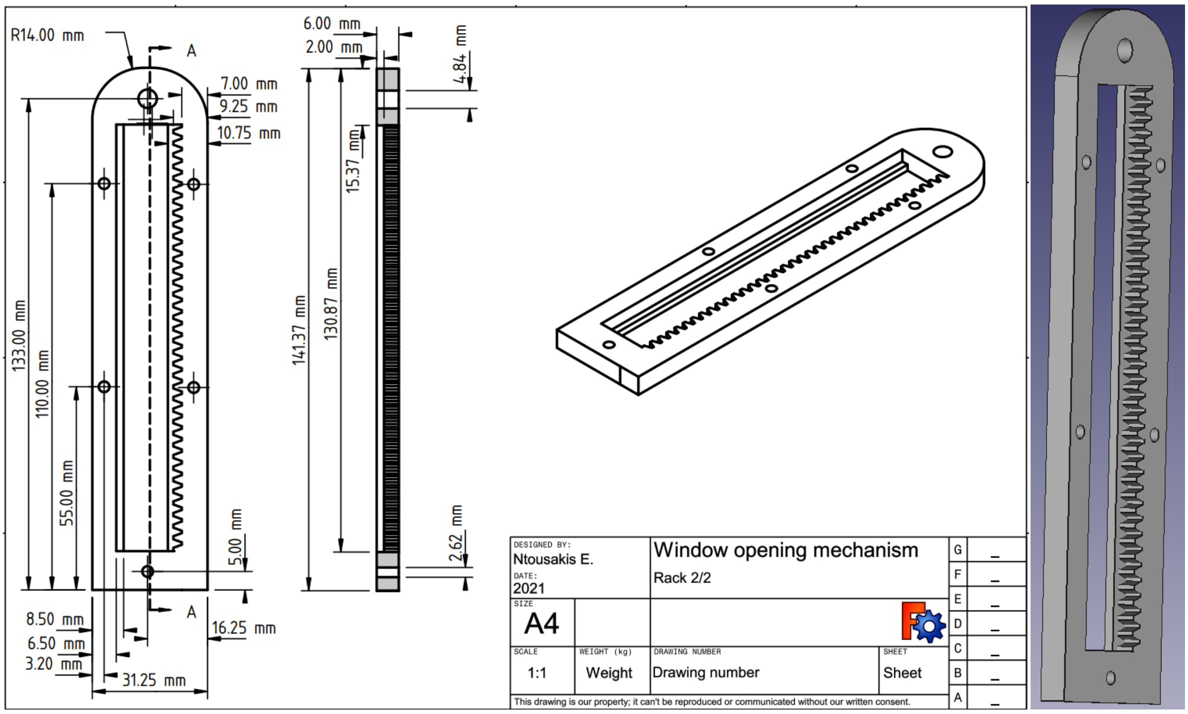

Figure 3.13: Front, left section, and isometric views of rack part 2.

Ventilation system

The six fans installed at the predefined holes of the plexiglasses consist the dynamic ventilation system. They are powered by the PSU and controlled by the microcontroller on the left corner.

Figure 3.14: The implementation of the dynamic ventilation system.

Irrigation system

The submerged water pump, the water tank and the 10mm tubes form the experimental irrigation system. Once the relay of the water pump is activated, the pump transfers water to the flowerpot, where the soil sensors are immersed.

Figure 3.15: The irrigation system of the experimental greenhouse.

Heating system

The infrared lamp of the heating system is installed inside the greenhouse, 60cm above the ground. The microcontroller of the irrigation and heating systems with their relays are placed outside of the greenhouse alongside a 220V AC plug.

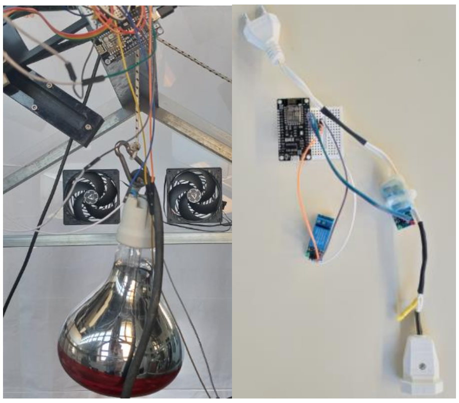

Figure 3.16: The infrared lamp and the microcontroller with the relay of the heating system.

3.4 Remote monitoring and control user interface software

Hobolink

The Hobolink web-based software can be accessed remotely via any web browser or mobile device. Hobolink allows easy configuration of sensors, logging rates, alarm notifications, or relay actions. It can be configured to send email or a text/SMS messages when conditions exceed set thresholds. Multiple levels of alarms and actions can be set for each sensor as well. Additionally, Hobolink interface integrates Google Maps to allow quick view of all HOBO devices' readings, alarm status and location. The HOBOlink dashboard enables instant visualization of current or historical data of a custom date range with graphs and can be customized to any kind of needs with the dashboard builder and the library of widgets. Lastly, the data can be manually exported or scheduled to be automatically delivered in "txt" or "csv" formats.

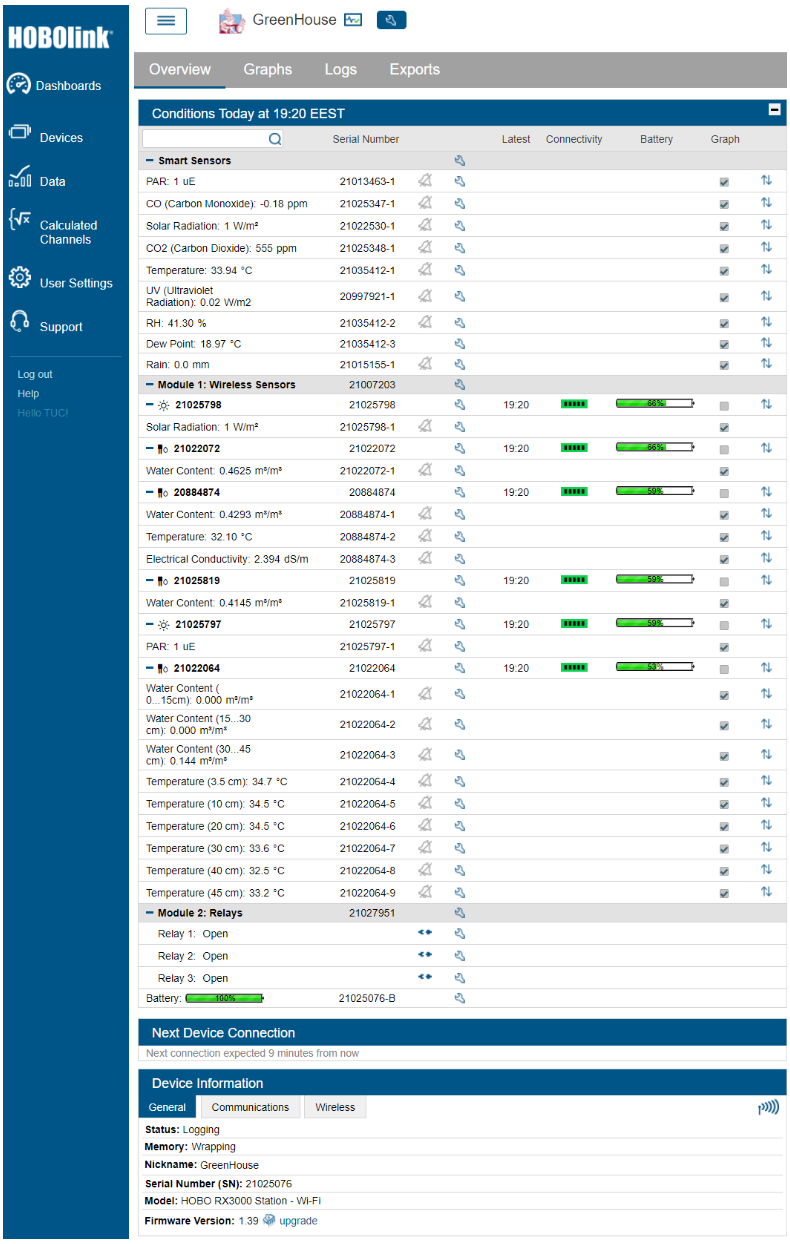

Figure 3.17: Hobolink user interface.

Meazon

Meazon provides a web-based platform to check the latest conditions of the active sensors and control its relays. It can be accessed remotely via any web browser or mobile device. The dashboard enables instant visualization of current, or historical data with graphs. Ultimately, the data can be manually saved in “xlsx” format.

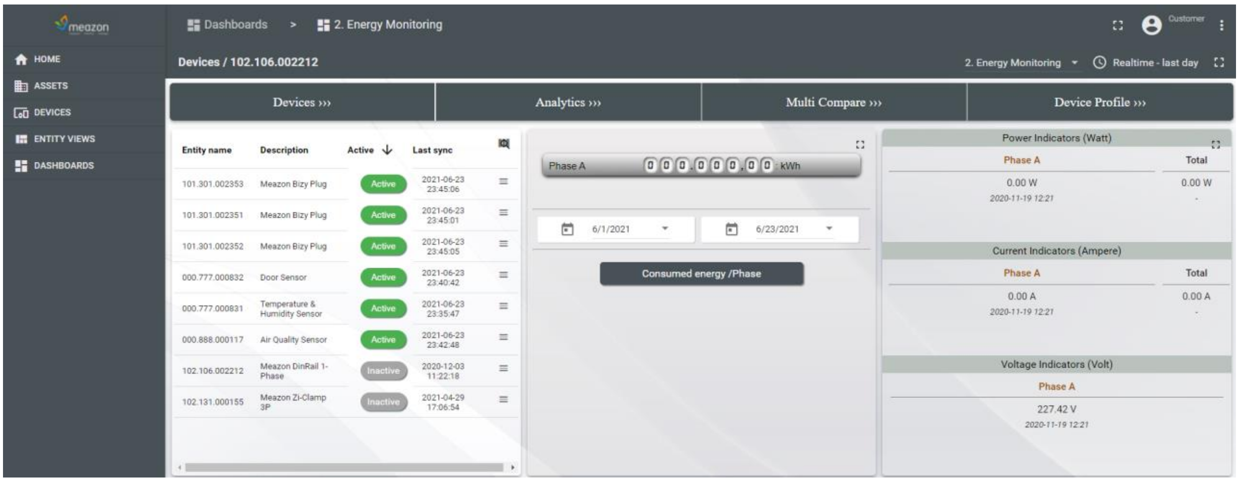

Figure 3.18: Meazon user interface.

Agenso

Agenso web-based software can be accessed remotely via any device with internet access. It can be configured to send alerts when conditions exceed set thresholds. Additionally, Agenso interface integrates Google Maps to allow quick view the devices’ readings, alarm status and location. The dashboard enables instant visualization of current or historical data and of weather forecast. Finally, the data can be saved in “xls” or “csv” formats and the graphs in “png”, “jpeg”, “pdf”, or “svg” image format.

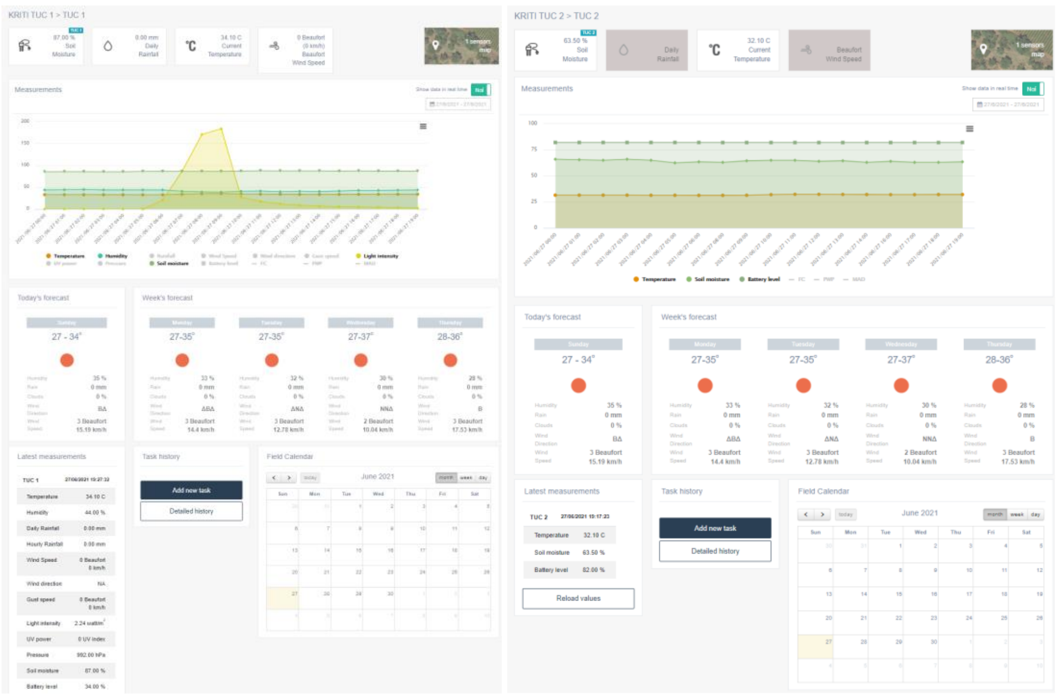

Figure 3.19: Agenso station 1 and 2 user interface.

Proposed GMCM system

The proposed greenhouse micro-climate monitoring systems was set to communicate with Cayenne IoT platform, which offers many possibilities and services as the previously mentioned platforms at zero cost.

Graphs are used to visualize real-time and historical data of the sensors and widgets to display and control the state of the actuators. Cayenne allows to create scheduled events or triggered actions on and between devices based upon their state. Three triggered actions were configured in this project. When the air temperature reaches 50°C, the fans are activated at full speed, but when the air temperature of the greenhouse drops below 10°C the heating system is activated. The third trigger turns off the irrigation system, when the water tank is empty. It is also possible to receive notifications and emails when has reached a certain state. As a last point, data can be exported in “csv” format for further analysis or process.

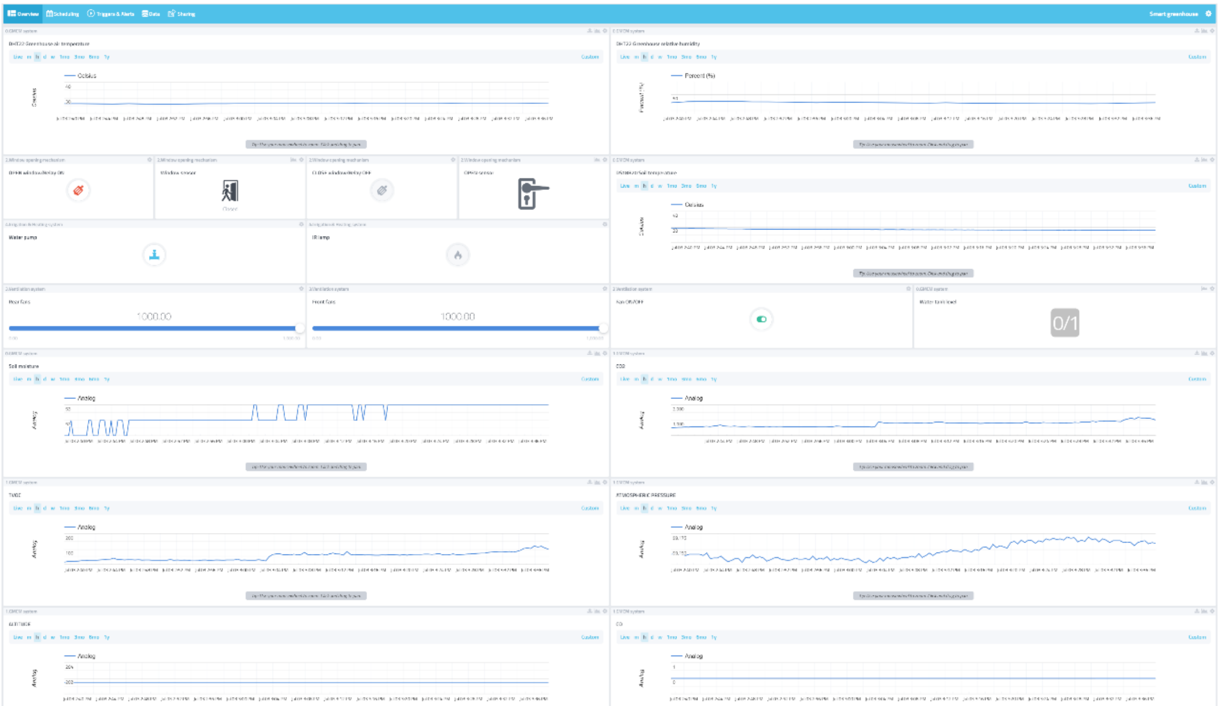

Figure 3.20: Cayenne user interface.

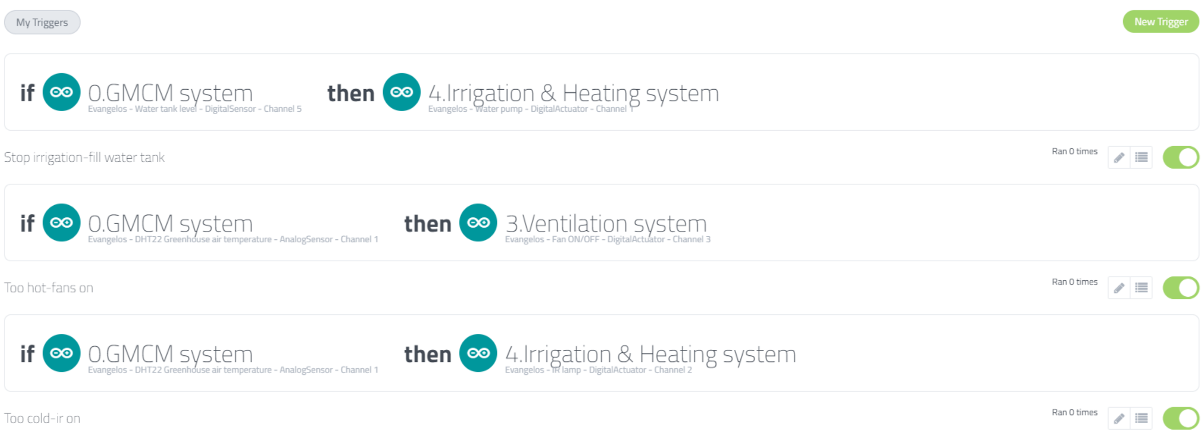

Figure 3.21: Automatic greenhouse micro-climate control with Cayenne triggered actions.

3.5 Sensors data and comparison

On June 21 all day long the room temperature is almost stable, approximately 29.00°C and the humidity level about 51.00%. It is observed that during the morning hours 07:00-10:00 a.m., when the room is exposed to sunlight as indicated by the photosynthetically active radiation (PAR) and solar radiation sensors (figure 3.23), the temperature rises by 2-3°C, reaching 32.00°C and the relative humidity falls by 5-6%, at 45.00%.

In case there is no intervention, the micro-climate conditions inside the greenhouse are almost the same as the room's conditions. Nevertheless, the microclimate parameters are observed to fluctuate 60 minutes later than the outdoor conditions. The soil temperature, contrary to the air temperature, rises by only 0.50°C reaching 28.00°C. The soil moisture is not prone to changes, unless the irrigation system is activated, when the soil moisture rises. These conditions inside the greenhouse are maintained for about 30 more minutes and the conditions readjust within 2 hours.

It is worth mentioning that the rain sensor shows no measurements as the testing takes place inside the IEESL laboratory. Furthermore, the Hobolink multi-depth sensor is immersed into the soil at the sensor's depths of 30-45cm.

Table 3.1: Outdoor conditions change during sunlight exposure (air temperature and relative humidity by Agenso and Hobolink systems).

Time/variable	AT-AGENSO	AT-HOBO	RH-AGENSO	RH-HOBO
06:00	29.00°C	29.00°C	51.00 %	51.00 %
09:00	32.00°C	31.00°C	45.00 %	46.00 %

Table 3.2: Greenhouse micro-climate conditions change during sunlight exposure (air temperature, relative humidity and soil temperature by Meazon air quality sensor, proposed GMCM system and Hobolink).

Time/variable	AT-MAQ	RH-MAQ	AT-GMCM	RH-GMCM	ST-GMCM	ST-HOBO
07:00	29.00°C	51.50 %	28.50°C	50.00 %	27.00°C	29.00°C
10:00	31.00°C	46.00 %	30.50°C	46.00 %	27.50°C	29.50°C

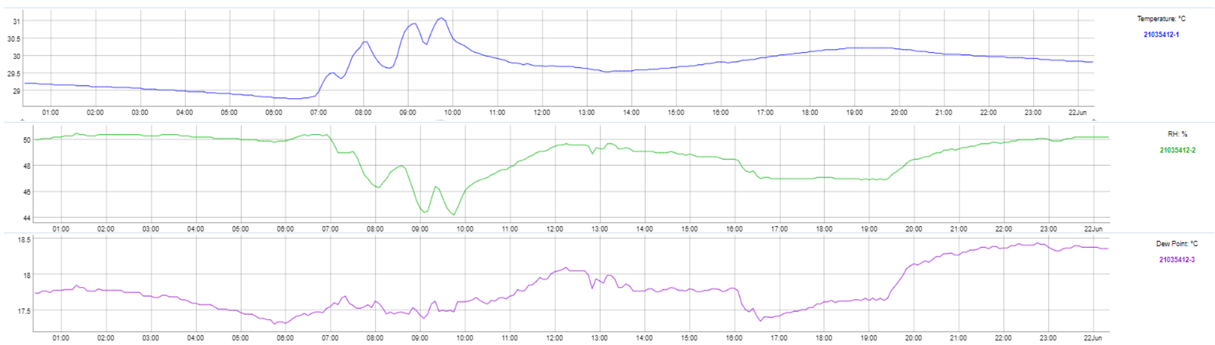

Figure 3.22: 24h data diagrams of Hobolink monitoring system (air temperature, relative humidity, dew point).

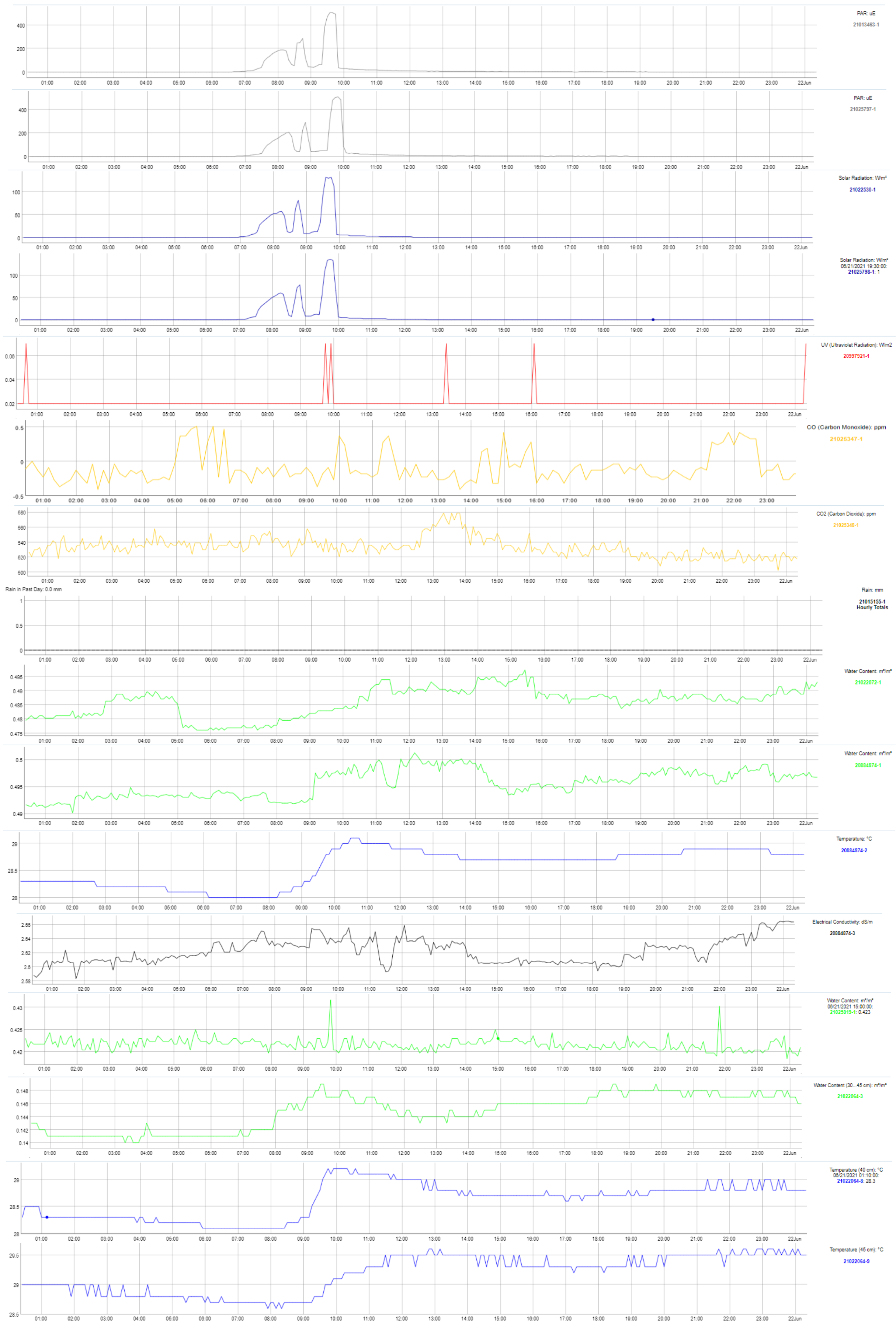

Figure 3.23: 24h data diagrams of Hobolink monitoring system (PA radiation, solar radiation, UV radiation, CO-CO_2 concentrations, rain, water content, soil temperature and electrical conductivity sensors).

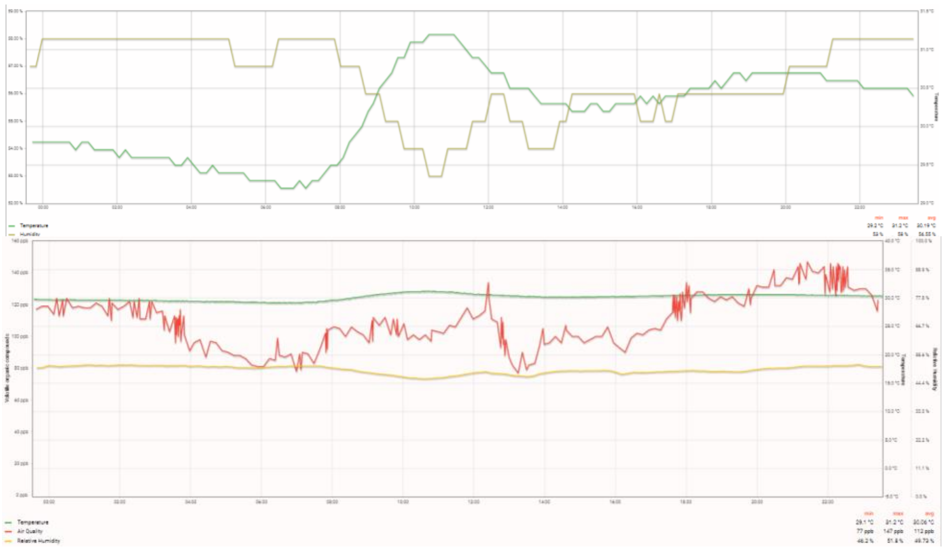

Figure 3.24: 24h data diagrams of Meazon air temperature-relative humidity and air quality sensors.

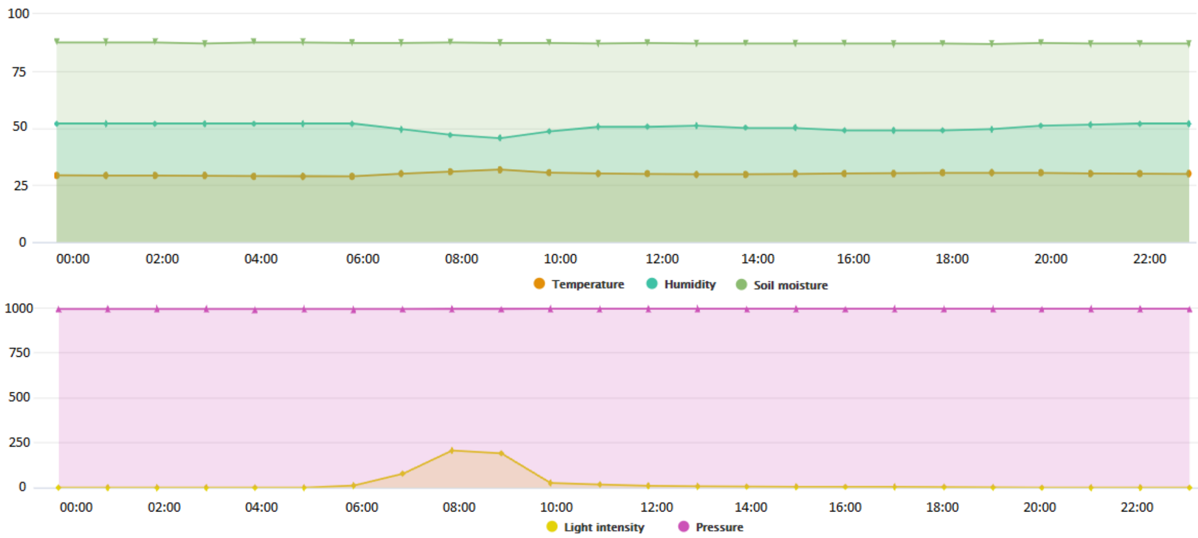

Figure 3.25: 24h data diagrams of Agenso monitoring system (temperature, relative humidity, soil moisture, air pressure, light intensity).

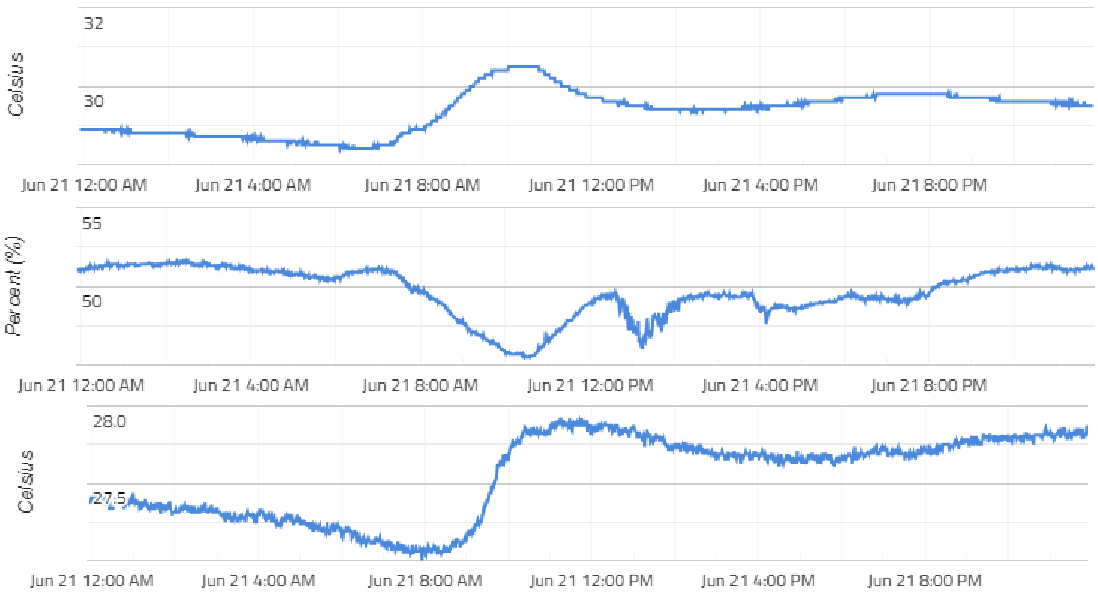

Figure 3.26: 24h data diagrams of proposed GMCM system 1 (temperature, relative humidity, soil temperature).

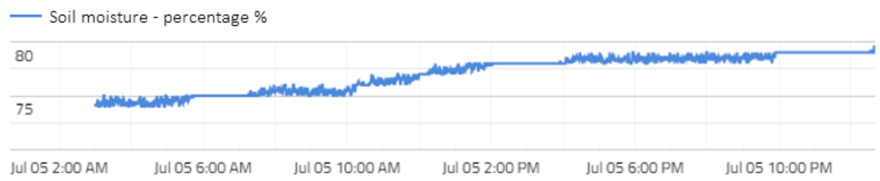

Figure 3.27: 24h data diagram of proposed GMCM system 1 (soil moisture sensor).

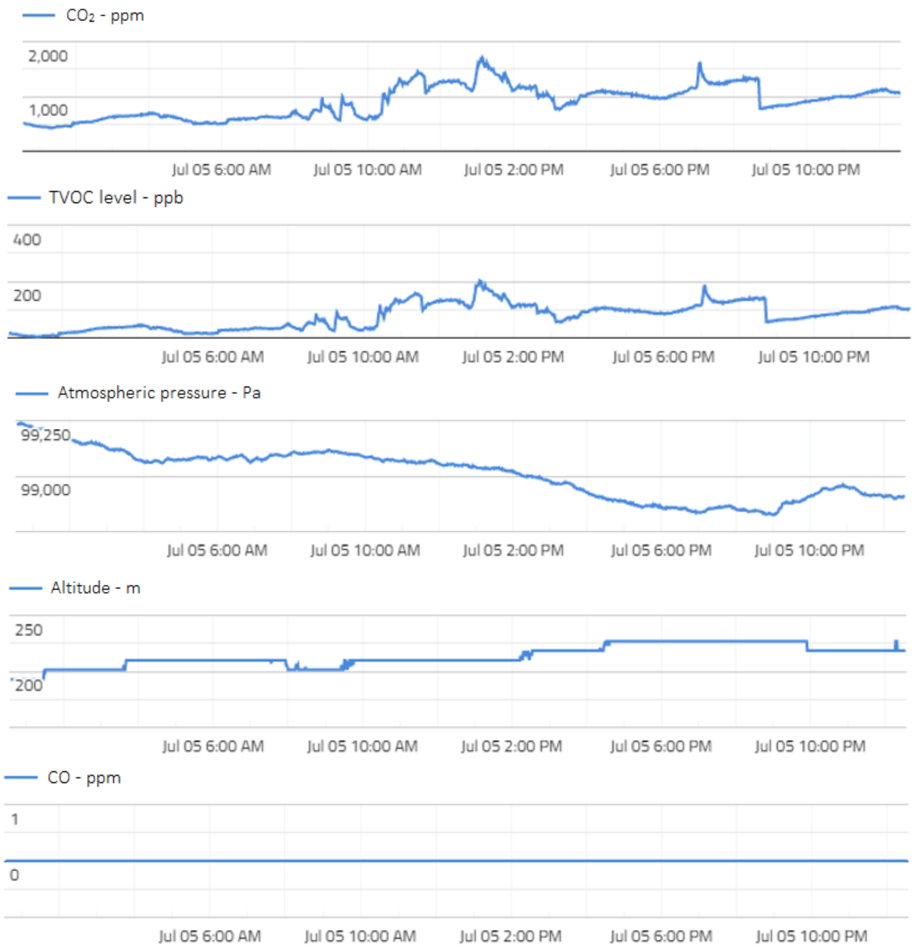

Figure 3.28: 24h data diagrams of proposed GMCM system 2 (CO_2 concentration, TVOC level, atmospheric pressure, altitude, CO concentration).

3.6 Actuators operation and results

1st test: Heating system

The first test took place on June 18 after 11:00 a.m., when there is no sunlight exposure and the outdoor conditions are stable. Between 11:20 and 13:50, the room temperature was approximately 27.50°C and the humidity slightly fluctuated between 48.00-49.00%.

During the first test, the heating system was activated for one hour, that is from 11:20 a.m. to 12:20 p.m. After activating the heating system, an increase of 3-6°C in the air temperature and a decrease of 6-12% in the relative humidity were observed. These conditions inside the greenhouse were reset in about one and a half hours (1.30 hours) after turning off the heating system. The soil temperature rose by 2.50-5.00°C and was reset around 17:00, after 4.30 hours. Last, there were no noticeable changes in soil moisture during the test period.

Note: The RXW-GP3 multi-depth sensor was installed at 30cm. As a result, 40cm measurements are 10 cm deep and the 45cm measurements are 15cm deep in the soil (figure 3.31).

Table 3.3: Outdoor conditions change after heating system activation (air temperature and relative humidity monitored by Hobolink and Agenso systems).

18/06/21	Room Temp (H)	Room Temp (A)	Room RH (H)	Room RH (A)
11:20	27.50°C	27.80°C	48.20 %	49.25 %
12:20	28.20°C	27.70°C	46.90 %	49.75 %
12:50	27.60°C	27.60°C	47.70 %	50.00 %
13:50	27.30°C	27.50°C	48.30 %	49.25 %

Table 3.4: Greenhouse micro-climate conditions change after heating system activation (air temperature, relative humidity, and soil temperature by Meazon air quality sensor, proposed GMCM system and Hobolink).

18/06/21	GH Temp (Meazon)	GH Temp (GMCM)	GH RH (Meazon)	GH RH (GMCM)
11.20	29.00°C	27.70°C	45.60 %	46.30 %
12.20	32.00°C	33.60°C	39.80 %	33.60 %
12.50	31.10°C	29.50°C	41.20 %	42.20 %
13.50	28.80°C	27.70°C	45.70 %	46.90 %

Table 3.5: Greenhouse micro-climate conditions change after heating system activation (soil temperature and soil temperature by proposed GMCM system and Hobolink).

18/06/21	GH ST (GMCM)	GH ST (H)	GH SM (H)
11:20	25.70°C	26.70°C	50.50 %
12:20	28.10°C	31.70°C	50.60 %
12:50	27.90°C	29.70°C	50.35 %
13:50	27.20°C	28.00°C	50.15 %

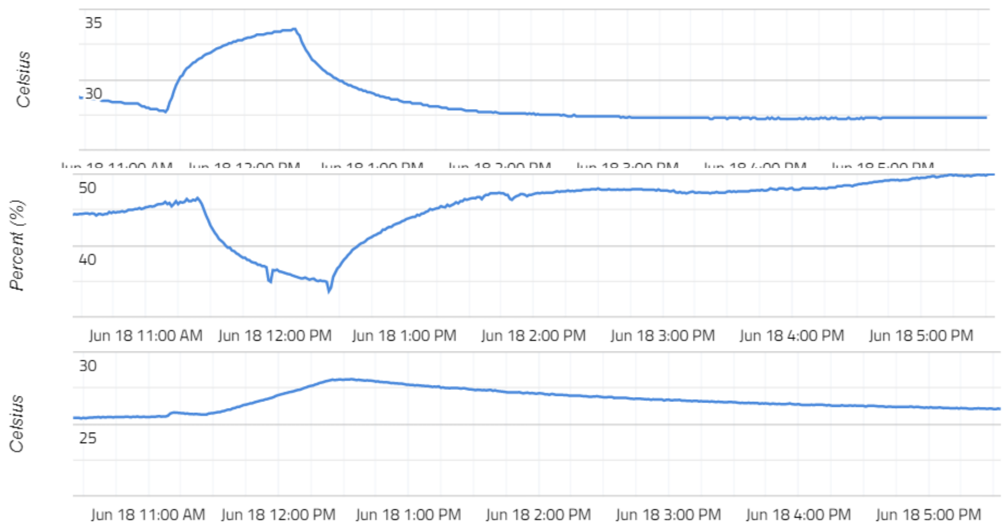

Figure 3.29: Diagrams of proposed GMCM system sensors after heating system activation (air temperature, relative humidity, soil temperature).

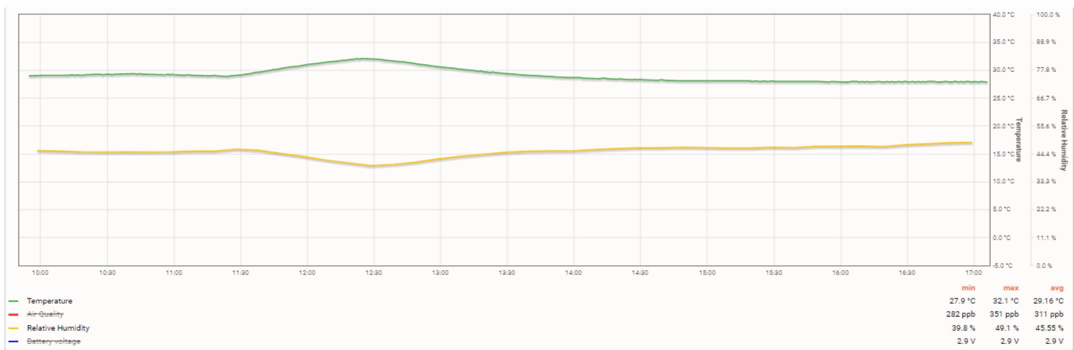

Figure 3.30: Diagram of Meazon air quality sensor after heating system activation (air temperature, relative humidity).

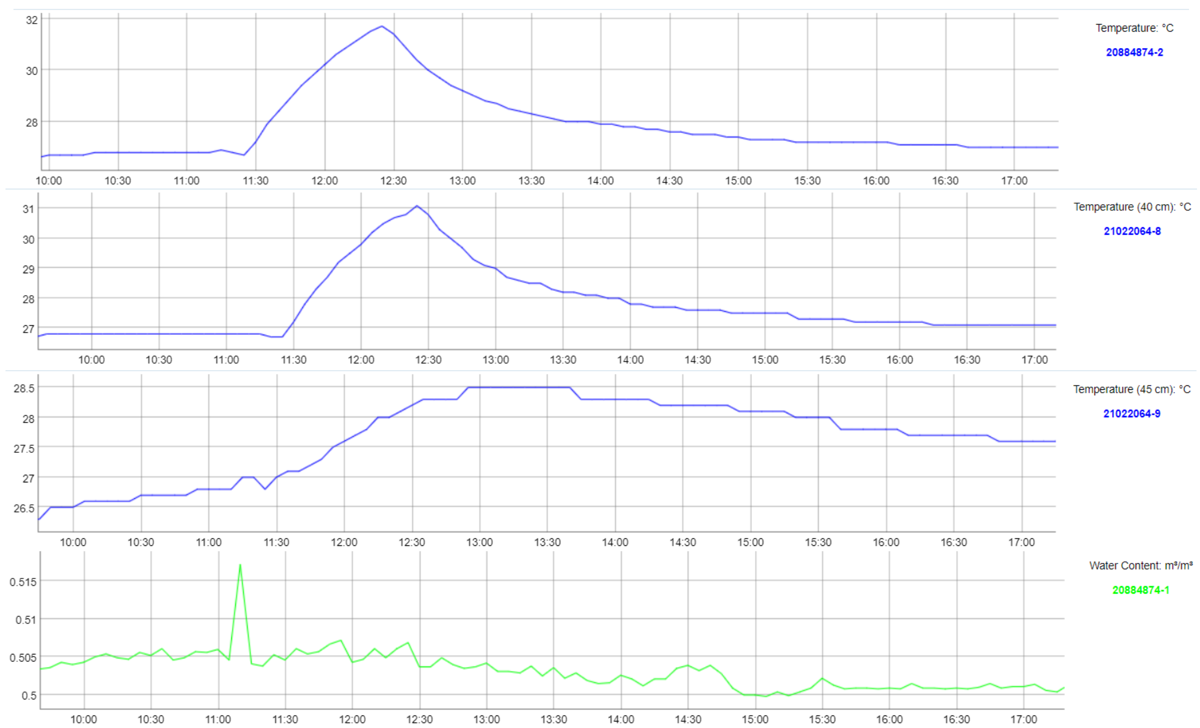

Figure 3.31: Diagrams of Hobolink sensors after heating system activation (RXW-T12 and RXW-GP3 multi-depth soil temperature and water content sensors).

2nd test: Heating and forced ventilation systems

The second test was conducted on June 18 at 11:00 a.m. At this point there is no sunlight exposure and the outdoor conditions are stable. Between 11:00 a.m. and 13:30, the room temperature was around 28.00°C and the humidity level 43.00-45.00%.

During the second test, the heating system was activated for one hour (from 11:00 a.m. to 12:00). After activating the heating system, the air temperature increased by 3-5°C while the relative humidity decreased by 4-7%. After activating the dynamic ventilation system, these conditions inside the greenhouse were reset in no more than half an hour (30 minutes). The soil temperature rose by 2.50-6.00°C and was reset around 13:30, in other words 1.30 hours after the activation of the fans. Last, there were no noticeable changes to soil moisture for the testing period.

The forced ventilation system managed to reset the micro-climate conditions in the greenhouse three times faster.

Table 3.6: Outdoor conditions change after heating and ventilation systems activation (air temperature and relative humidity monitored by Hobolink and Agenso systems).

19/06/21	Room Temp (H)	Room Temp (A)	Room RH (H)	Room RH (A)
11:00	28.40°C	28.70°C	42.60 %	43.00 %
12:00	28.60°C	28.70°C	41.30 %	43.50 %
12:30	28.30°C	28.55°C	41.80 %	44.25 %
13:30	28.20°C	27.35°C	43.50 %	45.75 %

Table 3.7: Greenhouse micro-climate conditions change after heating and ventilation systems activation (air temperature, relative humidity, and soil temperature by Meazon air quality sensor, proposed GMCM system and Hobolink).

19/06/21	GH Temp (Meazon)	GH Temp (GMCM)	GH RH (Meazon)	GH RH (GMCM)
11:00	30.00°C	29.00°C	40.40 %	39.50 %
12:00	32.90°C	33.60°C	36.30 %	32.25 %
12:30	30.20°C	28.40°C	38.80 %	40.60 %
13:30	28.60°C	27.80°C	43.40 %	43.40 %

Table 3.8: Greenhouse micro-climate conditions change after heating and ventilation systems activation (soil temperature and soil temperature by proposed GMCM system and Hobolink).

19/06/21	GH ST (GMCM)	GH ST (H)	GH SM (H)
11:00	26.00°C	27.40°C	49.50 %
12:00	28.60°C	33.40°C	50.00 %
12:30	27.60°C	29.80°C	49.90 %
13:30	26.50°C	27.40°C	49.50 %

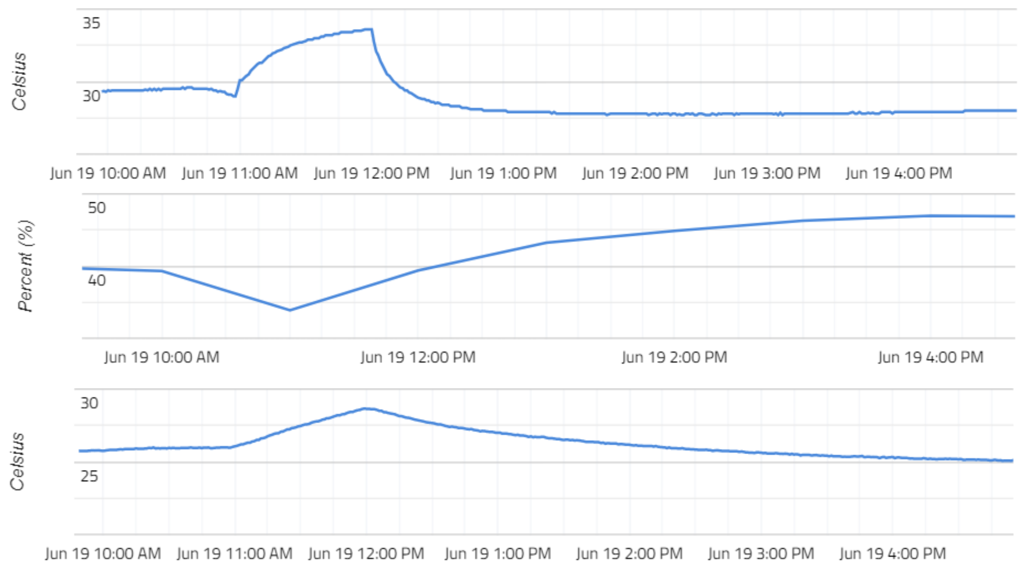

Figure 3.32: Diagrams of proposed GMCM system sensors after heating and ventilation systems activation (air temperature, relative humidity, soil temperature).

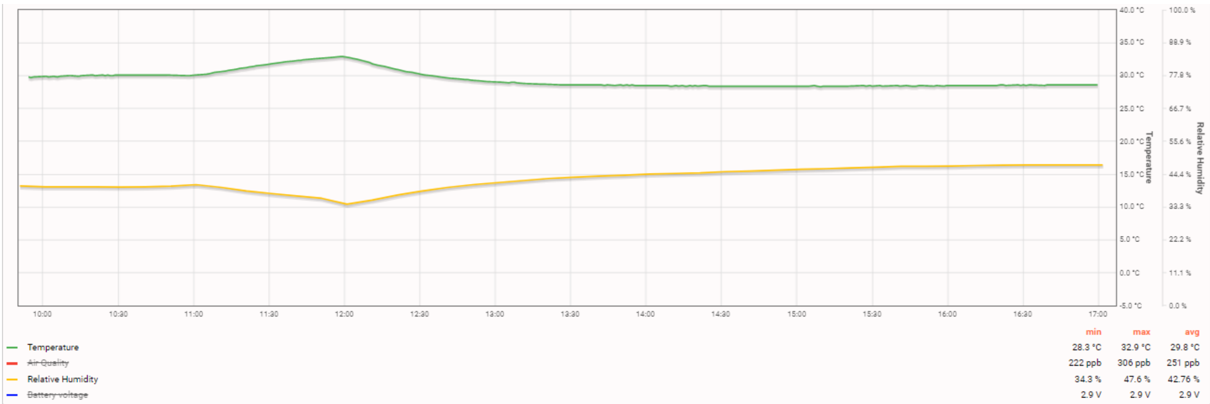

Figure 3.33: Diagram of Meazon air quality sensor after heating and ventilation systems activation (air temperature, relative humidity).

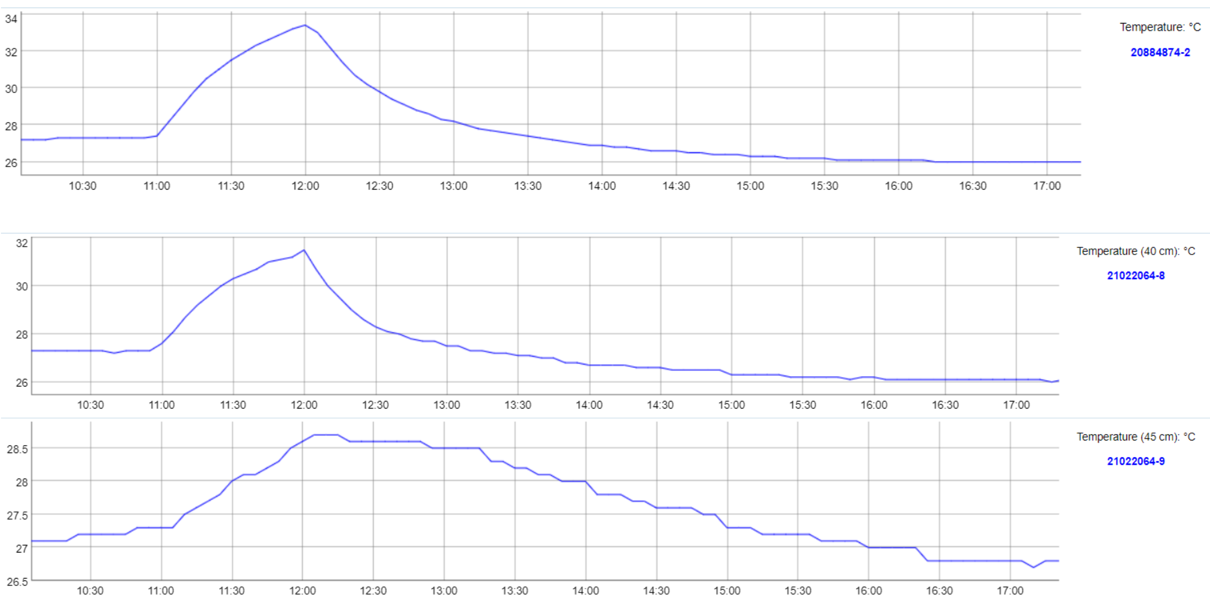

Figure 3.34: Diagrams of Hobolink sensors after heating and ventilation systems activation (RXW-T12 and RXW-GP3 multi-depth soil temperature and water content sensors).

3rd test: Heating and natural ventilation systems

The third test was conducted on June 18 at 11:00 a.m., when there is no sunlight exposure and the outdoor conditions are stable. Between 11:00 and 13:30, the room temperature was around 29.00°C and the humidity levels fluctuated between 45.00-48.00%.

During the third test, the heating system was activated for one hour from 11:00 to 12:00. After activating the heating system, a 3-5°C increase in the air temperature and an 8-12% decrease to the relative humidity were noted. After activating the natural ventilation system, these conditions inside the greenhouse were reset within 60 minutes. The soil temperature rose by 3-6°C and was reset around 15:00, 3 hours after opening the window. Lastly, there were no noticeable changes to soil moisture for the testing period.

The natural ventilation system managed to reset the micro-climate conditions in the greenhouse at two thirds of the time.

Table 3.9: Outdoor conditions change after heating and natural ventilation systems activation (air temperature and relative humidity monitored by Hobolink and Agenso systems).

20/06/21 status	Room Temp (H)	Room Temp (A)	Room RH (H)	Room RH (A)
11:00	29.30°C	29.50°C	44.60 %	46.50 %
12:00	29.50°C	29.50°C	44.60 %	47.00 %
12:30	29.20°C	29.40°C	45.50 %	47.75 %
13:00	29.10°C	29.30°C	46.20 %	48.50 %
13:30	29.10°C	29.30°C	46.80 %	48.75 %

Table 3.10: Greenhouse micro-climate conditions change after heating and natural ventilation systems activation (air temperature, relative humidity, and soil temperature by Meazon air quality sensor, proposed GMCM system and Hobolink).

20/06/21	GH Temp (Meazon)	GH Temp (GMCM)	GH RH (Meazon)	GH RH (GMCM)
11:00	29.70°C	28.80°C	45.00 %	45.00 %
12:00	33.20°C	34.10°C	37.30 %	34.80 %
12:30	31.90°C	30.50°C	40.20 %	41.70 %
13:00	30.80°C	29.50°C	43.00 %	44.10 %
13:30	30.20°C	29.10°C	44.90 %	45.60 %

Table 3.11: Greenhouse micro-climate conditions change after heating and natural ventilation systems activation (soil temperature and soil temperature by proposed GMCM system and Hobolink).

20/06/21 status	GH ST (GMCM)	GH ST (H)	GH SM (H)
11:00	25.40°C	26.60°C	48.70 %
12:00	28.40°C	33.30°C	48.90 %
12:30	28.20°C	30.80°C	49.70 %
13:00	27.90°C	29.80°C	49.40 %
13:30	27.90°C	29.30°C	49.30 %

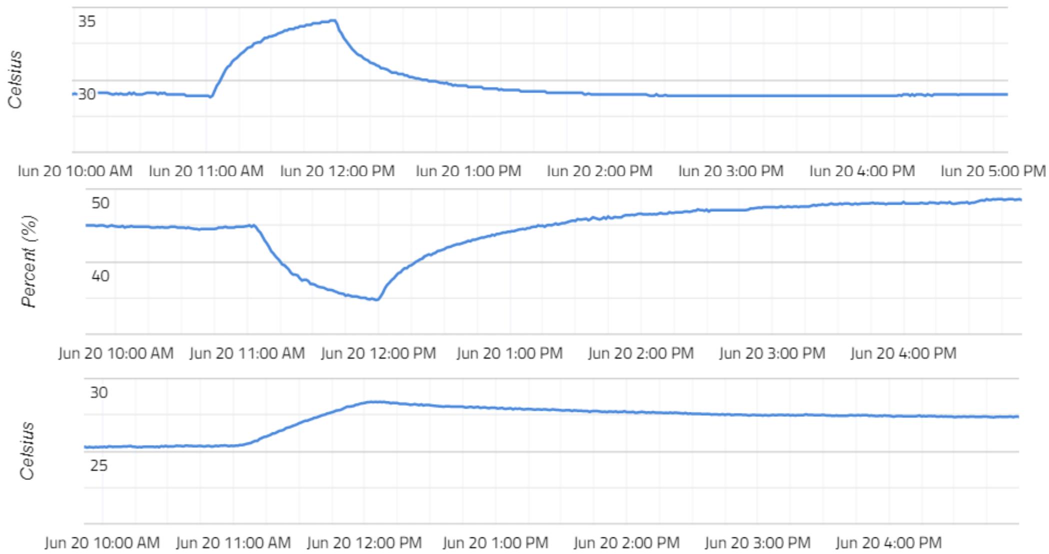

Figure 3.35: Diagrams of proposed GMCM system sensors after heating and natural ventilation systems activation (air temperature, relative humidity, soil temperature).

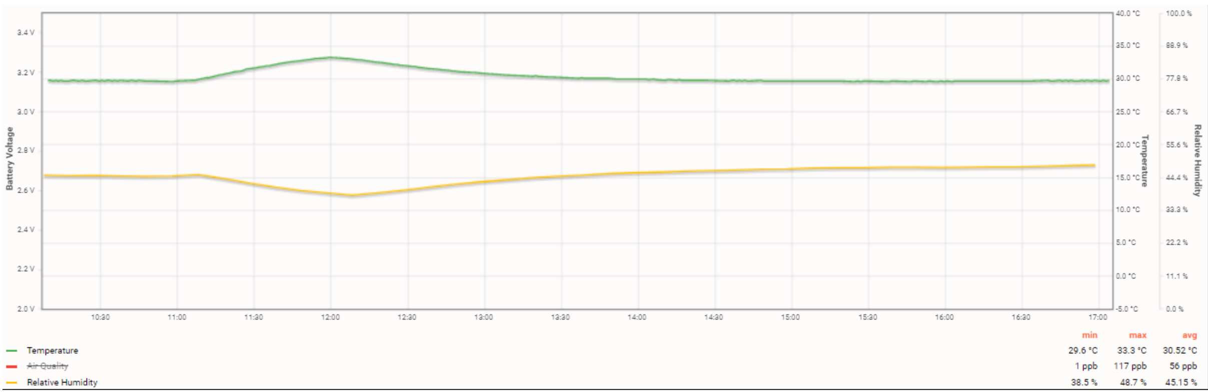

Figure 3.36: Diagram of Meazon air quality sensor after heating and natural ventilation systems activation (air temperature, relative humidity).

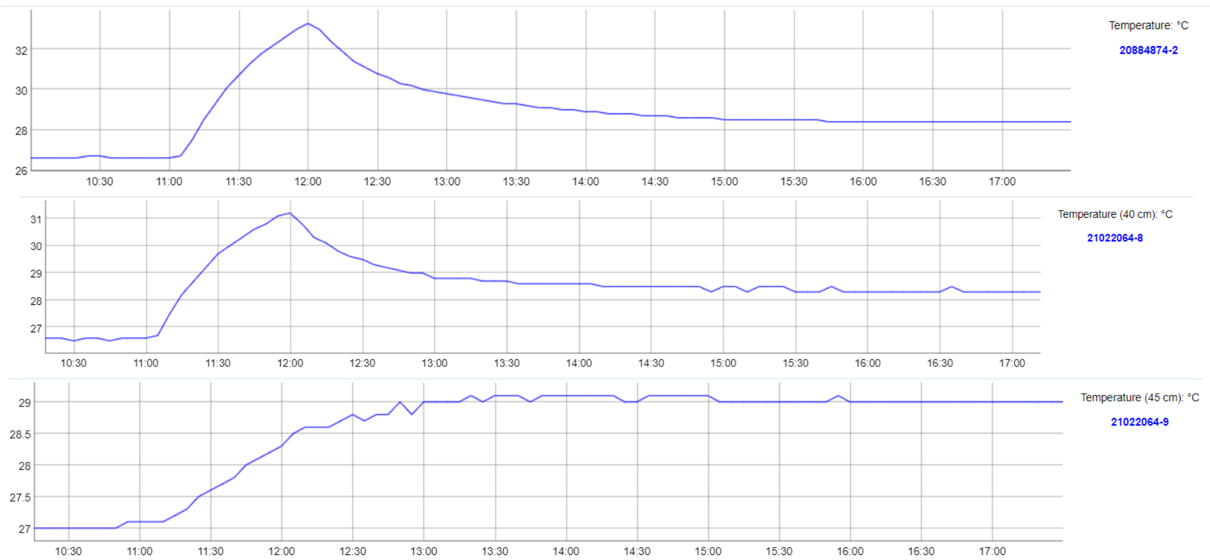

Figure 3.37: Diagrams of Hobolink sensors after heating and natural ventilation systems activation (RXW-T12 and RXW-GP3 multi-depth soil temperature and water content sensors).

It should be noted that a minor deviation among the sensors measurements is to be expected. First, each sensor inherently has a predefined deviation, draft to the measurements over time and duty cycles, different resolution and accuracy. Second, during the experimental measurements, each sensor was placed in a different place, height and with a different orientation. Ultimately, no significant deviation was observed among the measurements collected by the experiments and the research findings seemed to be reliable.

Conclusions

A proposed greenhouse micro-climate monitoring system was designed and installed in an experimental greenhouse model in Industrial Energy Environmental Systems Laboratory at Technical University of Crete. NodeMCU ESP8266 and ESP32 microcontrollers were used to collect data from the sensors, measuring air temperature, relative humidity, soil temperature, soil moisture, CO concentration, CO_2 concentration, TVOC level, air pressure and altitude. Data were uploaded via Wi-Fi to Cayenne IoT web-based platform, which offers remote monitoring features, including real-time or historical data visualization and export. The proposed Greenhouse Micro-Climate Monitoring system was compared with integrated monitoring systems created for industrial use, i.e. Hobolink, Meazon and Agenso. As it has become clear, the proposed GMCM system was successfully constructed, since it was a less expensive solution, giving sufficiently reliable measurements and its web-based interface provided a number of features similar to the integrated systems.

The building of the experimental greenhouse was the second stage of the research and thereby of this thesis. The experimental greenhouse effectively simulated a real greenhouse, while all necessary sensors and actuators incorporated in it worked flawlessly. The microcontroller of each system managing the actuators state was remotely controlled by Cayenne IoT web-based platform. Furthermore, several triggered actions were configured in Cayenne platform, which offered a level of automation in greenhouse micro-climate management. This is the result of the fact that the actuators are activated according to the sensors measurements. The heating system provided desirable air and soil temperature for plant growth, but it also decreased the air relative humidity in a short period of time. During the tests, after operating the heating system for one hour, the greenhouse needed 90 minutes to readapt itself to the outdoor conditions. The natural ventilation system reset the indoor conditions at two thirds of that time (60 minutes), while the dynamic ventilation systems at one third of that time (30 minutes). Lastly, the irrigation system served to increase soil moisture and prevent soil from drought.

This research focused on a proposed greenhouse micro-climate monitoring system. Therefore, I suggest that future research be made in use of photovoltaic solar panels in the system in question, so that it becomes a self-sustaining one. This advance may pave the way for the building of eco-friendly greenhouses.

Bibliography

[1] M. M. Anghelof, G. Suciu, R. Craciunescu, and C. Marghescu, “Intelligent System for Precision Agriculture,” *2020 13th Int. Conf. Commun. COMM 2020 - Proc.*, pp. 407–410, 2020, doi: 10.1109/COMM48946.2020.9141981.

[2] N. L. Panwar, S. C. Kaushik, and S. Kothari, “Solar greenhouse an option for renewable and sustainable farming,” *Renew. Sustain. Energy Rev.*, vol. 15, no. 8, pp. 3934–3945, 2011, doi: 10.1016/j.rser.2011.07.030.

[3] “How Does A Greenhouse Work?,” 2020. https://www.backyardgardenlover.com/how-does-a-greenhouse-work/ (accessed Mar. 15, 2021).

[4] I. Ardiansah, N. Bafdal, E. Suryadi, and A. Bono, “Greenhouse monitoring and automation using arduino: A review on precision farming and Internet of Things (IoT),” *Int. J. Adv. Sci. Eng. Inf. Technol.*, vol. 10, no. 2, pp. 703–709, 2020, doi: 10.18517/ijaseit.10.2.10249.

[5] “Smart Greenhouse | 2019 Guide to best Sensors and Remote Automated Monitoring Software,” 2019. https://www.postscapes.com/smart-greenhouses/ (accessed Mar. 15, 2021).

[6] Y. Mukazhanov, Z. Kamshat, O. Assel, N. Shayhmetov, and C. Alimbaev, “Microclimate control in greenhouses,” *Int. Multidiscip. Sci. GeoConference Surv. Geol. Min. Ecol. Manag. SGEM*, vol. 17, no. 62, pp. 699–704, 2017, doi: 10.5593/sgem2017/62/S27.089.

[7] N. Choab, A. Allouhi, A. El Maakoul, T. Kousksou, S. Saadeddine, and A. Jamil, “Review on greenhouse microclimate and application: Design parameters, thermal modeling and simulation, climate controlling technologies,” *Sol. Energy*, vol. 191, no. May, pp. 109–137, 2019, doi: 10.1016/j.solener.2019.08.042.

[8] A. Bhujel *et al.*, “Sensor Systems for Greenhouse Microclimate Monitoring and Control: a Review,” *J. Biosyst. Eng.*, vol. 2050, no. 2020, pp. 341–361, 2021, doi: 10.1007/s42853-020-00075-6.

[9] S. Gorjian *et al.*, “A review on opportunities for implementation of solar energy technologies in agricultural greenhouses,” *J. Clean. Prod.*, vol. 285, 2021, doi: 10.1016/j.jclepro.2020.124807.

[10] N. Gruda, “Impact of environmental factors on product quality of greenhouse vegetables for fresh consumption,” *CRC. Crit. Rev. Plant Sci.*, vol. 24, no. 3, pp. 227–247, 2005, doi: 10.1080/07352680591008628.

[11] R. K. Kodali, V. Jain, and S. Karagwal, “IoT based smart greenhouse,” *IEEE Reg. 10 Humanit. Technol. Conf. 2016, R10-HTC 2016 - Proc.*, 2017, doi: 10.1109/R10-HTC.2016.7906846.

[12] P. Defacio, L. Pickerel, and S. M. Rhyne, “Student Reference Greenhouse Operation and Management Writers,” vol. 34, no. 2, 2010, [Online]. Available: https://dese.mo.gov/sites/default/files/aged-Greenhouse Mngmnt Student Reference.pdf.

[13] “Nearly all life on Earth depends on photosynthesis.,” *Natl. Geogr. Mag.*, p. 6, 2020, [Online]. Available: https://media.nationalgeographic.org/assets/file/Photosynthesis_SECURED.pdf.

[14] “Essential pH Management in Greenhouse Crops: pH and Plant Nutrition | UGA Cooperative Extension,” 2015. https://extension.uga.edu/publications/detail.html?number=B1256&title=Essential pH Management in Greenhouse Crops: pH and Plant Nutrition (accessed Mar. 20, 2021).

[15] “e-Farming | Greenhouse Monitoring | Watchnet IoT Solutions Company,” 2021. https://www.watchnetiot.com/solution-by-industry-old/e-farming-and-greenhouse-farm-monitoring/ (accessed Mar. 19, 2021).

[16] “Innovative technologies in the NPEC greenhouse - NPEC,” 2020. https://www.npec.nl/news/innovative-technologies-in-the-npec-greenhouse/ (accessed Mar. 19, 2021).

[17] Α. Ασπράγκαθος and Χ. Μπεθάνης, “Χρήση Ηλιακών συστημάτων για θέρμανση/ψύξη θερμοκηπίων και μεθοδολογίες υπολογισμού θερμικών/ψυκτικών φορτίων,” Αριστοτέλειο Πανεπιστήμιο Θεσσαλονίκης, 2014.

[18] E. Kaiser, T. Ouzounis, H. Giday, R. Schipper, E. Heuvelink, and L. F. M. Marcelis, “Adding blue to red supplemental light increases biomass and yield of greenhouse-grown

tomatoes, but only to an optimum," *Front. Plant Sci.*, vol. 9, no. January, pp. 1–11, 2019, doi: 10.3389/fpls.2018.02002.
[19] "Green light: Is it important for plant growth? - MSU Extension," 2014. https://www.canr.msu.edu/news/green_light_is_it_important_for_plant_growth (accessed Mar. 19, 2021).
[20] "Hortidaily: global greenhouse news," 2021. https://www.hortidaily.com/article/9289092/boost-operational-efficiencies-with-lighting-control-system/ (accessed Mar. 19, 2021).
[21] "Greenhouse & Floriculture: Shade for Cooling Greenhouses | UMass Center for Agriculture, Food and the Environment," 2013. https://ag.umass.edu/greenhouse-floriculture/fact-sheets/shade-for-cooling-greenhouses (accessed Mar. 20, 2021).
[22] "Shade Systems," 2019. https://www.usgr.com/shade-heat-retention-systems/shade-systems/ (accessed Mar. 20, 2021).
[23] Z. Li, A. Yano, M. Cossu, H. Yoshioka, I. Kita, and Y. Ibaraki, "Shading and electric performance of a prototype greenhouse blind system based on semi-transparent photovoltaic technology," *J. Agric. Meteorol.*, vol. 74, no. 3, pp. 114–122, 2018, doi: 10.2480/agrmet.D-17-00047.
[24] Z. Li, A. Yano, and H. Yoshioka, "Feasibility study of a blind-type photovoltaic roof-shade system designed for simultaneous production of crops and electricity in a greenhouse," *Appl. Energy*, vol. 279, p. 115853, Dec. 2020, doi: 10.1016/j.apenergy.2020.115853.
[25] A. Slave and R. V Filkoski, "Modern technologies for utilization of geothermal energy and its influence to the environment," *Presing, J. Chamb. Auth. Archit. Eng. Maced. ISSN1857-744X*, vol. 10, no. November, pp. 5–15, 2011.
[26] "Greenhouse Heating Systems & Plant Growth Optimization | BioTherm Solutions," 2021. https://www.biothermsolutions.com/heat/ (accessed Mar. 20, 2021).
[27] A. Kavga, I. Konstas, and T. Panidis, "Assessment of infrared heating benefits in a production greenhouse," *Appl. Eng. Agric.*, vol. 31, no. 1, pp. 143–151, 2015, doi: 10.13031/aea.31.10747.
[28] "GRO Brooder Heaters | Hog Slat," 2021. https://www.hogslat.com/brooder-heaters-gro-series (accessed Mar. 20, 2021).
[29] "Natural or mechanical ventilation?," 2020. https://www.hortidaily.com/article/9243323/natural-or-mechanical-ventilation/ (accessed Mar. 19, 2021).
[30] Π. Αρέστης and Ζ. Καράλη, "ΜΕΛΕΤΗ ΕΝΕΡΓΕΙΑΚΩΝ ΑΝΑΓΚΩΝ ΘΕΡΜΟΚΗΠΙΩΝ ΚΑΙ ΠΡΟΤΑΣΕΙΣ ΓΙΑ ΤΗΝ ΧΡΗΣΗ ΑΝΑΝΕΩΣΙΜΩΝ ΠΗΓΩΝ ΕΝΕΡΓΕΙΑΣ ΓΙΑ ΤΗΝ ΚΑΛΥΨΗ ΜΕΡΟΥΣ ΤΩΝ ΕΝΕΡΓΕΙΑΚΩΝ ΑΝΑΓΚΩΝ ΤΟΥΣ," ΤΕΙ.ΔΕ, 2016.
[31] "Two types of temperature & humidity control - Greenhouse Management," 2017. https://www.greenhousemag.com/article/two-types-of-temperature--humidity-control/ (accessed Mar. 19, 2021).
[32] "Fogger or Mister? Which One Should I Use? : Drip Depot DIY Irrigation Support," 2019. https://help.dripdepot.com/support/solutions/articles/11000064167-fogger-and-mister-buying-guide (accessed Mar. 20, 2021).
[33] "Greenhouse environment control system," 2017. https://www.slideshare.net/ShekharTidke/greenhouse-environment-control-system (accessed Mar. 20, 2021).
[34] "Irrigation Systems | UMass Center for Agriculture, Food and the Environment," 2021. https://ag.umass.edu/greenhouse-floriculture/greenhouse-best-management-practices-bmp-manual/irrigation-systems (accessed Mar. 21, 2021).
[35] "Protected Crops - Irritec Corporate," 2021. https://www.irritec.com/protected-crops/ (accessed Mar. 21, 2021).
[36] "CO2 Fertilization - messergroup.com," 2020. https://www.messergroup.com/food/greenhouses/co2-fertilization (accessed Mar. 20, 2021).
[37] M. Ramezani, K. Shah, E. Doroodchi, and B. Moghtaderi, "Application of a novel calcium looping process for production of heat and carbon dioxide enrichment of greenhouses," *Energy Convers. Manag.*, vol. 103, pp. 129–138, Jun. 2015, doi: 10.1016/j.enconman.2015.06.044.
[38] S. Agnal, K. Kapoor, M. Musfik, and R. Sharma, "Automated Smart Greenhouse

Environment Using IoT," pp. 1665–1671, 2018.
[39] M. H. V. Shinde, "IOT based Greenhouse Automation System," *Int. J. Res. Appl. Sci. Eng. Technol.*, vol. 7, no. 5, pp. 606–609, 2019, doi: 10.22214/ijraset.2019.5103.
[40] A. S. Dilbaz, "Design and Implementation of a Smart Greenhouse," no. September, 2017.
[41] Ε. Ντερβίσι, Ι. Μίσκου, and Α. Κυπριώτης, "ΑΥΤΟΝΟΜΟ ΣΥΣΤΗΜΑ ΕΛΕΓΧΟΥ ΚΑΙ ΛΗΨΗΣ ΑΠΟΦΑΣΕΩΝ ΣΕ ΘΕΡΜΟΚΗΠΙΑΚΗ ΜΟΝΑΔΑ," ΤΕΙ ΔΕ, 2017.
[42] Α. ΓΡΙΒΑ, "ΑΥΤΟΝΟΜΟ ΘΕΡΜΟΚΗΠΙΟ ΜΕ ΣΥΣΤΗΜΑΤΑ ΠΡΟΣΤΑΣΙΑΣ ΚΑΙ ΑΝΤΛΗΣΗΣ ΝΕΡΟΥ ΜΕ ΤΗ ΧΡΗΣΗ ΜΙΚΡΟΕΛΕΓΚΤΗ ARDUINO, ΤΡΟΦΟΔΟΤΟΥΜΕΝΟ ΜΕ ΗΛΙΑΚΗ ΕΝΕΡΓΕΙΑ," ΑΡΙΣΤΟΤΕΛΕΙΟ ΠΑΝΕΠΙΣΤΗΜΙΟ ΘΕΣΣΑΛΟΝΙΚΗΣ, 2018.
[43] F. A. Khan, A. A. Ibrahim, and A. M. Zeki, "Environmental monitoring and disease detection of plants in smart greenhouse using internet of things," *J. Phys. Commun.*, vol. 4, no. 5, 2020, doi: 10.1088/2399-6528/ab90c1.
[44] Z. Wan, Y. Song, and Z. Cao, "Environment dynamic monitoring and remote control of greenhouse with ESP8266 NodeMCU," *Proc. 2019 IEEE 3rd Inf. Technol. Networking, Electron. Autom. Control Conf. ITNEC 2019*, no. Itnec, pp. 377–382, 2019, doi: 10.1109/ITNEC.2019.8729519.
[45] S. N. S. Al-Humairi, P. Manimaran, M. I. Abdullah, and J. Daud, "A Smart Automated Greenhouse: Soil Moisture, Temperature Monitoring and Automatic Water Supply System (Peaty, Loam and Silty)," *2019 IEEE Conf. Sustain. Util. Dev. Eng. Technol. CSUDET 2019*, pp. 111–115, 2019, doi: 10.1109/CSUDET47057.2019.9214661.
[46] M. T. Ismail, M. N. Ismail, S. S. Sameon, Z. M. Zin, and N. Mohd, "Wireless Sensor Network: Smart greenhouse prototype with smart design," *2nd Int. Symp. Agent, Multi-Agent Syst. Robot. ISAMSR 2016*, no. August, pp. 57–62, 2017, doi: 10.1109/ISAMSR.2016.7810003.
[47] K. Bounnady, P. Sibounnavong, K. Chanthavong, and S. Saypadith, "Smart crop cultivation monitoring system by using IoT," *Proceeding - 5th Int. Conf. Eng. Appl. Sci. Technol. ICEAST 2019*, pp. 2019–2021, 2019, doi: 10.1109/ICEAST.2019.8802584.
[48] "Raspberry Pi 4 Model B specifications – Raspberry Pi," 2021. https://www.raspberrypi.org/products/raspberry-pi-4-model-b/specifications/ (accessed Mar. 31, 2021).
[49] "Pros and Cons of Raspberry Pi: Detailed Guide in 2020," 2020. https://robu.in/5-pros-and-5-cons-of-raspberry-pi/ (accessed Mar. 31, 2021).
[50] H. Prskalo, J. Trstenjak, and B. Trstenjak, "Smart greenhouse based on the arduino platform," *Ann. DAAAM Proc. Int. DAAAM Symp.*, vol. 31, no. 1, pp. 282–289, 2020, doi: 10.2507/31st.daaam.proceedings.039.
[51] L. Nyanga and D. Q. Adams, "Greenhouse iot application for smart agriculture solutions," no. October, 2020, [Online]. Available: ThingSpeak; Flowcharts;
[52] H. Andrianto, Suhardi, and A. Faizal, "Development of smart greenhouse system for hydroponic agriculture," *2020 Int. Conf. Inf. Technol. Syst. Innov. ICITSI 2020 - Proc.*, pp. 335–340, 2020, doi: 10.1109/ICITSI50517.2020.9264917.
[53] K. Raviteja and M. Supriya, "Greenhouse Monitoring System Based on Internet of Things," *Lect. Notes Electr. Eng.*, vol. 637, pp. 581–591, 2020, doi: 10.1007/978-981-15-2612-1_56.
[54] P. Visconti, N. I. Giannoccaro, R. de Fazio, S. Strazzella, and D. Cafagna, "IoT-oriented software platform applied to sensors-based farming facility with smartphone farmer app," *Bull. Electr. Eng. Informatics*, vol. 9, no. 3, pp. 1095–1105, 2020, doi: 10.11591/eei.v9i3.2177.
[55] A. Vishwakarma, A. Sahu, N. Sheikh, P. Payasi, S. K. Rajput, and L. Srivastava, "IOT based greenhouse monitoring and controlling system," *2020 IEEE Students' Conf. Eng. Syst. SCES 2020*, 2020, doi: 10.1109/SCES50439.2020.9236693.
[56] "Arduino Buying Guide 2020: Complete Guide to Choose the Right Board," 2020. https://electropeak.com/learn/arduino-buying-guide-how-to-choose-right-arduino-board/ (accessed Mar. 28, 2021).
[57] Ö. Alpay and E. Erdem, "The control of greenhouses based on fuzzy logic using wireless sensor networks," *Int. J. Comput. Intell. Syst.*, vol. 12, no. 1, pp. 190–203, 2018, doi: 10.2991/ijcis.2018.125905641.
[58] A. Belkadi, D. Mezghani, and A. Mami, "DESIGN AND IMPLEMENTATION OF FLC APPLIED TO A SMART GREENHOUSE Fuzzy logic , IoT , Greenhouse cultivation needs an accurate

modelling and an optimised control system to ensure an adequate microclimatic condition for plants . It represents a complex task d," *Eng. Agrícola*, vol. 4430, pp. 777–790, 2020.
[59] Hobolink, "Hobolink monitoring system," vol. 11, no. 316, pp. 1–2, 2021, [Online]. Available: https://www.onsetcomp.com/products/data-loggers/rx3000/.
[60] Hunan Rika Electronics, "Rk200-07 UV Radiation Sensor / Ultraviolet Sensor / UV Index Sensor | Rika Sensors," 2021. https://www.rikasensor.com/rk200-07-uv-radiation-sensor.html (accessed Jun. 04, 2021).
[61] "About Meazon: leads IoT energy management using hi-tech as a leverage," 2021. https://meazon.com/about/ (accessed May 06, 2021).
[62] "Meazon 'Janus' Gateway Features," 2021. https://meazon.com/wp-content/uploads/2019/05/meazon-janus-gateway.pdf (accessed May 06, 2021).
[63] "Smart Plug Bizy Type F - Meazon Specs," 2021. https://meazon.com/wp-content/uploads/2019/05/meazon-bizy-type-f-plug.pdf (accessed May 06, 2021).
[64] MEAZON, "Humidity Sensor Humidity Sensor - Technical specifications," 2021.
[65] MEAZON, "Air Quality Sensor Wireless monitoring of VOC levels Air Quality Sensor - Technical specifications," 2021.
[66] "ESP8266 NodeMCU WiFi Devkit," 2021. Accessed: May 30, 2021. [Online]. Available: www.handsontec.com.
[67] "ESP32 Development Board - DEVKIT V1," 2021. https://grobotronics.com/esp32-development-board-devkit-v1.html (accessed May 30, 2021).
[68] "ESP32 ADC Tutorial - Read Analog Voltage in Arduino – DeepBlue," 2021. https://deepbluembedded.com/esp32-adc-tutorial-read-analog-voltage-arduino/ (accessed Jul. 05, 2021).
[69] "DHT22 Datasheet(PDF) - List of Unclassifed Manufacturers," 2021. https://www.alldatasheet.com/datasheet-pdf/pdf/1132459/ETC2/DHT22.html (accessed May 30, 2021).
[70] "DS18B20 Waterproof Temperature Sensor Cable Product Description," 2021. Accessed: May 30, 2021. [Online]. Available: https://dlnmh9ip6v2uc.cloudfront.net/datasheets/Sensors/Temp/DS18B20.pdf.
[71] "Capacitive_Soil_Moisture_Sensor_SKU_SEN0193-DFRobot," 2021. https://wiki.dfrobot.com/Capacitive_Soil_Moisture_Sensor_SKU_SEN0193 (accessed Jul. 05, 2021).
[72] "Liquid_Level_Sensor-FS-IR02_SKU__SEN0205-DFRobot," 2021. https://wiki.dfrobot.com/Liquid_Level_Sensor-FS-IR02_SKU__SEN0205 (accessed Jul. 05, 2021).
[73] "CCS811+ BME280 Multi-function Environmental Sensor Wiki - DFRobot," 2021. https://wiki.dfrobot.com/Multi_function_Environmental_Module_CCS811_BME280_SKU_SEN0335 (accessed Jul. 05, 2021).
[74] "Carbon_Monoxide_Gas_Sensor_MQ7___SKU_SEN0132_-DFRobot," 2021. https://wiki.dfrobot.com/Carbon_Monoxide_Gas_Sensor_MQ7___SKU_SEN0132_ (accessed Jul. 05, 2021).
[75] "Door magnet MC 37 B," 2021. https://blogmasterwalkershop.com.br/arquivos/datasheet/Datasheet MC-38.pdf (accessed May 30, 2021).
[76] "Creality 3D 42-40 Stepper Motor," 2021. https://grobotronics.com/creality-3d-42-40-stepper-motor.html (accessed May 30, 2021).
[77] "A4988 Stepper Motor Driver Module Pinout, Datasheet, Specs & Alternatives," 2019. https://components101.com/modules/a4988-stepper-motor-driver-module (accessed May 30, 2021).
[78] "How To Control Stepper Motor with A4988 Driver and Arduino," 2015. https://howtomechatronics.com/tutorials/arduino/how-to-control-stepper-motor-with-a4988-driver-and-arduino/ (accessed May 31, 2021).
[79] "P12 PWM PST CO | Pressure-optimised 120 mm PWM PST Fan for Continuous Operation | ARCTIC," 2021. https://www.arctic.de/en/P12-PWM-PST-CO/ACFAN00121A (accessed May 30, 2021).
[80] "Datasheet and description Avide Infra Bulb E27 250W Red," 2021.
[81] "5V Single-Channel Relay Module - Pin Diagram, Specifications, Applications, Working,"

2020. https://components101.com/switches/5v-single-channel-relay-module-pinout-features-applications-working-datasheet (accessed May 30, 2021).
[82] C. myDevices, “Cayenne Docs,” 2021. https://developers.mydevices.com/cayenne/docs/intro/ (accessed Jun. 11, 2021).